HOKKAIDO UNIVERSITY

Title	Investigation and Estimation of Restrained Expansion and Shrinkage Behavior of Expansive Concrete Structures
Author(s)	Prayuda, Hakas
Degree Grantor	北海道大学
Degree Name	博士(工学)
Dissertation Number	甲第15369号
Issue Date	2023-03-23
DOI	https://doi.org/10.14943/doctoral.k15369
Doc URL	https://hdl.handle.net/2115/91143
Type	doctoral thesis
File Information	Hakas_Prayuda.pdf

INVESTIGATION AND ESTIMATION OF RESTRAINED EXPANSION AND SHRINKAGE BEHAVOIRS OF EXPANSIVE CONCRETE STRUCTURES

A dissertation submitted to the Division of Engineering and Policy for Sustainable Environment, Graduate School of Engineering, Hokkaido University in partial fulfillment of the requirements for the Degree of Doctor of Philosophy in Engineering

by
HAKAS PRAYUDA

Examination Committee
Associate Professor Koji Matsumoto
Professor Takafumi Sugiyama
Professor Takashi Matsumoto

Division of Engineering and Policy for Sustainable Environment
Graduate School of Engineering
Hokkaido University
Sapporo, Japan

February 2023

INVESTIGATION AND ESTIMATION OF RESTRAINED EXPANSION AND SHRINKAGE BEHAVIORS OF EXPANSIVE CONCRETE STRUCTURES

Division of Engineering and Policy for Sustainable Environment

Graduate School of Engineering

Hokkaido University

Sapporo, Japan

February 2023

ABSTRACT

Expansive concrete is produced by using an expansive cement or expansive additive that introduces expansion in the concrete at early ages. Expansive concrete is used to reduce the tensile stress caused by restrained shrinkage in concrete structures. Basically, some standards, such as ACI 223R-10, JSCE No. 23, and JIS A 6202, have been regulated as a guideline for designing expansive concrete structures using either expansive cement or expansive additives. However, either the ACI or the JSCE design standard does not include many factors that affect the level of expansion in expansive concrete, such as cementitious replacement materials, curing method, and curing temperature. In addition, the existing standards includes only some types of expansive additive which are calcium oxide-based (CaO) and calcium sulfoaluminate-based (C-S-A). Meanwhile, there are many types of expansive additives or their combinations which produce different expansion levels and mechanisms. According to the limitation of those standards, this study proposes a method to estimate the restrained expansion strain from the free expansion strain of expansive concrete with several mix proportions and curing conditions, including the effects of amount of fly ash, amount of binder, amount of expansive additive, curing temperature, and curing method.

Finite element (FE) analysis is one of the comprehensive methods for estimating the strain level in expansive concrete to increase the flexibility and versatility of the design and analysis process. This research uses FE analysis to estimate the restrained expansion strain in expansive concrete structures. However, it was confirmed that the FE analysis using free expansion strain as the input always overestimates the actual restrained expansion strain of the expansive concrete. This is due to the difference in the expansion mechanism between the free and restrained conditions in the expansive concrete. During the initial hydration process, the expansive agent could rapidly react with water to produce a large number of expansive products. However, since there is no restraining compressive stress in the concrete, the expansive products do not fill much the pores in the concrete. In the case of expansive concrete under restraint, some portions of the expansive products are forced to enter the voids in the concrete, reducing the ability to produce expansion. Compression creep at the very early age also reduce the expansion ability of the expansive concrete under restraint. These two behaviors must be considered in the FE analysis to simulate the deformation caused by the expansion of expansive concrete under restraint, so the free expansion strain cannot be used solely as the input for the FE analysis. Quantification of the loss of expansion due to the two behaviors is very complex as it is very difficult to quantify them separately. Therefore, the effective free strain is defined in this study to be applied as the input in the FE analysis to simulate the deformation of expansive concrete under restraint.

Expansion and shrinkage were investigated through laboratory tests, field measurements, and FE analysis. Concrete expansion is measured in the laboratory under both unrestrained and restrained conditions. Through these laboratory measurements, it was to determine a reduction factor equation that can be used to estimate the effective free expansion strain. This research is continued by validating the proposed method by employing effective free strain to estimate early-age restrained expansion strain in expansive concrete for predicting early expansion and subsequent shrinkage in actual structures. The four structure types chosen for the validation in this

research are slabs on grade, slabs on beam, slabs on pile, and water tank walls. In all structures, estimations using FE analysis are performed by considering various factors that influence the expansion and shrinkage behavior of expansive concrete structures. From the results of this investigation, it can be concluded that the reduction factor used to determine the free strain can effectively estimate the restrained expansion strain in the studied expansive concrete structures. The level of expansion and shrinkage strains can be estimated by considering various factors affecting the expansion levels, such as mix proportion, degree of restraint, and measurement direction. In expansive concrete structures, structural configuration and degree of restraint significantly affect the level of expansion and shrinkage. The area with higher restraint conditions always produced lower restrained expansion strain.

ACKNOWLEDGEMENTS

TABLE OF CONTENTS

LIST OF TABLES

LIST OF FIGURES

LIST OF SYMBOLS/ABBREVIATIONS

Symbols/Abbreviations	Terms
ACI	American Concrete Institute
JSCE	Japan Society for Civil Engineers
JIS	Japan Industrial Standard
C-S-A	Calcium Sulfoaluminate
CaO	Calcium Oxide
MgO	Magnesium Oxide
C_4A_3S	Anhydrous Tetra Calcium Trialuminate Sulfate
$CaSO_4$	Calcium Sulfate
C3A	Tricalcium Aluminate
FEA	Finite Element Analysis
UEA	Expansive Additive Type U
EA	Expansive Additive
OPC	Ordinary Portland Cement
FA	Fly Ash
SiO_2	Silicon Dioxide (Silica)
Al_2O_3	Aluminum (II) Oxide
Fe_2O_3	Ferric Oxide
SO_3	Sulfur trioxide (Sulfite)
K_2O	Potassium Oxide
Na_2O	Sodium Oxide
MnO	Manganese (II) Oxide
SrO	Strontium (II) Oxide
$Ca(OH)_2$	Aluminum (II) Oxide
ASTM	American Standard for Testing Materials
ρ	Reinforcement Ratio (%)
CSCM	Continuous Surface Cap Model
E	Young's Modulus
fc'	Compressive Strength (MPa)
ft	Tensile Strength (MPa)
Gf	Fracture Energy
$\varepsilon_{eff, free}$	Effective Free Strain (μ)
ϕ	Reduction Factor
ε_{free}	Free Strain (μ)
W/B	Water to Binder Ratio
T	Temperature (°C)
TIS	Thailand Industrial Standard
SG	Slab on Grade
SB	Slab on Beam
SP	Slab on Pile
WT	Water Tank Wall

CHAPTER 1

INTRODUCTION

1.1 Background

Concrete is considered one of the most versatile construction materials due to its superior capabilities, such as high workability, excellent performance under compressive loading, and economic benefits. Concrete is a composite material composed of cement, water, fine aggregate, coarse aggregate, and other chemical and mineral admixtures in appropriate ratios to achieve the expected performance. The amount of concrete production as a construction material continues to increase, particularly in developing countries. Several previous researchers have predicted that cement production, as one of the components of concrete, will continue to increase until 2050 [1], [2]. On the other hand, concrete has significant disadvantages in terms of both mechanical properties and durability. The volume of concrete decreases with time because of drying shrinkage, thermal shrinkage, autogenous shrinkage, and carbonation shrinkage [3]. One of the most significant weaknesses of concrete is its inability to resist tensile forces. As a result, concrete is frequently combined with rebar reinforcement in various structures. The concrete has restraint due to reinforcement and the influence of adjacent members. When shrinkage occurs in restrained concrete, a certain amount of tensile stress may develop. The crack will be generated if the tensile stress under restraint exceeds the tensile stress capacity [4]. Cracks caused by shrinkage or volume reduction can reduce strength, durability and increase the risk of corrosion of rebar reinforcement [5].

Shrinkage occurs when the temperature decreases non-uniformly after heating due to the hydration process at the early age of the concrete. As a result of the temperature uniformity, the moisture in the inner of the concrete is lost due to self-desiccation at the early ages or by evaporation into the environment in the hardened stage. The decrease in relative humidity causes capillary stress in the micropores of concrete, compaction of the capillary pores, and macroscale shrinkage of the concrete members [5]–[7]. Various aspects contribute to shrinkage propagation in reinforced concrete structures, especially the influence of the configuration of the structures, such as dimension, reinforcement, adjacent structural members, base friction, mix proportion, curing conditions, and environmental exposure, including relative humidity and ambient temperature. These factors must be considered in order to produce concrete with high resistance to shrinkage cracking in concrete structures.

Several methods have been developed and studied to reduce cracking and corrosion in reinforced concrete structures caused by shrinkage at early age. The application of chemical admixtures to the surface area, the use of shrinkage-reducing admixture during the casting process, and using fibers as additional reinforcement are several methods that have been developed to prevent shrinkage cracking. In addition, utilizing expansive cement or expansive agent is one of the comprehensive solutions to compensate for concrete shrinkage. In the early stages of cement hydration, expansive concrete can increase the volume of concrete by producing a large amount of ettringite or calcium hydroxide. Under restrained conditions, the expansion or compressive stress generated compensates for the tensile stress caused by subsequent shrinkage. The utilization of an expansive additive to prevent shrinkage cracking in concrete is one of the most simple and practical methods. The construction procedure for an

expansive concrete structure is identical to conventional concrete. Some methods, such as applying chemical admixtures to the surface of concrete structures and controlling temperature and humidity during the curing period, necessitate additional work after the casting process. In addition, controlling temperature and humidity during the curing period might not be practical in actual construction. For shrinkage-reducing admixture, it only reduces physical shrinkage due to capillary tension, while expansive concrete can compensate for overall shrinkage by producing pre-compressive stress in concrete during the expansion process. Therefore, expansive concrete is a practical and suitable method for preventing cracking induced by overall shrinkage.

The use of expansive concrete as a method for preventing cracking due to shrinkage has been developed in various countries. Typically, expansive concrete in Europe and the United States is made from expansive cement, while in some other countries, it is manufactured by mixing expansive agents as additive materials into the concrete [8]. Besides, several standards have been regulated for the design procedure and classification of expansive concrete, including ACI 223R-10 for expansive cement [9], JSCE No.23, and JIS A 6202 for expansive concrete made with expansive additives [10], [11]. Meanwhile, several types of expansive agents have been developed in recent years, such as the C-S-A expansive agent, the CaO expansive agent, the MgO expansive agent, and a combination of the C-S-A, CaO, and MgO expansive agents. Expansive concrete is appropriate for thin structures with large surface areas, particularly those exposed to the environment, which increases the probability of cracking due to shrinkage. Expansive concrete has been used to construct several types of structures in many countries, including airport pavements, bridge girders, arch dams, basement concrete walls, industrial floors, slabs on beams and foundations, slabs on grades, basement walls, and water tank walls.

The expansion level of expansive concrete with restraint is influenced by various factors, such as degree of restraint (internal and external restraint), amount of binder, amount of expansive additive, type of expansive additive, water to binder ratio, type of curing, curing duration, curing temperature and exposure environment. Several parameters affecting the rate of expansion in actual structures can be managed. However, some are extremely uncontrollable, such as moisture loss, which is highly dependent on the condition of the environment. To prevent shrinkage cracking, the factors that affect the level of expansion in the construction site should be considered during the design process. However, limited studies provide information about the effectiveness of expansive additives in actual structures by considering the factors explained above, especially using ettringite and calcium sulfoaluminate-based expansive agent, which is used in this study. Thus, the main objective of this study is to investigate the expansion and shrinkage strain level in reinforced expansive concrete structures by considering the effect of restraint, type and amount of expansive additive, environmental conditions, and curing conditions.

1.2 Mechanism of shrinkage compensation

Expansive concrete is produced by using expansive cement or expansive additive that can introduce expansion or increase its volume at the early age of the hardening stage. **Figure 1.1** illustrates the expansion along time between normal and expansive concrete at an early age due to hydration from the cement and additive materials. Some new cement replacement materials have also been employed to produce ettringite or calcium during the hydration

process, which results in expansion. Meanwhile, expansive concrete expanded higher than normal concrete. The expansion process is generally effective during the curing periods and begins to shrink after the curing is completed. However, several investigations have discovered that concrete expands after the curing process is completed [12], [13]. The rate and duration of expansion in concrete are influenced by various factors, such as the structure configuration, the type and amount of expansive additive or expansive cement, and the exposure environment. Several expansive concrete expansion mechanisms have been proposed [14].

a. In swelling theory, the water absorption property of an expansive agent is regarded as an influencing factor for volume increment.
b. In crystal growth theory, the volume is increased due to the crystal growth of expansive crystalline indigents.
c. During hydration, the disintegration of expansive ingredients results in the formation of co-existing pores.
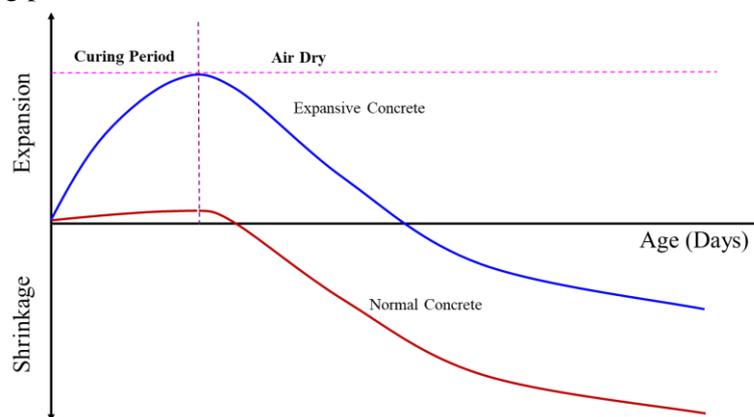
Figure 1.1 Volume change comparison between expansive and normal concrete [14]

According to ACI 223R-10 [9], three types of expansive cement and four types of expansive additive are used for concrete construction. Expansive cement is described as cement that can increase its volume to greater than Portland cement after setting time when mixed with water. Expansive cement can be classified into three types as follow.

a. Expansive cement type K is a mixture of Portland cement, anhydrous tetra calcium trialuminate sulfate (C_4A3S), calcium sulfate ($CaSO4$), and lime (CaO).
b. Expansive cement type M is a blended mixture of Portland cement, calcium aluminate cement, and calcium sulfate.
c. Expansive cement type S is a mixture of Portland cement with high tricalcium aluminate ($C3A$) and calcium sulfate.

An expansive additive or expansive component system combines Portland cement and expansive component that can increase its volume after setting time when mixed with water. Expansive additives must contain some iron powder, alumina powder, magnesia, calcium sulfoaluminate, and calcium oxide. Based on ACI 223R-10 [9], the expansive additive can be categorized into four types.

a. Expansive additive type K is a mixture of calcium sulfoaluminate and calcium sulfate that produces ettringite when mixed with Portland cement and water.
b. Expansive additive type M is a mixture of calcium aluminate and calcium sulfate.
c. Expansive additive type S is a mixture of tricalcium aluminate and calcium sulfate.

d.   Expansive additive type G is a mixture of aluminum dioxide and aluminum dioxide.

Several expansive additives with various chemical and mineral compositions have been applied in construction projects. This study used two types of expansive additives, namely C-S-A-based expansive agents and the combination of ettringite and calcium sulfoaluminate-based expansive agents. Various scientific studies have discovered several types of expansive additives that show different expansion capabilities. Nagataki & Gomi (1998) explained that expansive additives could be classified into two different types, namely C-S-A type and CaO type expansive agents [14]. C-S-A type expansive agent causes expansion by altering a mixture of calcium sulfoaluminate, lime, and anhydrite into ettringite. While the CaO type contributes to the expansion by forming calcium hydroxide. The formations of ettringite and calcium hydroxide are shown in **Eq. 1.1** and **Eq. 1.2**, respectively.

$$C_4A_3S + 8CaSO_4 + 6CaO + 96\ H_2O \rightarrow 3C_3A \cdot 3CaSO_4 \cdot 32H_2O \tag{1.1}$$

$$CaO + H_2O \rightarrow Ca\ (OH)_2 \tag{1.2}$$
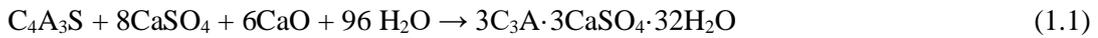
The mechanism of shrinkage compensating for normal and expansive concrete can be seen in **Figure 1.2**. The hardened concrete shrinks under dried conditions for typical normal concrete with free conditions. However, hardened concrete is not allowed to shrink freely under restrained conditions due to the effect of restraint. Tensile stress is developed under restraint during the shrinkage, and crack propagation may occur when the tensile stress exceeds the tensile strength of concrete. On the other hand, hardened expansive concrete in a free condition expand freely to fill an area with low stiffness or pressure. Meanwhile, compressive stress is generated because the concrete cannot expand freely under restraint conditions, and some expansive product fills the pores. As a result of compressive stress developed at the early age of expansive concrete, there is a decrease in tensile stress during shrinkage. This is one of the benefits of using expansive products to avoid shrinkage cracking in concrete.
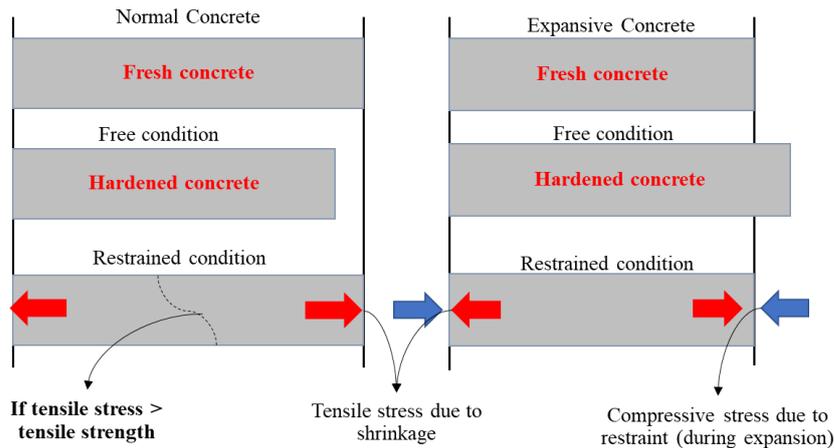
Figure 1.2 Mechanism of stress development in normal and expansive concrete

1.3 Aims and significance of this study

Nowadays, expansive concrete is considered an effective material for shrinkage cracking prevention or reducing shrinkage crack width. The expansion at an early stage controls the level of compensation of subsequently developed shrinkage stress in the expansive concrete.

In addition, fly ash is usually used in modern construction as cement replacement material to improve the performance of concrete, such as reducing the heat of hydration, which can cause thermal cracking. However, neither the ACI 223R-10 nor the JSCE design standard does not include the effect of cementitious replacement material on the level of expansion. Moreover, The ACI 223R-10 specifies the method for designing expansive concrete using expansive cement based on CaO and C-S-A agents with water curing.

It was discovered that various types of expansive additives had been used, particularly in Thailand, where a C-S-A expansive agent and a combination of ettringite and a C-S-A expansive agent were used. Additionally, several types of curing are frequently encountered, including moist and sealed curing. While the existing standards only focus on expansive concrete with water curing. With these constraints, existing standards do not encompass some circumstances encountered in the field, particularly in Thailand. The expansive concrete structures frequently incorporate fly ash as mineral admixtures and use different types of expansive additives and types of curing compared to existing standards. Therefore, it is necessary to conduct a field investigation of expansion and shrinkage strain behaviors by utilizing fly ash and different types of expansive additives and curing conditions.

The degree of restraint is one of the most critical factors affecting the level of expansion. Therefore, the existing expansive concrete design standards usually require a restrained expansion test. However, specimen dimensions and reinforcement ratios are limited for restrained expansion measurement in the standards, so they do not represent the actual condition of the expansive concrete structures. To increase the flexibility and versatility of the design and analysis process, finite element (FE) analysis is one of the efficient methods for estimating the strain level in reinforced expansive concrete structures. FE analysis in this study applies free expansion and shrinkage strain as input. However, there are two major behaviors to be considered for the restrained expansion mechanism that does not occur in the free expansion concrete. Some expansion losses can occur in restrained expansive concrete due to the effects of pores filling by expansive products and compression creep during the early expansion under restraint. Due to the loss of ability to generate expansion under restraint, the FE analysis using free expansion strain as input always overestimates the actual restrained expansion strain of the expansive concrete. An effective free strain is needed to determine the actual expansion level after compression creep occurs and a portion of expansive products have filled the pores.

This study proposes a method to estimate the restrained expansion strain of reinforced expansive concrete structures with and without fly ash, having different mix proportions, reinforcement ratios, and curing methods. This research consists of experimental works and finite element analysis. Experimental studies focus on expansive concrete properties such as free expansion, restrained expansion, and compressive strength. At the same time, the finite element analysis estimates the expansion level of expansive concrete restrained by internal and external restraint. Finally, the relationship between free and restrained expansion includes the effects of the amount of binder, amount of expansive additive, amount of fly ash, water to binder ratio, curing method, and curing temperature with various reinforcement ratios established.

1.4 Objectives of the study

Laboratory tests, field measurements, and FE analysis on the deformation during the hydration were investigated to fulfill the research gap. The performance of expansive concrete specimens was studied under different mix proportions, curing conditions, and restrained conditions. Field investigations were carried out on four different structures, i.e., slab on grade, slab on beam, slab on pile foundation, and water tank wall structures. Strain gauges are installed in several locations in each structure to study the effect of type and amount of expansive additive, the effect of internal and external restraint, and the effect of exposure environment on the level of expansion and shrinkage. FE analysis is used to estimate the expansion and shrinkage strain restraint for the prism specimens and expansive concrete structures. Based on the introduction and statement of problems, the main objectives of this research are as follows.

a. To evaluate the expansion rate of expansive concrete under free and restrained conditions with different mix proportions, curing methods, and reinforcement ratios.

b. To propose the reduction factor equations to generate effective free strain, which is used as input in FE analysis.

c. To estimate restrained expansion and shrinkage strain in prisms specimens and reinforced expansive concrete structures.

1.5 Outline of the dissertation

The purpose of this research is to propose a systematic and comprehensive method for estimating expansion and shrinkage strain for expansive concrete structures. This study is divided into two major sections: the experimental scale and the measurement of the actual structures. Generally, strain measurements are used to determine the expansion and shrinkage behavior of expansive concrete at both the experimental and actual structures. **Figure 1.3** shows the basic contents of each chapter and the progression of research from chapter 1 to chapter 5.

Chapter 1 describes the background of the research, problem statement, objectives, and significance. This chapter also discusses the mechanism of expansion strain in expansive concrete, allowing one to conclude that expansive additives are highly effective at preventing shrinkage cracking.

Chapter 2 focuses on experiments regarding the free expansion behavior of expansive concrete using prism specimens. This chapter addresses a number of parameters, such as the mix proportion (amount of binder, amount of fly ash, and amount of expansive additive) and curing condition (type of curing and curing temperature). The experiment in this chapter consists of measurements of free expansion strain and compressive strength. In chapter 3, the estimation method for restrained expansion strain is proposed based in part on the results of this test.

Chapter 3 describes the proposed method for estimating restrained expansion strain in expansive concrete using prism specimens. This experiment measured the restrained expansion strain with the same variation as in chapter 2 but with the addition of various reinforcement ratios. This chapter presents the reduction factor and effective free expansion strain equation used to estimate restrained expansion strain. Finite element (FE) analysis is performed as a tool to estimate restrained expansion strain. This chapter also uses the results from previous studies to verify the proposed method for estimating the restrained expansion strain.

Chapter 4 provided the proposed method for estimating restrained expansion and shrinkage strain in actual structures. In this chapter, direct field measurements of slabs on grade.

Slabs on beam. Slabs on pile and water tank walls were taken. Additionally, FE analysis is employed to study the expansion and shrinkage behavior of expansive concrete structures. In this proposed method, it is also possible to analyze the effectiveness of expansive concrete in preventing shrinkage, as well as the influence of internal and external restraints and the influence of the dimension of the structures on the expansion and shrinkage behavior of expansive concrete structures.

The results of chapters 2 through 4 are summarized in **chapter 5**, which clarifies the objectives and significance of this study. In addition, this chapter offers some suggestions for future research.
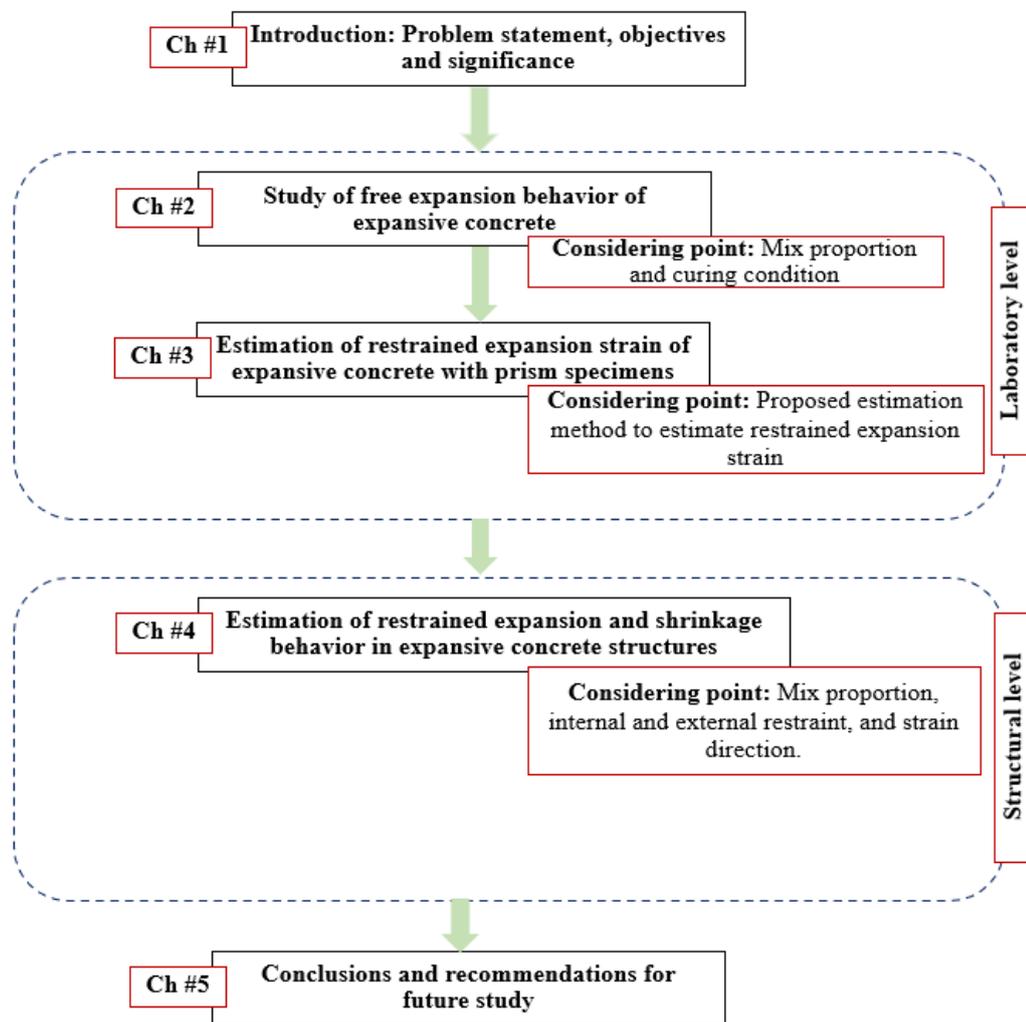
Figure 1.3 Research flow and organization of dissertation

References

[1]   M. Schneider, M. Romer, M. Tschudin, and H. Bolio, "Sustainable cement production-present and future," *Cem. Concr. Res.*, vol. 41, no. 7, pp. 642–650, 2011, doi: 10.1016/j.cemconres.2011.03.019.

[2]   M. S. Imbabi, C. Carrigan, and S. McKenna, "Trends and developments in green cement and concrete technology," *Int. J. Sustain. Built Environ.*, vol. 1, no. 2, pp. 194–216, 2012, doi: 10.1016/j.ijsbe.2013.05.001.

[3]   K. Huang, X. Shi, D. Zollinger, M. Mirsayar, A. Wang, and L. Mo, "Use of MgO

expansion agent to compensate concrete shrinkage in jointed reinforced concrete pavement under high-altitude environmental conditions," *Constr. Build. Mater.*, vol. 202, pp. 528–536, 2019, doi: 10.1016/j.conbuildmat.2019.01.041.

[4] J.-X. Zhang, H.-M. Lyu, S.-L. Shen, and D.-W. Hou, "Investigation of crack control of underground concrete structure with expansive additives," *J. Mater. Civ. Eng.*, vol. 33, no. 1, pp. 1–8, 2021, doi: 10.1061/(asce)mt.1943-5533.0003528.

[5] N. D. Van, E. Kuroiwa, J. Kim, H. Choi, and Y. Hama, "Influence of restrained condition on mechanical properties, frost resistance, and carbonation resistance of expansive concrete," *Materials (Basel).*, vol. 13, no. 2136, pp. 1–16, 2020.

[6] J. Zhang, K. Qi, and Y. Huang, "Calculation of moisture distribution in early-age concrete," *J. Eng. Mech.*, vol. 135, no. 8, pp. 871–880, 2009, doi: 10.1061/(asce)0733-9399(2009)135:8(871).

[7] Y. Gao, J. Zhang, and Y. Luosun, "Shrinkage stress in concrete under dry-wet cycles: An example with concrete column," *Mech. Time-Dependent Mater.*, vol. 18, no. 1, pp. 229–252, 2014, doi: 10.1007/s11043-013-9225-1.

[8] T. B. T. Nguyen, R. Chatchawan, W. Saengsoy, S. Tangtermsirikul, and T. Sugiyama, "Influences of different types of fly ash and confinement on performances of expansive mortars and concretes," *Constr. Build. Mater.*, vol. 209, pp. 176–186, 2019, doi: 10.1016/j.conbuildmat.2019.03.032.

[9] American Concrete Institute Committee, *ACI 223R-10 Guide for the use of shrinkage compensating concrete*. Farmington Hills: American Concrete Institute, 2010.

[10] Japan Society of Civil Engineers Committee, *JSCE No. 23: Recommended practice for expansive concrete*, no. 23. Tokyo: Concrete Library of JSCE, 1994.

[11] Japanese Standards Association, *JIS A 6202: Expansive additive for concrete*. Tokyo: Japanese Industrial Standard, 2017.

[12] H. Kabir and R. D. Hooton, "Evaluating soundness of concrete containing shrinkage-compensating MgO admixtures," *Constr. Build. Mater.*, vol. 253, pp. 1–11, 2020, doi: 10.1016/j.conbuildmat.2020.119141.

[13] V. C. Nguyen, X. S. Zhang, V. N. Nguyen, D. T. Phan, and G. Liu, "Experimental study on autogenous volume deformation of RCC mixed with MgO," in *IOP Conference Series: Materials Science and Engineering*, 2020, vol. 794, pp. 1–6. doi: 10.1088/1757-899X/794/1/012047.

[14] S. Nagataki and H. Gomi, "Expansive admixtures (mainly ettringite)," *Cem. Concr. Compos.*, vol. 20, no. 2–3, pp. 163–170, 1998, doi: 10.1016/s0958-9465(97)00064-4.

CHAPTER 2

STUDY ON FREE EXPANSION AND COMPRESSIVE STRENGTH

BEHAVIOR OF EXPANSIVE CONCRETE

2.1 Introduction

Expansive concrete is manufactured with expansive cement or expansive additives, which can increase its volume by generating large amounts of ettringite or calcium during the early stages of cement hydration. Recently, expansive concrete with expansive additives has been widely used in various civil construction in many countries, particularly in several Asian countries such as China, Japan, and Thailand. Concurrently with technological advancements, various expansive additives are continuously produced with high innovation and competitive low-cost production. Several studies on the type of expansive additive have also been discovered, including the use of calcium sulfoaluminate (C-S-A) [1]–[4], calcium oxide (CaO) [5]–[7], magnesium oxide (MgO) [8]–[10], ZY expansive agent [11], UAE expansive agent [12]–[14], and a combination of several types of expansive additive[15]–[18]. Each expansive agent has different characteristics and produces different expansive products depending on the hydration process, curing conditions, and calcining temperature [19]. For example, the expansive concrete with CaO and C-S-A based mainly experiences expansion at an early age during the curing period, while the expansive agent type MgO develops at a later age [18]–[23].

In addition to the type of expansive additive, several other factors also influence the expansion process of expansive concrete, including mix proportion, curing condition, restraint condition, and environmental exposure. The mix proportion is one of the most significant factors that affect the effectiveness of expansive concrete. Previous studies concluded that the amount of expansive additive is one of the most influential factors in the level of expansion on expansive concrete [6], [24]–[27]. Based on the research, it can be concluded that concrete expands due to the amount of expansive additive, concrete with a high amount of expansive additive produces a larger amount of expansive product. In addition, binder content also influences the performance of expansive concrete. Based on the results of previous studies, it can be concluded that the higher binder content in expansive concrete will produce a higher level of expansion [28].

In recent years, pozzolanic additives have been widely used in concrete construction to reduce cement consumption and use unutilized industrial wastes. Fly ash is a pozzolanic material that has conventionally used as a construction material. Moreover, fly ash has also been shown to influence the level of expansion in expansive concrete. This is because fly ash contains CaO, which can increase the volume of concrete during the hydration period [29]–[33]. In addition, the water to binder ratio also affects the level of expansion in expansive concrete. The high water to binder ratio produces a high degree of expansion. This is due to the water supply availability for the hydration process in expansive concrete, which assists the expansive agent in producing sufficient expansive product [34]–[36].

Curing conditions in expansive concrete has a significant effect on the expansion process. Despite using the same mix proportion, the results of expansive products will vary depending on the curing method. This is due to the fact that the expansion process of expansive concrete is highly dependent on the availability of water, moisture conditions, and temperature. Previous studies on the effect of the curing method on expansive concrete have also been

developed [4], [24], [37]–[39]. After the curing process is completed, the expansion of certain types of expansive additives begins to shrink. In addition, the investigation revealed that water curing always results in a higher degree of expansion than moist and sealed curing. This is because the specimens are submerged in water to maintain their moisture content during the curing process. The temperature during curing also influences the expansion rate [35], [40]–[42].

Due to the complexity of the design process for expansive concrete structures, it is necessary to conduct a more comprehensive experiment on the basic properties of expansive concrete. Subsequently, the results of this experiment will be used in the future design or analysis process for expansive concrete structures. Various design guidelines are available for expansive concrete, including ACI 223R-10 [43] for expansive cement and JSCE No. 23 and JIS A 6202 [44], [45] for expansive concrete containing expansive additives. However, the existing standards do not account for several factors, such as the effect of fly ash, the effect type of curing, and the effect of curing temperature. This study investigates the basic properties of expansive concrete by considering the mix proportion and curing conditions that influence the degree of expansion. Compressive strength and free expansion measurements were conducted in this study. The expansive agent is a blend of ettringite (CaO) and calcium sulfoaluminate (C-S-A).

2.2 Experimental program

2.2.1   General information

In this study, the laboratory test focuses on measuring the length change under free conditions with prism specimens and the unconfined compressive strength of expansive concrete. The objective of this experiment is to collect the data and investigate the variables that influence the degree of expansion on expansive concrete. Moreover, this experiment aims to identify a relationship between free expansion and compressive strength in expansive concrete. The results of this test will be used as input for the FE analysis in Chapter 3. Four series with different compositions are used in this study, as shown in **Table 2.1**. The first series investigates the effect of expansive additive dosage and curing conditions. Similar parameters are used for series II and III, but a different amount of binder is used. Thus, the effect of the amount of binder can be investigated by comparing the results of series I to series III. While series IV focuses on the effect of curing temperature with two different types of curing. The curing temperature used in series I to III is 28 °C, while in series IV, the curing temperature is 28 °C, 35 °C, and 40 °C.

Table 2.1 Specimen variations for each series

Variations Component	Series I	Series II	Series III	Series IV
Amount of Binder (kg/m^3)	280	340	380	280; 380
Amount of EA (kg/m^3)	0; 20; 30; 40	0; 20; 30; 40	0; 20; 30; 40	20; 30
Type of EA	C-S-A + CaO	C-S-A + CaO	C-S-A + CaO	C-S-A + CaO
Amount of FA (%)	20	20	20	20
Water to Binder Ratio	0.66	0.51	0.47	0.66; 0.47
Curing Condition	Moist; Sealed	Moist; Sealed	Moist; Sealed	Moist; Sealed
Curing Period (Days)	3	3	3	3
Curing Temperature (ºC)	28	28	28	28; 35; 40

2.2.2 Materials and mix proportions

The concrete constituent materials used in this study consisted of a binder, fine aggregate, coarse aggregate, water, and superplasticizer. The binders used in this experiment consist of Ordinary Portland Cement (OPC), Fly Ash (FA), and Expansive Additive (EA). OPC is manufactured by Siam Cement Group Co., Ltd, Thailand, cement type 1 based on ASTM C150 [46]. Fly ash class 2b according to TIS 2135 [47] or class C according to ASTM C618 [48] were used in this study from the Mae Moh power plant. Meanwhile, the expansive additive used is a blended ettringite and calcium sulfoaluminate (CaO + C-S-A) based expansive agent. The major chemical composition of binders, including expansive additives, can be seen in **Table 2.2**.

Table 2.2 Chemical composition of binders (Portland cement, fly ash, and expansive additive)

Binder	SiO_2	Al_2O_3	Fe_2O_3	CaO	MgO	SO_3	K_2O	Na_2O
OPC	18.98	5.33	3.16	65.34	1.15	2.65	0.21	0.16
FA	36.18	20.21	13.89	18.74	2.69	3.74	2.24	1.14
EA	2.12	4.75	0.14	61.09	0.73	26.46	-	-

Table 2.3 provides the tested mix proportions of concrete in all series. In this experiment, the total binder content varied from 280 kg/m³ (series I), 340 kg/m³ (series II), and 380 kg/m³ (series III). The replacement percentages of fly ash were up to 20% of the weight of the total binder, while the amounts of expansive additive were between 0 kg/m³ to 40 kg/m³. Water to binder ratios varied between 0.47 to 0.66 depending on the slump value target. To investigate the effects of curing temperature on the level of expansion strain in unrestrained conditions, mixtures in series IV were used by varying the curing temperature. In series IV, each specimen was exposed to curing temperatures of 28 °C, 30 °C, and 35 °C. The standard curing temperature for series other than series IV is 28 °C.

Table 2.3 Mix proportions of the tested concrete

Series	Symbol	w/b	Binders (kg/m³)			Water (kg/m³)	Aggregate (kg/m³)		Admixture (g/m³)	
			OPC	FA	EA		Fine	Coarse	Type D	Type F
Series I	EA0B280	0.66	226	54	0	185	827	1073	784	560
	EA20B280		206	54	20					
	EA30B280		196	54	30					
	EA40B280		186	54	40					
Series II	EA0B340	0.51	288	52	0	175	816	1060	680	2040
	EA20B340		268	52	20					
	EA30B340		258	52	30					
	EA40B340		248	52	40					
Series III	EA0B380	0.47	322	58	0	180	795	1032	760	1330
	EA20B380		302	58	20					
	EA30B380		292	58	30					
	EA40B380		282	58	40					
Series IV	EA30B280	0.66	206	54	20	185	827	1073	784	560
	EA20B380	0.47	302	58	20	180	795	1032	760	1330
	EA30B380		292	58	30					

In addition, sand from the natural aggregate was used as the fine aggregate, whereas crushed limestone was used as the coarse aggregate. Gradations of the fine and coarse

aggregates were tested as per ASTM C33 [49]. Crushed limestone with a maximum size of 19 mm was used as the coarse aggregate. The properties of aggregates are given in **Table 2.4**. Chemical admixtures were added to control the initial slump within a range of 15 ± 2 cm. A type D (water-reducing and retarding) and a type F (high-range water-reducing) admixtures were added to adjust the initial slump at constant water to binder ratio. The specifications for the types of admixtures are explained in ASTM C494 [50].

Table 2.4 Properties of fine and coarse aggregates

Properties	Fine aggregate	Coarse aggregate
Absorption (%)	1.08	0.34
Specific gravity (SSD)	2.60	2.83
s/a at minimum void (by volume)	0.44	
Minimum void (%)	23.52	

2.2.3 Test methods

The experiment in this study consisted of two main parts, including length change measurement in unrestrained conditions and the unconfined compressive strength of concrete. Length change measurement in free condition was conducted based on ASTM C157 [51] using prisms specimens with sizes of 75 × 75 × 285 mm3 (see **Figure 2.1**). The specimens were demolded 8 hours after casting (final setting time), and the initial length was measured. In this study, free expansions and FE analysis measurement started at 8 hours of age. All specimens in this study were demolded 8 hours after casting (final setting time), and the initial length was measured. Aside from measuring length changes, the compressive strength of $100 \times 100 \times 100$ mm^3 concrete cubic specimens was measured in an unconfined condition. Compressive strength test results were used as the input data for the material properties in the FE analysis. Compressive strength tests conforming to ASTM C39 [52] were conducted on specimens aged 3, 7, and 28.
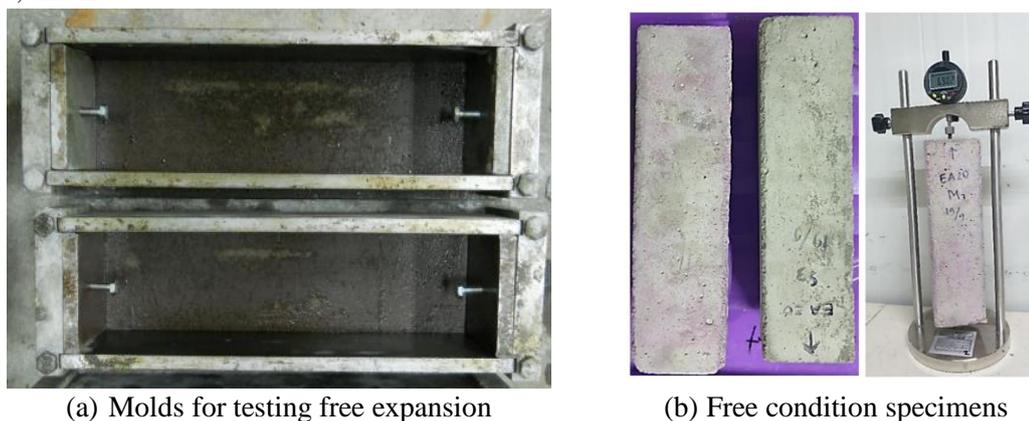
(a) Molds for testing free expansion   (b) Free condition specimens
Figure 2.1 Mold and specimens for length change measurement in free condition

Two types of curing conditions applied in this study are moist curing and sealed curing with 3 days for series I to IV. Wet clothes were applied to the concrete surfaces during the curing process to provide moist curing, while sealed curing applied plastic wraps to all surfaces of the specimens. It should be noted that from the observation during the tests, expansion increased until 3 days of curing age and was almost constant regardless of the curing methods. Therefore, the expansion strains of the specimens were measured for up to 3 days, and the expansion at 3 days was considered the maximum expansion. During the measurement process,

the specimens were placed in a control room with a relative humidity of 70 ± 5% and a temperature of 28 °C. However, for the measurement in series IV, the curing temperature varies from 28 °C, 35 °C, and 40 °C for moist and sealed curing.

2.3 Results and discussion

This study discusses the results of compressive strength and free expansion strain using prism specimens for expansive concrete. The experiment in this study measured the compressive strength at ages 3, 7, and 28 days. Meanwhile, measurement of free expansion strain on prism specimens was carried out during the curing period. The result of this study discusses the main factors that influence the level of expansion in expansive concrete, including the amount of expansive additive, binder dosage, curing method, and curing temperature.

2.3.1 Influence of amount of expansive additive

Compressive strength test was carried out on unconfined specimens in all series I-VI at 3, 7, and 28 days of the specimen age. The test results for each mixture proportion are the average of three samples. **Figure 2.2** shows the compressive strength results for specimens with amount of binder of 280 kg/m^3 (series I), **Figure 2.3** shows the compressive strength results for amount of binder of 340 kg/m^3 (series II), and **Figure 2.4** shows the compressive strength results for the amount of binder of 380 kg/m^3 (series III). Each series varies the amount of expansive additive by 0, 20, 30, and 40 kg/m^3 so that the effect of expansive additive on the compressive strength of concrete can be observed.

(a) Series I – Moist curing   (b) Series I – Sealed curing
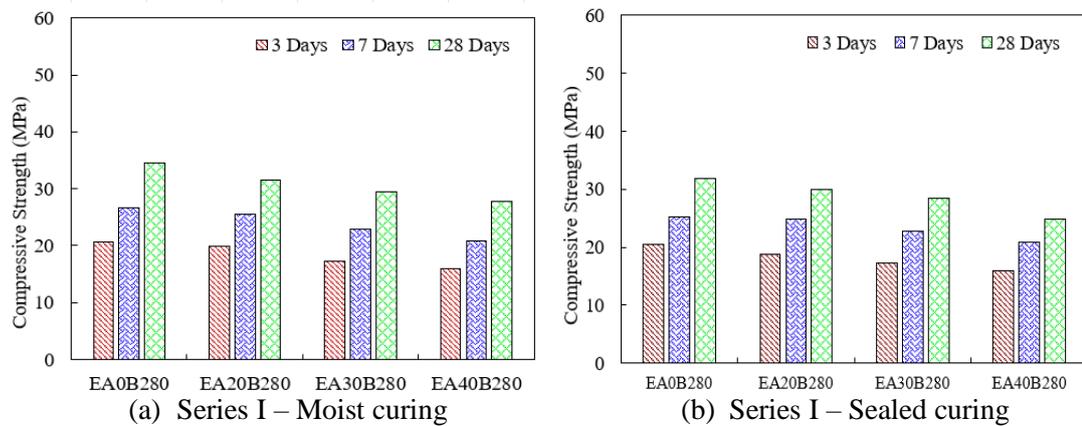
Figure 2.2 Compressive strength with amount of binder 280 kg/m^3 (Series I)

(a) Series II – Moist curing   (b) Series II – Sealed curing
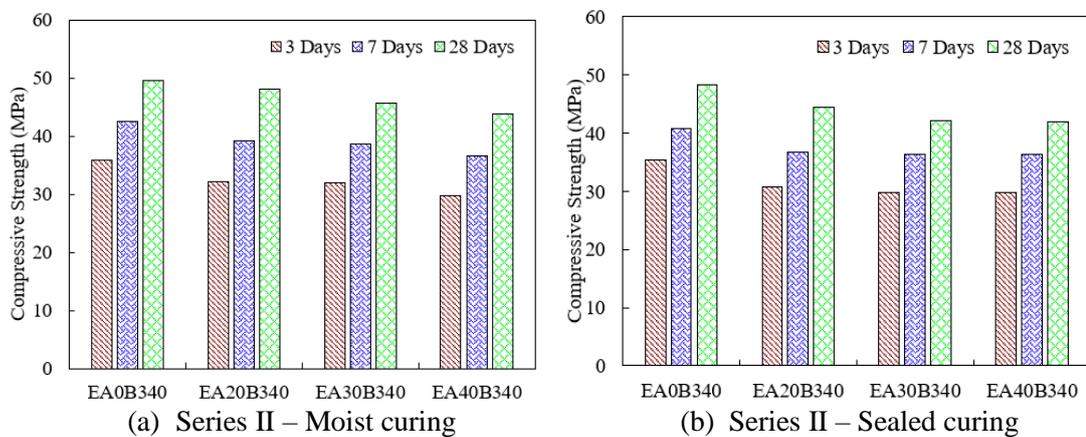
Figure 2.3 Compressive strength with amount of binder 340 kg/m^3 (Series II)

(a) Series III – Moist curing   (b) Series III – Sealed curing

Figure 2.4 Compressive strength with amount of binder 380 kg/m³ (Series III)
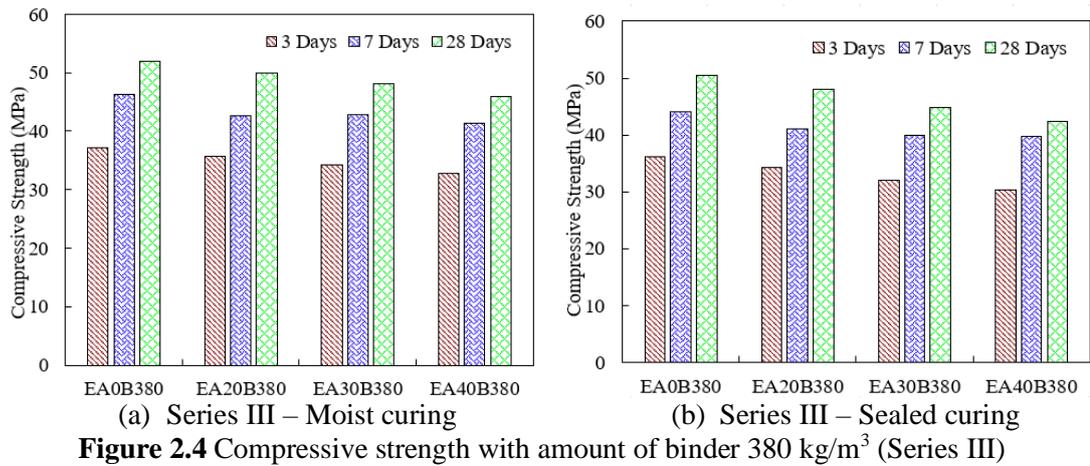
This research employs two types of curing: moist and sealed. For series I to III, the curing temperature and relative humidity are 28 °C and 70 ± 5%, respectively. The test results indicate that the compressive strength has increased with age due to the influence of cement hydration and increased stiffness. In series I to III, it is demonstrated that the compressive strength decreases as the amount of expansive additives increases, both at an early age and when the specimens are 28 days. Several factors contribute to the decrease in the compressive strength of concrete caused by expansive additives, including the formation of micro-cracks due to large expansion. Moreover, the addition of the expansive additive results in a reduction in the amount of cement used. This decrease in cement dosage results in a decrease in compressive strength.

(a) Moist Curing   (b) Sealed curing

Figure 2.5 Compressive strength comparison of normal and expansive concrete
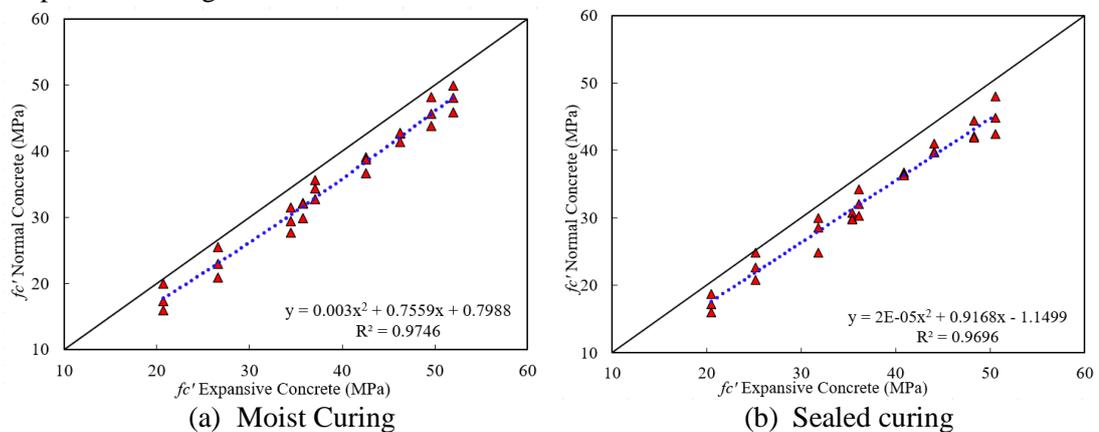
Figure 2.5 compares the compressive strength results of normal and expansive concrete with different curing types. The results of this test indicate that the compressive strength of expansive concrete is always lower than the compressive strength of normal concrete. Therefore, the use of expansive additives is also the result of considering the quality of the concrete. When utilizing large amounts of expansive additives, compressive strength can experience a significant decrease. Based on JSCE No. 23, it is recommended to use an expansive additive of no more than 30 kg/m³ as a cementitious material for CaO and C-S-A-based expansive additives. It should be noted that the compressive strength test of this concrete was carried out on unconfined specimens. For the compressive strength behavior of confined concrete, further research is required. Due to the effect of expansion products filling pores in

concrete during the expansion process under restrained conditions, confinement in concrete is likely to affect the compressive strength of expansive concrete.

This study also investigated the free expansion strain of normal and expansive concrete with varying amounts of binder, expansive additive, and curing conditions. The free expansion strain measurement results calculate the effective free strain and estimate the restrained expansion strain. **Figure 2.6** shows the result of the free expansion strain for series I (280 kg/m^3 of binder content). **Figure 2.7** shows the result of the free expansion strain for series II (340 kg/m^3 binder content). **Figure 2.8** shows the free expansion strain results for series III (380 kg/m^3 of binder content). The measurement of free expansion strain was carried out during the curing period, which is 3 days.

(a) Series I – Moist curing   (b) Series I – Sealed curing
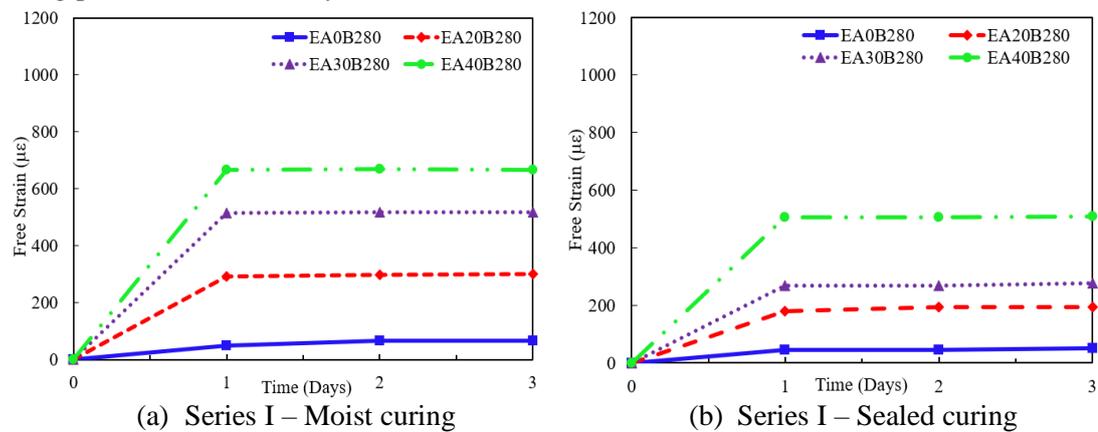
Figure 2.6 Free expansion strain with the amount of binder 280 kg/m^3 (Series I)

The results of the free expansion strain in series I to series III (**Figure 2.6** to **Figure 2.8**) show that the free expansion strains increased significantly on the first day after the final setting time and became nearly constant until the curing periods were completed. This indicates that the reaction rate of the expansive additive is very fast on the CaO + C-S-A-based expansive agent. The behavior of the expansive agent also affects the duration and rate of expansion of the expansive concrete. The expansion behavior resembles the pattern in both moist and sealed curing samples. In both moist and sealed curing, the free expansion strain investigation results indicate that as the amount of expansive additives increases, so does the level of expansion. This is because the high amount of expansive agent produced a high amount of expansive product in concrete.

(a) Series II – Moist curing   (b) Series II – Sealed curing
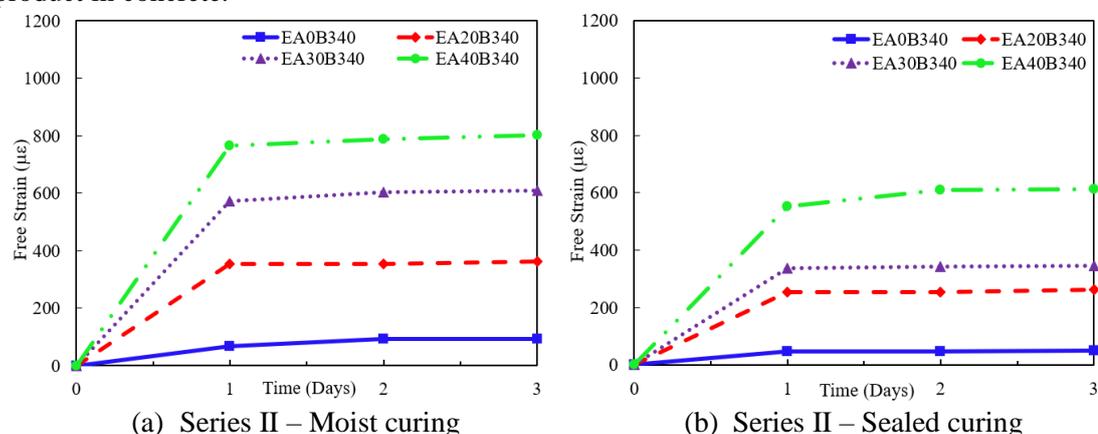
Figure 2.7 Free expansion strain with the amount of binder 340 kg/m^3 (Series II)
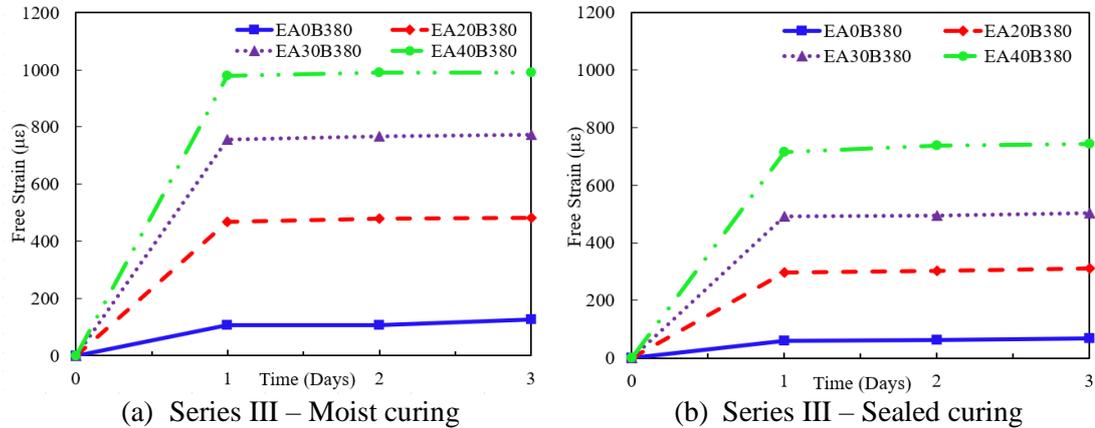
(a) Series III – Moist curing   (b) Series III – Sealed curing
Figure 2.8 Free expansion strain with the amount of binder 380 kg/m^3 (Series III)

2.3.2   Influence of amount of binder

The amount of binder significantly impacts the compressive strength of concrete, as shown in **Figure 2.9**. **Figure 2.9** shows compressive strength results at an early age and 28 days for expansive concrete with the same amount of expansive additive but different binder dosages. The compressive strength test results at an early age and 28 days of age indicated that the compressive strength increased as the amount of binder increased. Cement content in concrete is proportional to the amount of binder used, but the amount of expansive agent used remains constant. This increase in the amount of cement causes an increase in the bonding strength. Consequently, the compressive strength of concrete increases as the amount of binder increases. This increase in compressive strength occurs both in moist and sealed curing. This shows the beneficial aspect of the compressive strength due to the high binder content. However, using a binder composed of the main ingredient in the form of cement must also be considered from an economical and efficient point of view. The cost of producing concrete will rise due to the extensive use of cement. The effect of the amount of binder on expansive concrete must therefore be investigated thoroughly and appropriately.
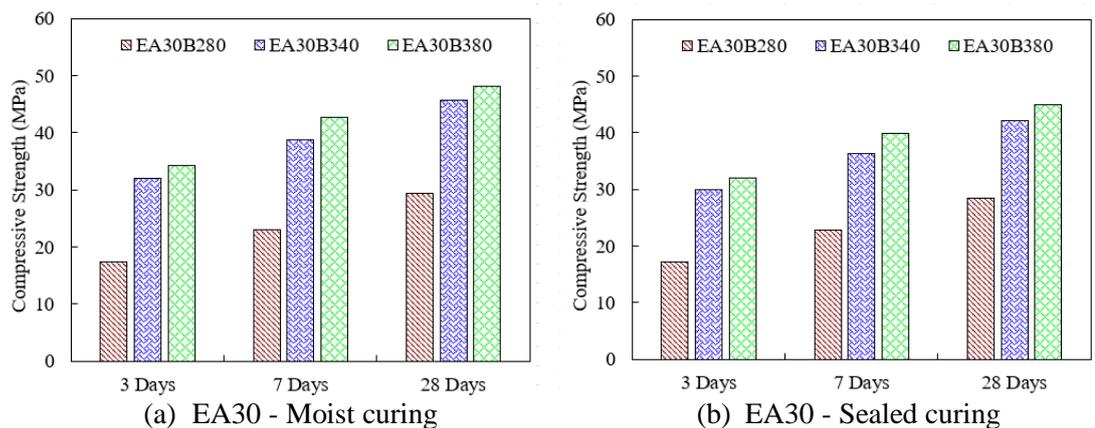
(a) EA30 - Moist curing   (b) EA30 - Sealed curing
Figure 2.9 Compressive strength with different binder dosages

The relationship between the amount of binder and the maximum free expansion strain can be seen in **Figure 2.10**. The test results indicate that, despite using the same amount of expansive agent, the free expansion strain is produced differently depending on the binder dosage. As the amount of binder used increases, so does the degree of expansion. The expansion strain primarily occurs in the paste, whose volume increases as the amount of binder increases.

This increase in paste volume increases the probability that the resulting expansive product will be sufficient and optimal. In addition, with high amount of binder cause the water to binder ratio become lower, indicate that expansive concrete with high amount of binder were using lower water to binder ratio. This indicate that with low w/b cause faster hydration process cause the degree of expansion also increase during the early age.

(a) Moist curing (b) Sealed curing
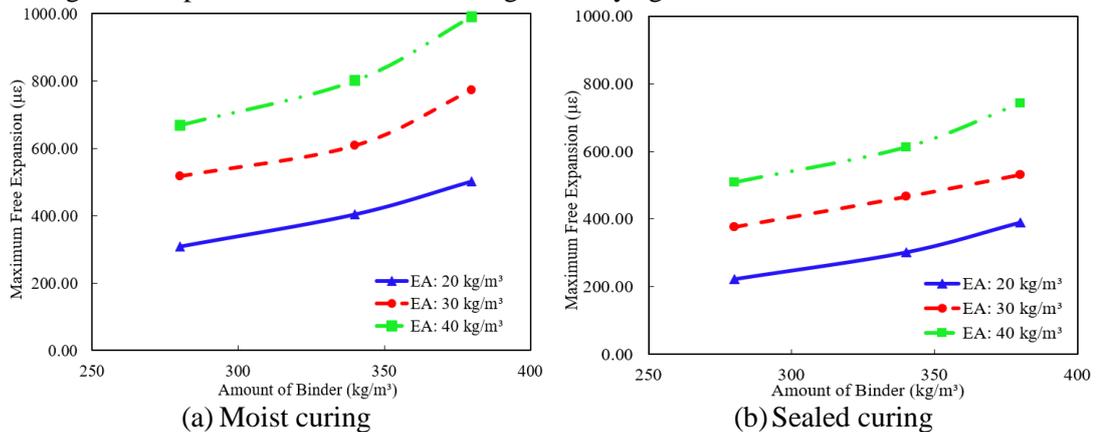
Figure 2.10 Maximum free expansion strains with different amount of binder

2.3.3 Influence of type of curing

Figure 2.11 shows the compressive strength comparison between moist and sealed curing with the same curing temperature and curing periods. To prevent the evaporation and drying of the concrete, specimens undergoing moist curing were wrapped with wet clothes and then wrapped with plastic. While in sealed curing, specimens are only coated with plastic to prevent concrete from evaporating during the hydration process. **Figure 2.11** shows that the compressive strength of concrete with moist curing is higher than that of specimens with sealed curing. However, the difference in compressive strength between the two-curing technique is insignificant. During the hydration process, the inner temperature of concrete rises relative to its exterior, and this temperature difference can result in moisture loss and evaporation. However, the appearance of wet cloth in moist curing causes the surface of the concrete to remain constantly moist, and the concrete absorbs the water in the wet cloth, aiding the hydration process and decreasing the chances of moisture loss and evaporation. Meanwhile, in sealed curing, plastic wrap only serves to help reduce evaporation during the hydration process. Therefore, concrete with moist curing produces a higher compressive strength than sealed curing.
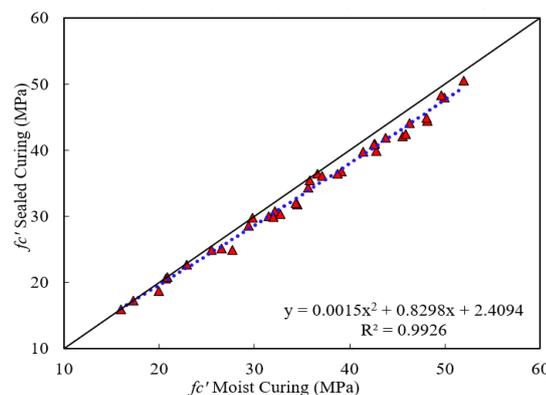
Figure 2.11 Concrete compressive strength comparison of moist and sealed curing

Two different curing types during the 3 days curing periods were applied to investigate the effects of the curing types on the measured free expansion strains. Maximum expansion strain indicates that expansive concrete with moist curing has a larger free expansion strain than expansive concrete with sealed curing, as shown in **Figure 2.12**. The main purpose of using moist curing is to provide moisture to specimens by applying wet clothes on the surface, while sealed curing prevents moisture loss from the specimens. As water is necessary for the reaction of the expansive agent, expansive concrete usually is sensitive to curing conditions. By maintaining the moisture during the hydration process, moist curing results in a more expansive product than sealed curing. Therefore, moist curing results in larger expansion than specimens of sealed concrete. Moist curing more effective methods to supply water to the mixtures will produce larger expansion. From the experimental results in series I, II, and III, it can be concluded that the amount of expansive additive, amount of binder, and curing types significantly affect the free expansion strain.
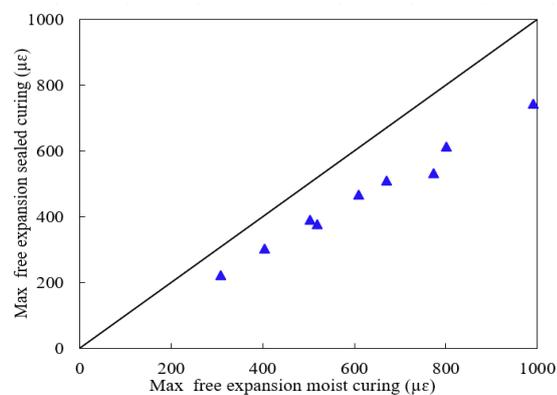
Figure 2.12 Maximum free expansion comparison of moist and sealed curing

2.3.4 Influence of curing temperature

Figure 2.13 shows the compressive strength of expansive concrete cured under various conditions. This compressive strength test subjected specimens to 28 °C, 35 °C, and 40 °C curing temperatures. Each result in **Figure 2.13** shows that the compressive strength increases as the curing temperature increases. Due to the high curing temperature, the temperature outside of the concrete is comparable to the temperature inside. The temperature naturally accelerates the hydration process in concrete, causing it to harden more rapidly. As a result of the rapid hardening process, concrete with a higher curing temperature attains a higher compressive strength and a faster increase in strength. The effect of curing temperature on the free expansion strain of expansive concrete with different curing conditions is shown in **Figure 2.14**.

The study in series IV uses 3 variations of curing temperature, namely 28 °C, 35 °C, and 40 °C. The results show that the free expansion strain of expansive concrete is affected by curing temperature. Due to the higher curing temperature, both moist and sealed curing resulted in increased expansion. When the curing temperature is high, the reaction of the expansive additive is accelerated, which causes the expansive product to be produced at an earlier age. In addition, the stiffness of the paste at an early age is not too high since the concrete is still weak and not fully hardened, thus causing the expansive product to expand more efficiently and produce a higher level of expansion. It should be noted that the specimens in this study were demolded and cured at temperatures of 28°C, 35°C, 40°C, and RH 70±5%, which covers the ranges of temperature and RH in Thailand. However, some standards regarding expansive

concrete may use different curing standards and relative humidity, this depends on the environmental conditions in each country. This difference in curing conditions also affects the level of free expansion. As a result of the high curing temperature and different curing conditions used in this study, the hydration and expansion rates are faster during an early age.

(a) EA30B380 – Moist curing　　　　　　(b) EA30B380 – Sealed curing
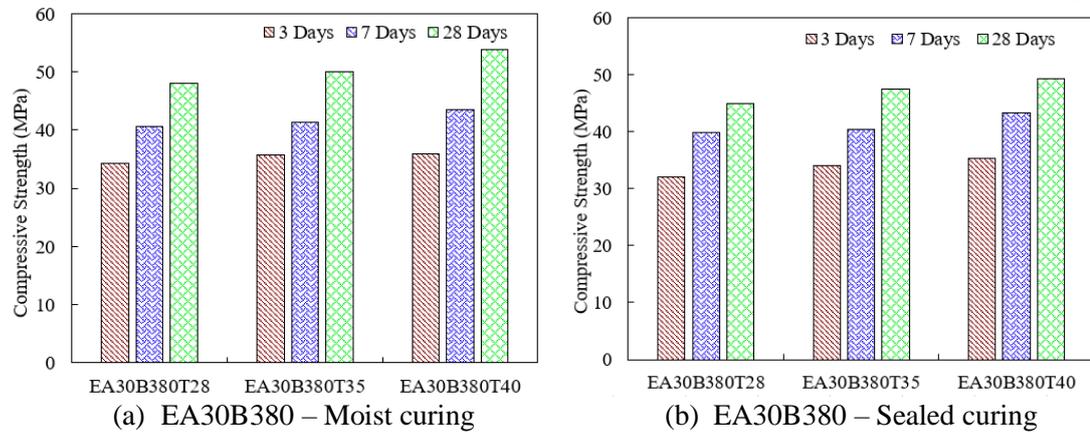
Figure 2.13 Compressive strength with different curing temperatures (Series IV)

(a) EA30B380 – Moist curing　　　　　　(b) EA30B380 – Sealed curing
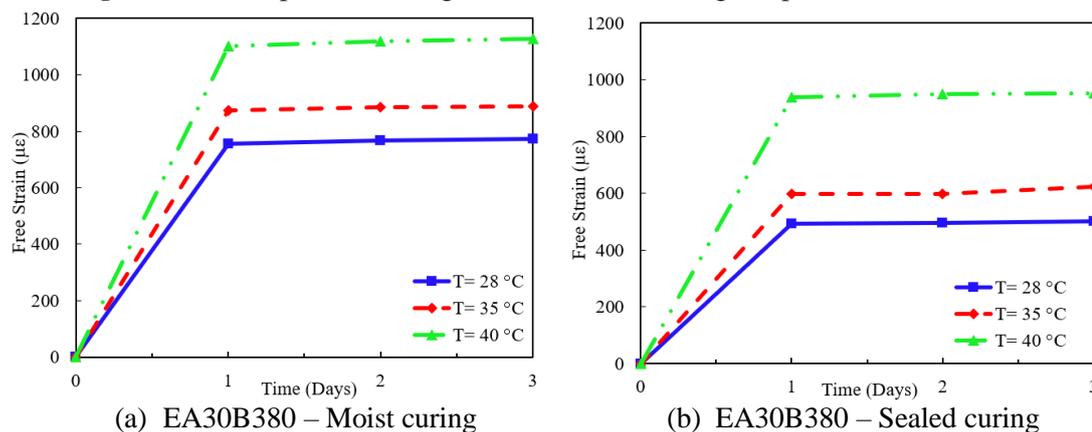
Figure 2.14 Free expansion of concrete with different temperatures (series IV)

2.3.5   Correlation between concrete strength and free expansion strain

The main purpose of using an expansive additive is to compensate for subsequent restrained shrinkage tensile strain, which causes shrinkage cracking. A high expansion rate is more effective for shrinkage crack control. However, a high expansion rate can cause an excessive decrease in the compressive strength of the expansive concrete. On the other hand, too low of the expansion rate is insufficient to compensate for the subsequent shrinkage. Therefore, both effectiveness in controlling shrinkage cracking and possible sacrifice of compressive strength must be considered together in designing a proper expansion rate and so expansive additive content for the expansive concrete. Since the test results on compressive strength reported in the previous section indicated that compressive strength gradually decreases when the amount of expansive additive increases. Therefore, one of the concerns when determining the required amount of expansive additive is the simultaneous consideration of compressive strength with the expansion. The relationships between the strength of concrete and the level of expansion under moist and sealed curing obtained in this study are presented in **Figure 2.15**. A higher amount of expansive additive demonstrates a higher level of expansion in both curing conditions. It can be seen from **Figure 2.15** that the strength of the expansive

concrete slightly decreases when the level of expansion, indicated by maximum free expansion in the figure, increases for all tested binder contents and curing conditions.

(a) Moist curing (b) Sealed curing
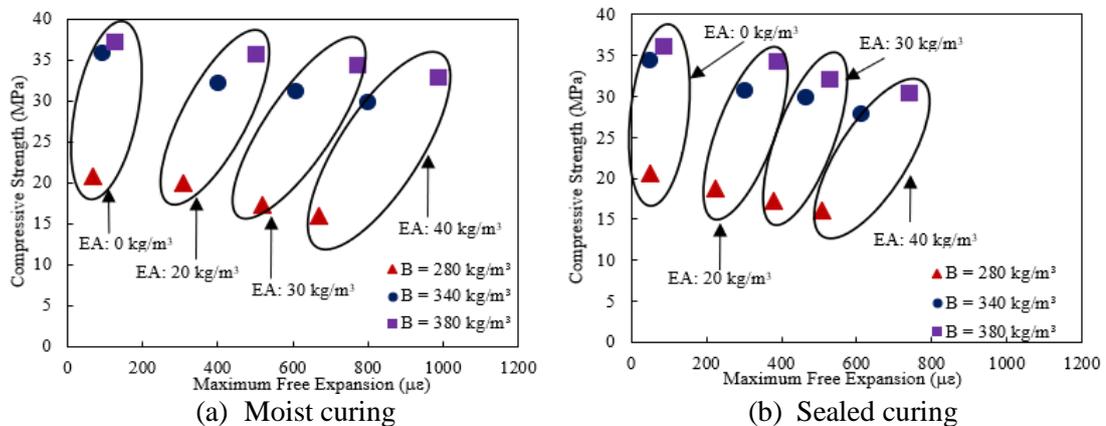
Figure 2.15 Relationship between compressive strength and maximum free expansion

2.4 Conclusions

This study can draw several conclusions based on the compressive strength and free expansion strain of expansive concrete specimens.

a) The amount of expansive additive significantly affects the degree of concrete expansion. A high amount of expansive additive used produces a higher free expansion strain. However, high amounts of expansive additives used in expansive concrete cause the compressive strength to decrease. The formation of microcracks causes a decrease in compressive strength in the concrete due to large expansion.

b) Utilizing a large amount of binder increases the free expansion strain and compressive strength. This is because expansion occurs predominantly in the paste region, causing significant product expansion in specimens with high binder dosages.

c) Moist curing of expansive concrete results in higher free expansion and compressive strength than concrete with sealed curing.

d) The curing temperature significantly influences the compressive strength and free expansion strain of expansive concrete. The compressive strength and free expansion strain also increased with increasing curing temperature.

References

[1]   T. Kim, K. Y. Seo, C. Kang, and T. K. Lee, "Development of eco-friendly cement using a calcium sulfoaluminate expansive agent blended with slag and silica fume," *Appl. Sci.*, vol. 11, no. 1, pp. 1–24, 2021, doi: 10.3390/app11010394.

[2]   C. Li, P. Shang, F. Li, M. Feng, and S. Zhao, "Shrinkage and mechanical properties of self-compacting SFRC with calcium-sulfoaluminate expansive agent," *Materials (Basel).*, vol. 13, no. 3, pp. 1–14, 2020, doi: 10.3390/ma13030588.

[3]   D. Sirtoli, M. Wyrzykowski, P. Riva, and P. Lura, "Autogenous and drying shrinkage of mortars based on portland and calcium sulfoaluminate cements," *Mater. Struct.*, vol. 53, no. 5, pp. 1–14, 2020, doi: 10.1617/s11527-020-01561-1.

[4]   P. Carballosa, J. L. G. Calvo, and D. Revuelta, "Influence of expansive calcium sulfoaluminate agent dosage on properties and microstructure of expansive self-compacting concretes," *Cem. Concr. Compos.*, vol. 107, no. 103464, pp. 1–12, 2020, doi: 10.1016/j.cemconcomp.2019.103464.

[5]   H. Zhao *et al.*, "Mechanical properties and autogenous deformation behavior of early-

age concrete containing pre-wetted ceramsite and CaO-based expansive agent," *Constr. Build. Mater.*, vol. 267, pp. 1–9, 2021, doi: 10.1016/j.conbuildmat.2020.120992.

[6] H. Zhao *et al.*, "Effects of pre-soaked zeolite and CaO-based expansive agent on mechanical properties and autogenous deformation of early-age concrete," *Constr. Build. Mater.*, vol. 261, no. 120370, pp. 1–11, 2020, doi: 10.1016/j.conbuildmat.2020.120370.

[7] P. Shen *et al.*, "Investigation on expansion effect of the expansive agents in ultra-high performance concrete," *Cem. Concr. Compos.*, vol. 105, pp. 1–13, 2020, doi: 10.1016/j.cemconcomp.2019.103425.

[8] V. C. Nguyen, X. S. Zhang, V. N. Nguyen, D. T. Phan, and G. Liu, "Experimental study on autogenous volume deformation of RCC mixed with MgO," in *IOP Conference Series: Materials Science and Engineering*, 2020, vol. 794, pp. 1–6. doi: 10.1088/1757-899X/794/1/012047.

[9] H. Kabir and R. D. Hooton, "Evaluating soundness of concrete containing shrinkage-compensating MgO admixtures," *Constr. Build. Mater.*, vol. 253, pp. 1–11, 2020, doi: 10.1016/j.conbuildmat.2020.119141.

[10] F. Jiang, M. Deng, L. Mo, and W. Wu, "Effects of MgO expansive agent and steel fiber on crack resistance of a bridge deck," *Materials (Basel).*, vol. 13, no. 14, pp. 1–16, 2020, doi: 10.3390/ma13143074.

[11] M. Miao, Q. Liu, J. Zhou, and J. Feng, "Effects of expansive agents on the early hydration kinetics of cementitious binders," *Materials (Basel).*, vol. 12, no. 12, 2019, doi: 10.3390/ma12121900.

[12] W. Sun, H. Chen, X. Luo, and H. Qian, "The effect of hybrid fibers and expansive agent on the shrinkage and permeability of high-performance concrete," *Cem. Concr. Res.*, vol. 31, no. 4, pp. 595–601, 2001, doi: 10.1016/S0008-8846(00)00479-8.

[13] J. Guo, S. Zhang, T. Guo, and P. Zhang, "Effects of UEA and MgO expansive agents on fracture properties of concrete," *Constr. Build. Mater.*, vol. 263, p. 120245, 2020, doi: 10.1016/j.conbuildmat.2020.120245.

[14] J. Guo, T. Guo, S. Zhang, and Y. Lu, "Experimental study on freezing and thawing cycles of shrinkage-compensating concrete with double expansive agents," *Materials (Basel).*, vol. 13, no. 8, 2020, doi: 10.3390/MA13081850.

[15] H. Li, Y. Wang, Y. Wang, J. Liu, and Q. Tian, "Effect of CaO and MgO based expansive agent on deformation and mechanical properties of concrete-filled steel tubes," *Constr. Build. Mater.*, vol. 250, p. 118723, 2020, doi: 10.1016/j.conbuildmat.2020.118723.

[16] L. Coppola *et al.*, "The combined use of admixtures for shrinkage reduction in one-part alkali activated slag-based mortars and pastes," *Constr. Build. Mater.*, vol. 248, no. 118682, pp. 1–8, 2020, doi: 10.1016/j.conbuildmat.2020.118682.

[17] H. Zhao *et al.*, "Effects of CaO-based and MgO-based expansion agent, curing temperature and restraint degree on pore structure of early-age mortar," *Constr. Build. Mater.*, vol. 257, pp. 1–14, 2020, doi: 10.1016/j.conbuildmat.2020.119572.

[18] J. Guo, S. Zhang, C. Qi, L. Cheng, and L. Yang, "Effect of calcium sulfoaluminate and MgO expansive agent on the mechanical strength and crack resistance of concrete," *Constr. Build. Mater.*, vol. 299, no. 123833, pp. 1–10, 2021, doi: 10.1016/j.conbuildmat.2021.123833.

[19] A. Mahmood, A. B. M. A. Kaish, N. F. B. A. Gulam, S. N. Raman, M. Jamil, and R. Hamid, "Effects of MgO-based expansive agent on the characteristics of expansive concrete," *Eng. Proc.*, vol. 11, no. 14, pp. 1–6, 2021, doi: 10.3390/asec2021-11165.

[20] J. B. Liyanage and R. P. Gamage, "The hydration and volume expansion mechanisms of modified expansive cements for sustainable in-situ rock fragmentation: A review," *Energies*, vol. 14, no. 5965, pp. 1–26, 2021, doi: 10.3390/en14185965.

[21] L. Wang *et al.*, "Influence of reactivity and dosage of MgO expansive agent on

shrinkage and crack resistance of face slab concrete," *Cem. Concr. Compos.*, vol. 126, no. 104333, pp. 1–13, 2022, doi: 10.1016/j.cemconcomp.2021.104333.

[22] F. Cao, M. Miao, and P. Yan, "Hydration characteristics and expansive mechanism of MgO expansive agents," *Constr. Build. Mater.*, vol. 183, pp. 234–242, 2018, doi: 10.1016/j.conbuildmat.2018.06.164.

[23] J. Han, D. Jia, and P. Yan, "Understanding the shrinkage compensating ability of type K expansive agent in concrete," *Constr. Build. Mater.*, vol. 116, pp. 36–44, 2016, doi: 10.1016/j.conbuildmat.2016.04.092.

[24] Q. Cao, Q. Gao, R. Wang, and Z. Lin, "Effect of fibers and expansive agent on shrinkage of self-consolidating concrete under two curing schemes," *J. Mater. Civ. Eng.*, vol. 31, no. 9, pp. 1–9, 2019, doi: 10.1061/(asce)mt.1943-5533.0002761.

[25] V. Corinaldesi, A. Nardinocchi, and J. Donnini, "The influence of expansive agent on the performance of fibre reinforced cement-based composites," *Constr. Build. Mater.*, vol. 91, pp. 171–179, 2015, doi: 10.1016/j.conbuildmat.2015.05.002.

[26] Q. Xia, H. Li, A. Lu, Q. Tian, and J. Liu, "Damage analysis of concrete members containing expansive agent by mechanical and acoustic methods," *Eng. Fail. Anal.*, vol. 74, pp. 95–106, 2017, doi: 10.1016/j.engfailanal.2016.12.020.

[27] S. Z. Zhang, Q. Tian, and A. Q. Lu, "Influence of CaO-based expansive agent on the deformation behavior of high performance concrete," *Appl. Mech. Mater.*, vol. 438–439, pp. 113–116, 2013, doi: 10.4028/www.scientific.net/AMM.438-439.113.

[28] R. Dumaru, *Performance of expansive concrete under the influence of mix proportions, restraining conditions and curing conditions*. Bangkok: Sirindhorn International Institute of Technology, Thammasat University, 2021.

[29] D. T. Nguyen, R. Sahamitmongkol, and S. Tangtermsirikul, "Prediction of net expansion of expansive concrete under restraint," *Res. Dev. J.*, vol. 21, no. 3, pp. 75–84, 2010.

[30] P. Sutthiwaree, R. Sahamitmongkol, and S. Tangtermsirikul, "Effect of internal curing on expansion and shrinkage of expansive concrete," *Thammasat Int. J. Sci. Technol.*, vol. 20, no. 4, pp. 46–55, 2015.

[31] G. Peiwei, L. Xiaolin, and T. Mingshu, "Shrinkage and expansive strain of concrete with fly ash and expansive agent," *J. Wuhan Univ. Technol. Mater. Sci. Ed.*, vol. 24, no. 1, pp. 150–153, 2009, doi: 10.1007/s11595-009-1150-4.

[32] G. Peiwei, X. Shao-yun, C. Xiong, L. Jun, and L. Xiao-lin, "Research on autogenous volume deformation of concrete with MgO," *Constr. Build. Mater.*, vol. 40, pp. 998–1001, 2013, doi: 10.1016/j.conbuildmat.2012.11.025.

[33] M. A. A. Sherir, K. M. A. Hossain, and M. Lachemi, "Self-healing and expansion characteristics of cementitious composites with high volume fly ash and MgO-type expansive agent," *Constr. Build. Mater.*, vol. 127, pp. 80–92, 2016, doi: 10.1016/j.conbuildmat.2016.09.125.

[34] M. S. Meddah, M. Suzuki, and R. Sato, "Influence of a combination of expansive and shrinkage-reducing admixture on autogenous deformation and self-stress of silica fume high-performance concrete," *Constr. Build. Mater.*, vol. 25, no. 1, pp. 239–250, 2011, doi: 10.1016/j.conbuildmat.2010.06.033.

[35] T. L. Nguyen, R. Sahamitmongkol, and S. Tangtermsirikul, "Expansion and compressive strength of concrete with expansive additive," *Reearch Dev. J.*, vol. 19, no. 2, pp. 40–49, 2008.

[36] L. Wang, C. Shu, T. Jiao, Y. Han, and H. Wang, "Effect of assembly unit of expansive agents on the mechanical performance and durability of cement-based materials," *Coatings*, vol. 11, no. 6, pp. 1–10, 2021, doi: 10.3390/coatings11060731.

[37] R. R. Alvaro, B. G. Fonteboa, S. Seara-Paz, and K. M. A. Hossain, "Internally cured high performance concrete with magnesium based expansive agent using coal bottom

ash particles as water reservoirs," *Constr. Build. Mater.*, vol. 251, pp. 1–13, 2020, doi: 10.1016/j.conbuildmat.2020.118977.

[38] G. J. L. Calvo, D. Revuelta, P. Carballosa, and J. P. Gutiérrez, "Comparison between the performance of expansive SCC and expansive conventional concretes in different expansion and curing conditions," *Constr. Build. Mater.*, vol. 136, pp. 277–285, 2017, doi: 10.1016/j.conbuildmat.2017.01.039.

[39] G. J. L. Calvo, P. Carballosa, A. Castillo, D. Revuelta, J. P. Gutiérrez, and M. Castellote, "Expansive concretes with photocatalytic activity for pavements: Enhanced performance and modifications of the expansive hydrates composition," *Constr. Build. Mater.*, vol. 218, pp. 394–403, 2019, doi: 10.1016/j.conbuildmat.2019.05.135.

[40] M. Ish-Shalom and A. Bentur, "Properties of type K expansive cement of pure components: Hydration of unrestrained paste of expansive component," *Cem. Concr. Res.*, vol. 4, no. 4, pp. 519–532, 1974, doi: 10.1016/0008-8846(74)90003-9.

[41] Y. Dong, J. Zhang, X. Chen, and H. Yang, "Influence of curing temperature on the deformation properties of magnesium oxide micro-expansive concrete," *Int. Conf. Civil, Transp. Environ.*, pp. 552–558, 2016, doi: 10.2991/iccte-16.2016.91.

[42] L. Mo, M. Deng, and M. Tang, "Effects of calcination condition on expansion property of MgO-type expansive agent used in cement-based materials," *Cem. Concr. Res.*, vol. 40, no. 3, pp. 437–446, 2010, doi: 10.1016/j.cemconres.2009.09.025.

[43] American Concrete Institute Committee, *ACI 223R-10 Guide for the use of shrinkage compensating concrete*. Farmington Hills: American Concrete Institute, 2010.

[44] Japanese Standards Association, *JIS A 6202: Expansive additive for concrete*. Tokyo: Japanese Industrial Standard, 2017.

[45] Japan Society of Civil Engineers Committee, *JSCE No. 23: Recommended practice for expansive concrete*, no. 23. Tokyo: Concrete Library of JSCE, 1994.

[46] ASTM International, *C150/C150M-16: Standard specification for portland cement*, ASTM Inter. West Conshohocken: ASTM International, 2015. doi: 10.1520/C0150.

[47] Thailand Standards Association, *TIS 2135-2545: Coal fly ash for use as an admixture in concrete*. Bangkok: Thailand Industrial Standard, 2003.

[48] ASTM International, *ASTM C618-19: Standard specification for coal fly ash and raw or calcined natural pozzolan for use in concrete*. West Conshohocken: ASTM International, 2019. doi: 10.1520/C0618-19.2.

[49] ASTM International, *ASTM C33/C33M-18: Standards specification for concrete aggregates*. West Conshohocken: ASTM International, 2018. doi: 10.1520/C0033.

[50] ASTM International, *ASTM C494/C949M-19: Standard specification for chemical admixtures for concrete*. West Conshohocken: ASTM International, 2019.

[51] ASTM International, *ASTM C157/C157M-08 Standard test method for length change of hardened hydraulic cement mortar and concrete*. West Conshohocken, 2008. doi: 10.1002/9781118702956.ch15.

[52] ASTM International, *ASTM C39/C39M-20: Standard test method for compressive strength of cylindrical concrete specimens*. 2020.

CHAPTER 3

ESTIMATION OF RESTRAINED EXPANSION STRAIN OF REINFORCED EXPANSIVE CONCRETE

3.1 Introduction

As one of the most common construction materials, concrete has many advantages, including high resistance to compressive loads, high workability, durability, and low-cost materials. However, concrete also has a significant drawback of volume change along time may occur due to autogenous shrinkage, drying shrinkage, and carbonation shrinkage [1]. Concrete utilization is often composed of rebar reinforcement, which causes internal restraint. In addition, friction from neighboring structures and the influence of adjacent structural members cause external restraint. Therefore, using concrete as a construction material cannot be avoided from internal and external restraints. Due to early age shrinkage, restrained volume change in concrete frequently causes tensile stress development during the hardening process. When the tensile stress caused by shrinkage exceeds the tensile stress capacity, crack propagation is caused by shrinkage-induced tensile stress in the restrained concrete [2], [3]. In addition, cracking could lead to serviceability issues, such as increased permeability and corrosion of rebar reinforcement, resulting in decreased durability and increased maintenance costs [3].

Expansive concrete is one method that can be used to prevent restrained shrinkage cracking in concrete. Special materials in the form of expansive cement or expansive additives can increase the volume by generating a large amount of expansive product during the early stage of the hardening process. However, the effectiveness of this expansive concrete is also dependent on the configuration of the structure and the degree of restraint. In concrete with restraint conditions, the expansion of expansive products has difficulty due to the presence of restraint. Thus, the expansion process induces compressive stress between the expansive product or volume expansion to the other members that serve as restraints. This compressive stress can eliminate the tensile stress at the early age of the expansive concrete, thereby preventing shrinkage. In addition, restraint causes the expansive product to expand into areas with low stiffness, such as areas without restraint or concrete pores. Consequently, by utilizing expansive concrete, restrained concrete can reduce permeability and the volume of pores in the concrete [4]–[7]. Previous research has also been conducted on the effect of restraint on the level of expansion, using both prism specimens with a single rebar reinforcement [8]–[11] and cylindrical specimens with steel tubes [12]–[15].

In general, the sources of restraint in concrete structures are divided into two categories: internal and external restraints. In concrete structures, internal restraint is typically assumed to be provided by reinforcing bars, while external restraint depends on the configuration and function of the structure. It is very difficult to estimate the relationship between the level of expansion and the degree of restraint in expansive concrete structures due to the structure complexity. Before using expansive concrete in restraint conditions, ACI 223R-10 and JSCE No. 23 require an experiment to estimate the relationship between the level of expansion and the degree of restraint in expansive concrete [16], [17]. The objective of the restrained expansion strain measurement is to predict the amount of expansion that will occur in actual structures. However, these restrained expansion strain experiments are limited under certain conditions. This experiment can only accommodate a limited range of reinforcement ratios. In

addition, this restrained expansion strain test cannot accurately represent the conditions of actual structures because the strain measurements are taken in only one direction (longitudinal), while the actual expansion may vary in each direction depending on the configuration of structures.

Estimation of the degree of expansion in expansive concrete during the design process, particularly for actual structures, is still uncommon. This presents many challenges during the design process, particularly in regions where certain specifications are not yet included in the design guideline for expansive concrete structures. Therefore, an approach to the estimation method for expansive concrete is conducted in this study. The estimation method was conducted by using FE analysis. In order to improve the adaptability and versatility of design and analysis processes, FE analysis is one of the most effective techniques for estimating the strain level in reinforced expansive concrete structures. Estimation of restrained expansion strain via FE analysis can speed up the design process for expansive concrete without the need for direct experimentation. In addition, FE analysis can estimate the restrained expansion strain in a manner that is more accurate and representative of the actual condition. FE analysis has been used in various studies to evaluate the expansion and shrinkage behavior of expansive concrete under restraint, including experimental validation [13], [18]–[22], dan field investigation [23], [24]. Several studies applied experimental free expansion strain as an input in FE analysis to investigate the strain behavior of expansive concrete [22], [23]. Based on these studies, the FE analysis using free expansion strain as input always overestimates the actual restrained expansion strain of the expansive concrete.

To analyze the length change of concrete under restrained conditions, concrete length change strain with time in the free condition is usually employed as the input in the FE model. However, two major behaviors are to be considered for the restrained expansion mechanism that does not occur in the free expansion concrete. The method of FE analysis in this study applies free expansion strain as input data, considering expansion loss due to pores filling of expansive products and early age compressive creep for estimating the restrained expansion. This research determines the effective free expansion strain of expansive concrete, which eliminates the free expansion strain after loss of expansion due to the effects of pores filling by expansive product fan compression creep during the early stage of restrained expansion. A reduction factor is introduced to account for expansion loss to generate effective free expansion strain. This effective free expansion strain is used as input in the FE analysis to estimate the restrained expansion strain. Reduction factors are generated by considering factors affecting the expansion rate, such as mix proportion, curing type, temperature, and reinforcement ratio.

This study proposes a method to estimate the restrained expansion strain of reinforced expansive concrete. Before using the free expansion strain as an input to the FE analysis, the reduction factor is applied to the free expansion strain as an estimation method. This study includes both experimental and numerical analysis. The experimental work consisted of a test of compressive strength, free expansion strain (see chapter 2), and also restrained expansion strain measurement. All mix proportion and curing condition variations between unrestrained and restrained expansion strains are similar. However, the effect of the reinforcement ratio is varied for each series using reinforcement ratios of 0.35%, 0.79%, and 1.13%. From this analysis, it is possible to calculate a reduction factor in order to generate effective free expansion strain. In prior studies, this estimation method was also utilized to confirm the applicability of the reduction factor. Through this research, it is expected that an efficient and

comprehensive method for estimating the restrained expansion strain of expansive concrete will be developed.

3.2 Experimental program

3.2.1 General information

This study aimed to develop a method for estimating the expansion strain in expansive concrete under restraint. In the early stages of this investigation, prism specimens were measured. The length change measurement under restrained conditions is required to validate the estimation results. This research begins by conducting experiments with restrained expansion strain. The specimens condition is similar to the free expansion strain test in Chapter 2. The variation of the restrained expansion strain test is shown in **Table 3.1**. Using experimental data and finite element simulations for series I through IV, reduction factor equations will be derived to generate effective free expansion strain. The results of the effective free expansion strain will be input into the finite element analysis in order to predict the expansion strain in expansive concrete under restrained conditions.

Table 3.1 Specimen variations for each Series

Variations Component	Series I	Series II	Series III	Series IV
Amount of Binder (kg/m^3)	280	340	380	280; 380
Amount of EA (kg/m^3)	0; 20; 30; 40	0; 20; 30; 40	0; 20; 30; 40	20; 30
Type of EA	C-S-A + CaO	C-S-A + CaO	C-S-A + CaO	C-S-A + CaO
Amount of FA (%)	20	20	20	20
Water to Binder Ratio	0.66	0.51	0.47	0.66; 0.47
Curing Condition	Moist; Sealed	Moist; Sealed	Moist; Sealed	Moist; Sealed
Curing Period (Days)	3	3	3	3
Curing Temperature (ºC)	28	28	28	28; 35; 40
Reinforcement ratio (%)	0.35; 0.79; 1.13	0.35; 0.79; 1.13	0.35; 0.79; 1.13	0.35; 0.79; 1.13

After the reduction factor and effective free expansion strain have been successfully calculated, back analysis is performed on all existing series using FE simulation. However, this simulation utilizes the effective free expansion strain from the generated equation. Several previous studies were utilized in this investigation to estimate the restrained expansion strain in expansive concrete. **Table 3.2** presents data from previous researchers that will be used as components to validate the estimation results of restrained expansion strain.

Table 3.2 Specimen variations for additional series

Variations Component	Series V [25]	Series VI [26]
Amount of Binder (kg/m^3)	365	350
Amount of EA (kg/m^3)	20	5; 15; 20
Type of EA	SEA, FEA, CEA (CaO Type)	HEA (C-S-A Type)
Amount of FA (%)	0; 20	20; 30
Water to Binder Ratio	0.53	0.50
Reinforcement Ratio (%)	0.79; 1.13	0.79; 1.57; 3.13; 8.04
Curing Condition	Moist	Sealed
Curing Period (Days)	7	7
Curing Temperature (ºC)	28	28

3.2.2 Materials and mix proportions

Binders used in this experiment consist of Ordinary Portland Cement (OPC), Fly Ash (FA), and Expansive Additive (EA). OPC manufactured by Siam Cement Group Co., Ltd,

Thailand, was used as a major binder material for all tested concrete mixtures. Based on ASTM C150 [27], the cement used in this study is classified as type I. The fly ash used is Class 2b according to TIS 2135 [28] or Class C per ASTM C 618 [29] from Mae Moh power plant, Thailand. Series I to IV used the combined ettringite and calcium sulfoaluminate systems (C-S-A + CaO type). Series V and VI used calcium oxide-based (CaO type) and calcium sulfoaluminate (C-S-A type) expansive additives, respectively [25], [26]. The major chemical compositions of all binders and expansive additives used in the current and previous studies are shown in **Table 3.3.**

Table 3.3 Chemical composition of binders (Portland cement, fly ash, and expansive additive)

Binder	SiO_2	Al_2O_3	Fe_2O_3	CaO	MgO	SO_3	K_2O	Na_2O
OPC	18.98	5.33	3.16	65.34	1.15	2.65	0.21	0.16
FA	36.18	20.21	13.89	18.74	2.69	3.74	2.24	1.14
EA	2.12	4.75	0.14	61.09	0.73	26.46	-	-
SEA	0.18	4.61	0.88	54.59	4.08	24.42	0.23	0.15
FEA	7.47	9.89	2.67	47.54	1.95	20.38	0.38	0.19
CEA	0	17.12	0.04	47.47	0.17	30.74	0	0.1
HEA	4.35	0.96	1.14	78.84	0.93	10.95	0.05	0.01

OPC: Ordinary Portland Cement; **FA**: Fly Ash; **EA, SEA, FEA, CEA, HEA**: Expansive Agent

In addition, sand from the natural river was used as the fine aggregate, whereas crushed limestone was used as the coarse aggregate. Gradations of the fine and coarse aggregates were tested as per ASTM C33 [30]. Crushed limestone with a maximum size of 19 mm was used as the coarse aggregate. The properties of aggregates are given in **Table 3.4**. Chemical admixtures were added to control the initial slump within a range of 15 ± 2 cm. A type D (water-reducing and retarding) and a type F (high-range water-reducing) admixtures were added to adjust the initial slump at constant water to binder ratio. The specifications for the types of admixtures are explained in ASTM C494 [31].

Table 3.4 Properties of fine and coarse aggregates

Properties	Fine aggregate	Coarse aggregate
Absorption (%)	1.08	0.34
Specific gravity (SSD)	2.60	2.83
s/a at minimum void (by volume)	0.44	
Minimum void (%)	23.52	

In the mix proportions, Ordinary Portland cement, expansive additive (EA), and fly ash (FA) from Mae Moh power plant were used as binders in this study. **Table 3.5** provides the tested mix proportions of concrete in all series. In this experiment, the total binder content varied from 280 kg/m³ (series I), 340 kg/m³ (series II), and 380 kg/m³ (series III). While the total binder used through the results of previous studies is 365 kg/m³ for series V and 350 kg/m³ for series VI. The replacement percentages of fly ash were between 0% to 30% of the weight of the total binder, while the amounts of expansive additive were between 0 kg/m^3 to 40 kg/m^3. Water to binder ratios varied between 0.47 to 0.66 depending on the slump value target. To study the effects of curing temperature on the level of expansion strain in free and restrained conditions, mixtures in series IV were used by varying the curing temperature. In series IV,

each specimen was exposed to curing temperatures of 28 °C, 30 °C, and 35 °C. The standard curing temperature for series other than series IV is 28 °C.

Table 3.5 Mix proportions of the tested concrete

Series	Symbol	w/b	Binders (kg/m³)			Water (kg/m³)	Aggregate (kg/m³)		Admixture (g/m³)	
			OPC	FA	EA		Fine	Coarse	Type D	Type F
Series I (Binder: 280 kg/m³)	EA0B280	0.66	226	54	0	185	827	1073	784	560
	EA20B280		206	54	20					
	EA30B280		196	54	30					
	EA40B280		186	54	40					
Series II (Binder: 340 kg/m³)	EA0B340	0.51	288	52	0	175	816	1060	680	2040
	EA20B340		268	52	20					
	EA30B340		258	52	30					
	EA40B340		248	52	40					
Series III (Binder: 380 kg/m³)	EA0B380	0.47	322	58	0	180	795	1032	760	1330
	EA20B380		302	58	20					
	EA30B380		292	58	30					
	EA40B380		282	58	40					
Series IV (Binder: 280 and 380 kg/m³)	EA30B280	0.66	206	54	20	185	827	1073	784	560
	EA20B380	0.47	302	58	20	180	795	1032	760	1330
	EA30B380		292	58	30					
Series V (Binder: 365 Kg/m³)	SEA20FA0	0.53	345	0	20	194	806	1024	-	-
	SEA20FA20		272	73	20					
	FEA20FA0		345	0	20					
	FEA20FA20		272	73	20					
	CEA20FA0		345	0	20					
	CEA20FA20		272	73	20					
Series VI (Binder: 350 Kg/m³)	HEA5FA20	0.50	275	70	5	175	814	1026	-	-
	HEA15FA20		265	70	15					
	HEA20FA20		260	70	20					
	HEA5FA30		240	105	5					
	HEA15FA30		230	105	15		810	1021		
	HEA20FA30		225	105	20					

3.2.3 Test methods

The restraining apparatus was arranged for the restrained expansion test, as shown in **Figure 3.1**. The restraining ratios were varied by selecting the appropriate size and number of steel rebar. The sizes of specimens were changed according to the reinforcement ratios. Series I to V used specimen sizes of $100 \times 100 \times 350$ mm³ for the reinforcement ratios of 0.79% (DB10) and 1.13% (DB12), while the $150 \times 150 \times 500$ mm³ specimens were used for the reinforcement ratio of 0.35% (DB10). Two steel plates were fastened by nuts at both ends of the specimens to create the restraint, as shown in **Figure 3.2** and **Table 3.6**. In series VI, the $100 \times 100 \times 350$ mm³ specimen sizes were applied. However, the rebar configurations in series VI were different from the other series. In series VI, the reinforcement ratios were 0.79% with 1DB10, 1.57% with 2DB10, 3.14% with 4DB10, and 8.04% with 4DB16, as shown in **Figure 3.3**. To measure the restrained expansion strain, a strain gauge was attached at the center span of the specimens with the test method for specimens with restrained conditions conformed to ASTM C878 [32]. The expansion measurement in restrained condition started at 8 hours of age after casting.

Figure 3.1 Specimens for length change measurement in restrained condition
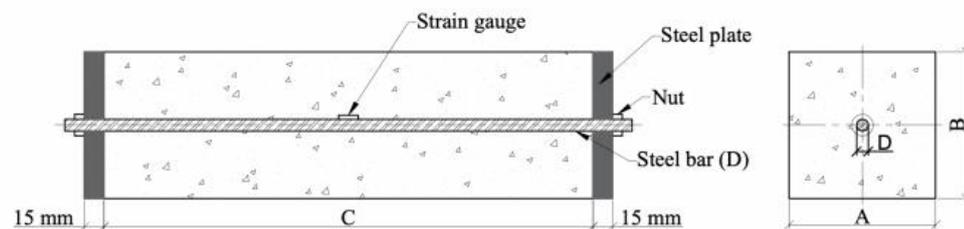
Figure 3.2 Specimens size for length change measurement in restrained condition

Table 3.6 Details of restrained specimen

Series ID	Reinforcement Ratio (%)	Rebar (D) (mm)	A (mm)	B (mm)	C (mm)
I-IV	0.35	1DB10	150	150	500
I-VI	0.79	1DB10	100	100	350
I-V	1.13	1DB12	100	100	350
VI	1.57	2DB10	100	100	350
VI	3.13	4DB10	100	100	350
VI	8.04	4DB16	100	100	350

(a) ρ: 0.79% (1DB10) (b) ρ: 1.57% (2DB10) (c) ρ: 3.14% (4DB10) (d) ρ: 8.04% (4DB16)
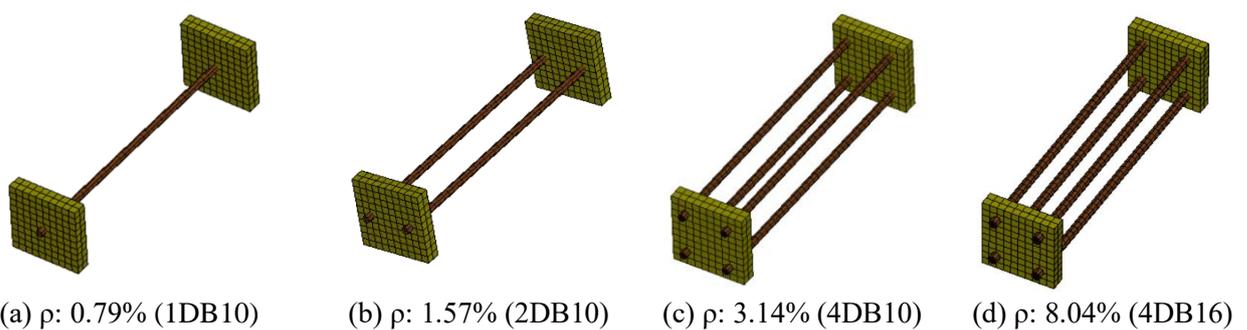
Figure 3.3 Rebar configurations for Series VI

All specimens in this study were demolded 8 hours after casting (final setting time), and the initial length was measured. Two types of curing conditions applied in this study are moist and sealed curing, with 3 days for series I to IV and 7 days for series V to VI. Wet clothes were applied to the concrete surfaces during the curing process to provide moist curing, while sealed curing applied plastic wraps to all surfaces of the specimens. It should be noted that from the observation during the tests, expansion increased until 3 days of curing age and was almost constant regardless of the curing methods. Therefore, the expansion strains of the specimens

were measured for up to 3 days, and the expansion at 3 days was considered the maximum expansion. During the measurement process, the specimens were placed in a control room with a relative humidity of 70 ± 5% and a temperature of 28 °C. However, for the measurement in series IV, the curing temperature varies from 28 °C, 35 °C, and 40 °C for moist and sealed curing.

3.3 Finite element analysis
3.3.1 Geometry and boundary conditions

The finite element (FE) analysis LS Dyna software [33] was used to investigate the expansion and shrinkage strains in the studied reinforced expansive concrete structures. In finite element (FE) analysis, the configuration and boundary conditions are the fundamental factors that must be considered. The dimensions and configuration of each model correspond to those of the experimental specimen. In this simulation, concrete, rebar reinforcement, and steel plate are modeled. Concrete and steel plates are assumed to be eight-node solid elements, while rebar reinforcement is assumed to be two-node beam elements. The meshing size used also varies according to the dimensions of each specimen. **Figure 3.4** shows an example of a geometry for the FE model to investigate the restrained expansion strain on expansive concrete.
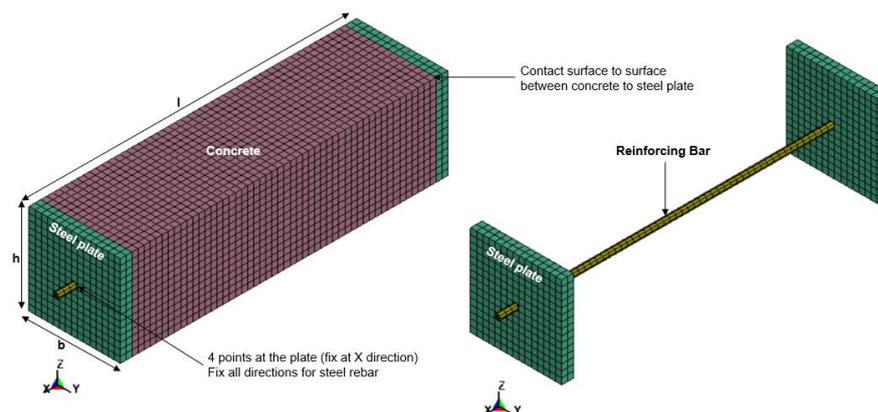
Figure 3.4 An example of three-dimensional FE model of the tested specimen

Fixed conditions for displacement and rotation were applied to the x, y, and z directions at the rebar near the edge of the concrete. In addition, the 4 selected nodes of the steel plate that are directly exposed to bold are also fixed in the longitudinal direction. The surface contact between the steel plate and the concrete is assumed using the contact surface to surface with a friction coefficient of 0.20 for the friction contact between the steel surface and the concrete surface. Meanwhile, the contact between rebar and concrete uses beams in solid tools by specifying the bond stress and slip relationship between concrete and rebar reinforcement. The correlation between body stress and the slip relationship used in this analysis refers to the 1990 CEB-FIB [34]. In this FE analysis, the boundary conditions, model configuration, and test setup closely resemble actual experimental conditions.

3.3.2 Materials models

The material model is one of the most important analysis factors in FE simulation. Ls-Dyna has provided various material models for general purposes and specific functions. Some material models require users to input complex properties, while others simplify the input and can generate the required material properties. This simulation utilizes three material models,

MAT 159 Continuous Surface Cap Model (CSCM) to describe concrete, MAT 024 Piecewise Linear Plasticity to define steel plate and rebar reinforcement, and MAT 001 Add Thermal Expansion to determine the concrete's expansion strain. The volume II software user's manual explains each material model for the LS-Dyna numerical tools [35].

The MAT 159 continuous surface cap model (CSCM) was first developed to simulate the behavior of concrete structures for the National Cooperative Highway Research Program of the United States Department of Transportation [36]. MAT 159 is one of the material models offered by Ls Dyna and is widely utilized for concrete materials subject to various loading. The ability to automatically generate the input parameters of the material model based on the concrete strength is one of the benefits of this material model. Only general concrete properties data, such as mass density, Poisson's ratio, compressive strength, maximum aggregate size, and rate effect, are required to generate concrete parameters. The MAT 159 algorithm computes the stress-strain relationship of concrete based on its compressive strength by using the CEB-FIB Standards [34]. The relationship between stress and strain generated by Ls-Dyna based on uniaxial compressive strength is illustrated in **Figure 3.5**. The benefits of this material model for generating concrete behavior based on uniaxial compressive strength make it simple for users to analyze the behavior of reinforced concrete structures under different loading conditions. In addition, this model material can generate strain-softening behavior after post-peak in concrete using the quadratic fitting equations regression analysis.
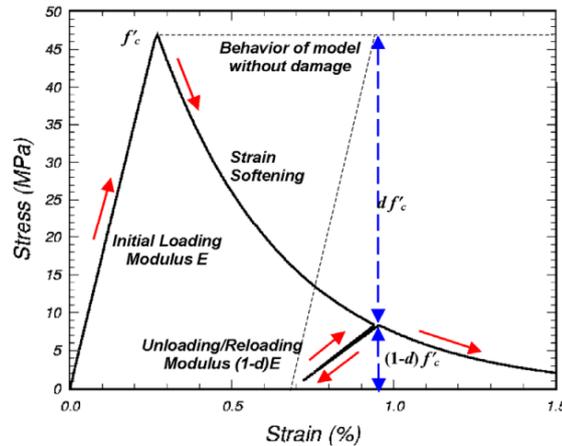
Figure 3.5 Illustration of the generated stress-strain of compressive strength [35], [36]

The value of compressive strength is divided into two sections to produce the stress-strain relationship of the concrete material under compression. The initial section assumes that the concrete is in an elastic state up to the peak stress or compressive strength, while the second section describes the strain-softening state. Only the value of Young's modulus is required in elastic conditions, which can be calculated using **Eq. 3.1**, while **Eq. 3.2** can be used to calculate tensile strength.

$$E = 4700\sqrt{fc'} \tag{3.1}$$

$$ft = 0.3\,(fc')^{2/3} \tag{3.2}$$

To concrete under compression behavior, **Eq. 3.3** and **Eq. 3.4** can be used to calculate the softening strain, while to concrete under tension behavior, **Eq. 3.5** and **Eq. 3.6** can be used

to calculate the softening strain. Refer to the provided manual for a comprehensive analysis of the method for generating strain-strain relationships on MAT 159 [35]–[38].

$$\text{Softening Function in compression} = (1\text{-}dc)\, fc' \qquad (3.3)$$

$$dc = \frac{d_{max}}{B}\left|\frac{1+B}{1+B\; exp^{-A(\tau_d - r0_d)}} - 1\right| \qquad (3.4)$$

$$\text{Softening Function in tension} = (1\text{-}dt)\, ft \qquad (3.5)$$

$$dt = \frac{0.999}{D}\left|\frac{1+D}{1+D\; exp^{-C(\tau_b - r0_b)}} - 1\right| \qquad (3.6)$$

Where *fc'* is compressive strength (MPa), *E* is young's modulus, d is strain softening function, *dmax* is maximum damage level, A and B are the constant parameters for softening shape under compression, C and D are the constant parameters for softening shape under tension, $\tau - r_0$ is parameters for damage difference in compression and tension.

Eq. 3.7 is used to calculate the maximum damage level under compression by taking into account the effect of multidimensional stress, which can be calculated using **Eq. 3.8** and **Eq. 3.9**. This multidimensional stress calculation is also detailed in CEB FIP 1990 [34].

$$d_{max} = \left(\frac{\sqrt{3J_2}}{J_1}\right)^{1.5} \qquad (3.7)$$

$$J_1 = \sigma_1 + \sigma_2 + \sigma_3 \qquad (3.8)$$

$$J_2 = \frac{1}{6}\left[(\sigma_1 - \sigma_2)^2 + (\sigma_2 - \sigma_3)^2 + (\sigma_3 - \sigma_1)^2\right] \qquad (3.9)$$

Where J_1 is the first invariant stress tensor and J_2 is the second invariant stress tensor.

To calculate strain softening under compression and tension conditions, the softening parameters A and B for compression and C and D for tension are required. This analysis requires fracture energy as one of the primary components, which can be determined from compressive strength using **Eq. 3.10** to **Eq. 3.12**. While the initial fracture energy can be calculated using the values in **Table 3.7**, its value is dependent on the maximum aggregate size. While the stress difference can be calculated using **Eq. 3.13** and **Eq. 3.14**. Finally, all these equations produce a stress-strain relationship for the model material for concrete.

$$G_f = G_{f0}\left(\frac{fck' + 8}{10}\right)^{0.7} \qquad (3.10)$$

$$G_{fc} = 2r0_d L \left(\frac{1+B}{A.B}\right)\log(1+B)2L\left|\frac{1+B}{A^2}\right| \qquad (3.11)$$

$$G_{ft} = r0_b L \left(\frac{1+D}{C.D}\right)\log(1+D) \qquad (3.12)$$

$$\tau_d - \tau_{0d} = \lfloor\sqrt{x} - \sqrt{x_0}\rfloor\sqrt{\frac{fc'}{L}} \qquad (3.13)$$

$$\tau_b - \tau_{0b} = \lfloor\sqrt{E}\rfloor\left(\frac{x-x_0}{L}\right) \tag{3.14}$$

Where G_f is fracture energy (N mm/mm^2), G_{f0} is initial fracture energy (N mm/mm^2), Dmax is the maximum size of aggregate (mm), and L is meshing size (mm).

Table 3.7 Base values of fracture energy G_{f0} [38]

D_{max} (mm)	G_{f0} (N mm/mm^2)
8	0.025
16	0.030
32	0.038

However, this CSCM material model is highly dependent on the compressive strength of concrete, and it is difficult to define the behavior of certain types of concrete based on the compressive strength. Therefore, this material model also provides space for users to define more complete concrete material properties according to the condition of the concrete. Users must input fracture energy, torsion, and triaxial compression behavior [36], [39]. For a comprehensive explanation utilizing MAT 159, various previous case studies utilizing this material model have been conducted [40]–[46].

This numerical simulation adopted material piecewise linear plasticity (MAT 024) to the steel plates dan reinforcing bars model. In MAT 024, users can also input the stress-strain behavior of the steel and consider the strain rate effect. Failure in this analysis is based on the plastic strain or a defined minimum time step. This model material generally applies to isotropic, elastoplastic materials with stress-strain relationship characteristics that are too complex to be modeled by a bilinear representation [35]. The main parameters that must be input into this material model include mass density, Poisson's ratio, young modulus, force yield, tangent modulus, and strain rate. By utilizing these parameters, MAT 024 is able to generate stress-strain relationships, or von automatically misses stress and plastic strain relationships. In addition, this material model permits users to input the necessary stress-strain curves as material properties. **Figure 3.6** show an illustration of the stress-strain curve generated by MAT 024. The results of the previous study provide a detailed explanation of the implementation of MAT 024 for various types of numerical simulation interests using Ls-Dyna [47]–[51].
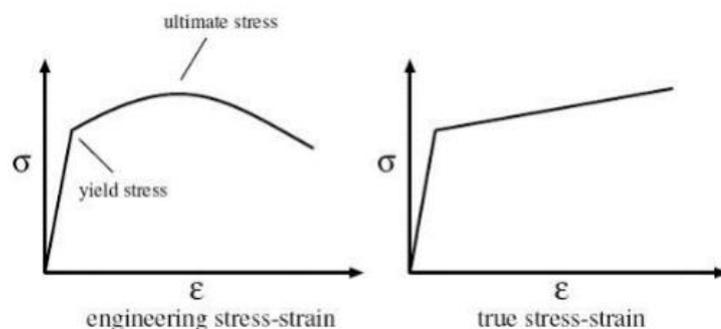
Figure 3.6 Illustration of stress and strain relationship from MAT 024 [52]

In addition to the two materials described previously, this study also employs Mat Add Thermal Expansion, an option for any material model in Ls Dyna with a thermal expansion property. This thermal expansion option applies to nonlinear solid, shell, and thick shell elements. Local thermal expansion coefficients for each material must be used as input for this

material properties. Thus, different inputs are required for each type of material when utilizing various materials.

3.3.3 Determination of effective free expansion strain

To analyze or predict the length change of concrete under restrained conditions, the FE model employs the concrete length change strain with time in free conditions as an input. This study adopts the concept that experimental results for specimens in free conditions predict concrete expansion strain levels under restrained conditions. However, two significant behaviors must be considered in the restrained expansion mechanism that does not occur in the concrete with the free condition. Due to the difference in the expansion mechanism caused by the influence of restraint, the length change strain under free conditions of expansive concrete cannot be used directly as input to predict the restrained expansion strain. **Figure 3.7** illustrates the expansion mechanism between free and restrained expansion.
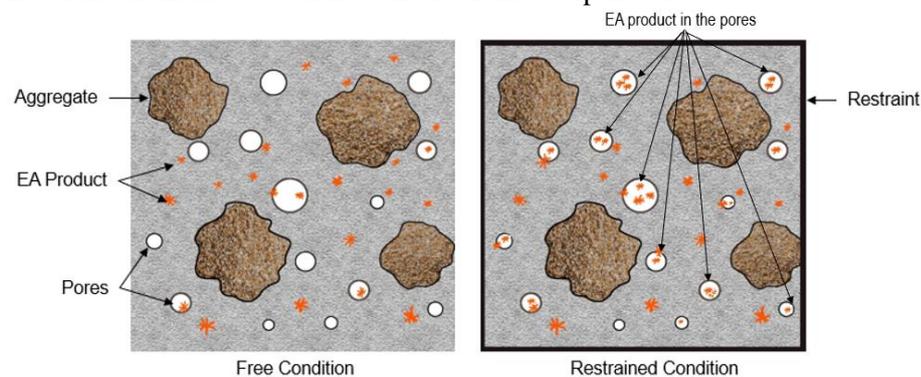
Figure 3.7 Illustration of expansion mechanism between free and restrained conditions

Loss of expansion can occur in expansive concrete under restrained conditions due to the expansive product filling the pores and compression creep during early expansion under restrained conditions. As there is no restraining stress in the case of free expansion, expansive products are more effective at producing expansion than in the case of restrained expansion. Under restraining stress, a portion of the expansive products is forced to enter the voids in concrete, reducing their expansion capacity. Also, compression creep does not occur in free expansion concrete because the free expansion does not generate compressive stress. On the other hand, the restraint causes compressive stress in the expanding concrete, so compression creep arises at an early age in the restrained expansion concrete. These two behaviors cause a loss of ability to produce expansion in restrained expansive concrete compared to unrestrained expansive concrete. Explanation of these two differences in expansion mechanism between free and restrained conditions is also supported by previous researchers [4], [53], [54].

These two different behaviors of the free expansion strain cannot be modeled in the FA analysis to predict the restrained expansion strain, so the experimentally determined free expansion strain cannot be used directly as an input in the FE analysis. However, these two behaviors must be considered in the FE analysis to simulate the deformation due to the expansion of expansive concrete under restraint. The calculation of the amount of expansion lost due to these two behaviors is very complex and challenging to calculate separately. Therefore, the effective free strain is defined in this study to be simply applied as the input in the FE analysis to simulate the deformation of expansive concrete under restraint. Due to the loss of ability to generate expansion under restraint, the FE analysis using free expansion strain

as input data always overestimates the actual restrained expansion strain of the expansive concrete. The overestimation of calculated restrained expansive concrete is also explained in previous studies [22], [23].
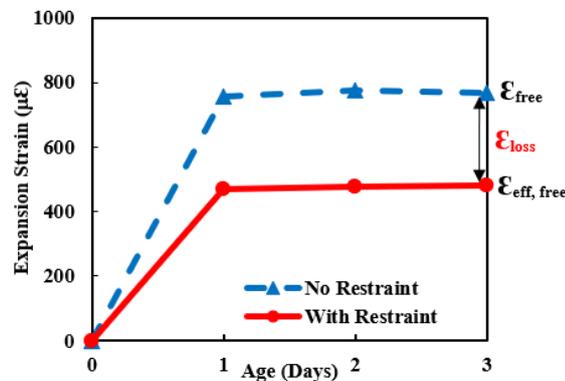
Figure 3.8 Free expansion strain with and without reduction factor

$$\varepsilon_{eff,\,free}= \phi \times \varepsilon_{free} \tag{3.15}$$

Where $\varepsilon_{eff,\,free}$ is the effective free strain (μ), ϕ is the reduction factor, and ε_{free} is measured free expansion strain of the unrestrained expansive concrete (μ).

An investigation is needed to determine the effective free strain, which is the actual expansion level after compression creep occurs and a portion of expansive products have filled the pores. This effective free strain will be the main input in FE analysis instead of the free expansion strain for estimating the restrained expansion strain of the expansive concrete. For simplicity, a reduction factor concept introduced to account for the loss of free expansion in this research is shown in **Figure 3.8**. Effective free strain can be obtained from the measured free strain of unrestrained expansive concrete by applying the reduction factor (ϕ) as illustrated in **Eq. 3.15**. This study introduced a reduction factor equation to determine the effective free strain for input in FE analysis. The value of the reduction factor of each test case from series I to Series IV was varied until the restrained expansion strain from FE analysis matched with the experimental result. The equation to determine a regression technique then obtained the reduction factor. The data from series V and VI were then used for the equation verification. Two equations were proposed based on two curing conditions (moist and sealed curing), which can be used to determine reduction factors for mixtures with various amount of expansive additive, amount of binder, amount of fly ash, water to binder ratios, curing temperature, and reinforcement ratios.

3.4 Results and discussions

This chapter explains the estimation method of restrained expansion strain of expansive concrete based on the reduction factor approach. As previously explained, this study estimates the restrained expansion strain using the free expansion strain derived from experimental results. Due to the difference in expansion mechanism between free and restrained conditions for expansive concrete, the free expansion strain cannot be used as a direct input in FE analysis. Consideration must be given to the loss of expansion strain due to the entry of expansion product into the pores and compressive creep of restrained expansive concrete during the expansion process. Therefore, it is necessary to reduce the free expansion strain, also known as

the effective free expansion strain. This section explains the procedure for generating a reduction factor equation in order to obtain an effective free strain.

3.4.1 Reduction factor equations

An illustration of the estimation results of the restrained expansion strain on the expansive concrete can be seen in **Figure 3.9**. **Figure 3.9a** shows the restrained expansion strain without considering the loss of ability to produce the expansion due to the effect of restraint (free expansion as input in FE analysis). The results of the FE analysis indicate that the restrained expansion strain was overestimated. Therefore, the free expansion strain must be reduced prior to its use as an input in the FE analysis. The method used in this research is to produce a reduction factor equation. The first step to generating the reduction factor equation is to perform FE analysis by varying the value of the reduction factor between 0.40 to 1.00. **Figure 3.9b** illustrates the results of a FE analysis with various reduction factors. The analysis was conducted by predicting the appropriate reduction factor value for each specimen from series I to IV. **Figure 3.9c** shows an example of the estimation of restrained expansion strain utilizing a reduction factor of 0.70. The simulation for predicting the reduction factor is followed by generating the reduction factor equation. The effects of loss of ability to produce expansion under restraint are considered in this study by using a reduction factor as demonstrated by **Eq. 3.16**.

(a) Without applying reduction factor

(b) Applying reduction factor

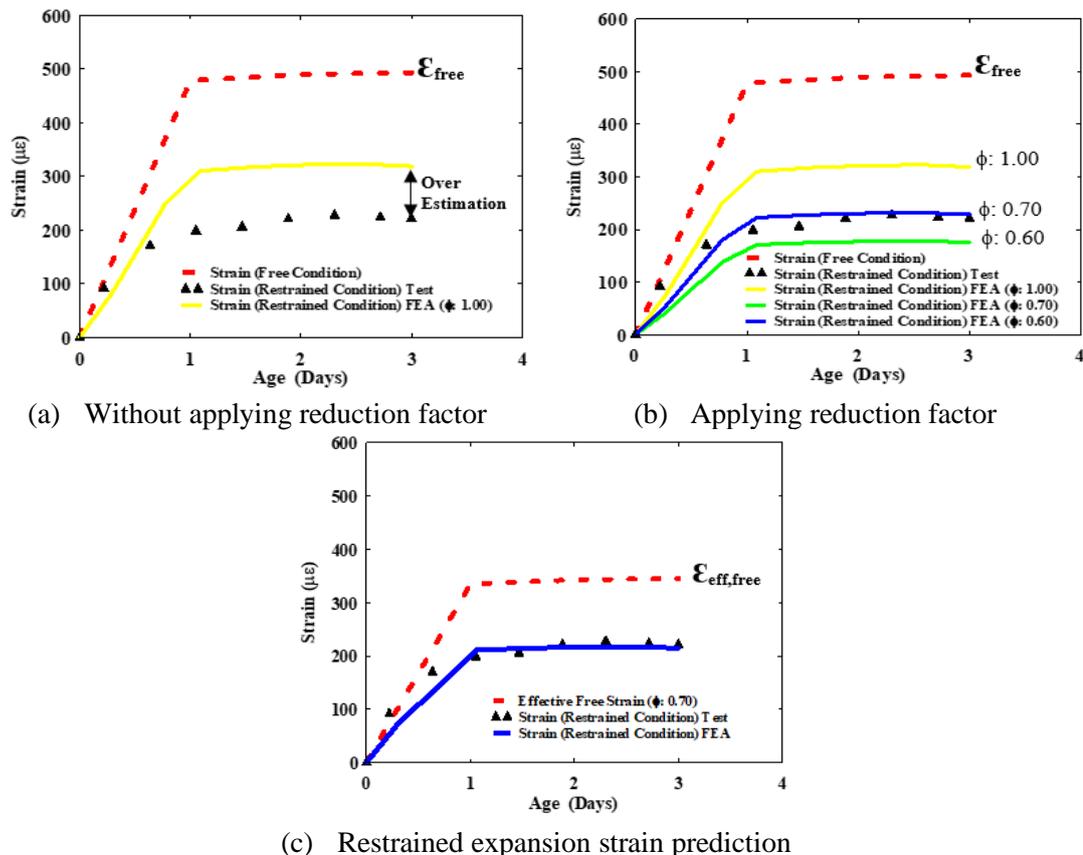(c) Restrained expansion strain prediction

Figure 3.9 Expansion strain comparison between finite element analysis and experiment

This reduction factor is generated using a regression equation with the help of the MATLAB program. The results of the investigation show that the FE analysis with the effective

free strain was successful to simulate the restrained expansion strain of the expansive concrete specimen under rebar restraint. Therefore, reduction factor equations which can be used to calculate the effective free strain of expansive concrete are developed as one of the main objectives of this study by considering various factors that affect the level of expansion, i.e., expansive additive dosage, fly ash content, binder content, water to binder ratio, curing method, curing temperature, and reinforcement ratio. After calculating the reduction factor, the analysis is continued by estimating the restrained expansion strain using effective free strain.

The reduction factor of each test case was obtained by FE analysis for the best fit to the test results. A total of 269 test cases were used for the equation determination. After obtaining the values of the reduction factor for all test cases, the MATLAB program was utilized to obtain the reduction factor equation with the polynomial form, as shown in **Eq. 3.16**. The constant for each parameter is divided into two conditions based on the curing type, as shown in **Table 3.8**. After obtaining the reduction factor, the effective free strain can be calculated using **Eq. 3.17**. **Eq. 3.16** has some limitations according to the range of test data. So, the equations can only be used for moist and sealed curing with the applicable range of expansive additive dosages from 0 to 40 kg/m^3, fly ash contents from 0% to 30% of the total binder, binder contents from 280 to 380 kg/m^3, water to binder ratios from 0.47 to 0.66, curing temperature from 28°C to 40°C, and reinforcement ratio up to 8.00%. However, these ranges are considered to cover the typical ranges of application in normal concrete structures.

$$\phi = x_1B^{x2} + x_3EA^{x4} + x_5FA^{x6} + x_7\rho^{x8} - x_9(W/B)^{x10} + x_{11}T^{x12} + x_{13}, \quad \phi \leq 1.00 \tag{1}$$

Where ϕ is reduction factor, B is binder content (kg/m^3), EA is expansive additive dosage (kg/m^3), FA is fly ash content (% of total binder), ρ is reinforcement percentage (%), W/B is water to binder ratio, and T is curing temperature (°C).

Table 3.8 Constant values for reduction factor equation for moist and sealed curing methods

Curing	X_1	X_2	X_3	X_4	X_5	X_6	X_7
Moist	-0.401	-0.327	-0.011	0.839	-0.161	0.006	0.337
Sealed	-0.926	-0.254	-0.010	0.892	-0.150	0.002	0.088
Curing	X_8	X_9	X_{10}	X_{11}	X_{12}	X_{13}	
Moist	-0.347	0.447	1.666	1.549	-0.301	0.115	
Sealed	-0.933	0.685	3.801	1.000	-0.275	0.360	

$$\varepsilon_{eff, free} = \phi \times \varepsilon_{free} \tag{2}$$

Where $\varepsilon_{eff, free}$ is the effective free strain (μ), ϕ is the reduction factor, and ε_{free} is measured free expansion strain of the unrestrained expansive concrete (μ).

3.4.2 Comparison of restrained expansion strain

After obtaining the reduction factor equation, the next step is validating the restrained expansion strain estimation using the effective free expansion strain. This simulation is performed for all series I through IV. In addition, series V and series VI are used to observe the level of reliability of the effective free strain and to validate the estimation results of restrained expansion strain. **Figure 3.10** shows the comparison results between the experimental and the FE analysis. **Figure 3.10a** and **Figure 3.10b** shows the correlation between the estimation results of restrained expansion strain in series I through series IV with various curing types. While **Figure 3.10c** and **Figure 3.10d** show the correlation results for series V and VI,

respectively. The correlation of the obtained results is 0.9691 (96.91%) for specimens with moist curing and 0.9666 (96.66%) for specimens with sealed curing, as determined by the reanalysis used to verify the reliability level of the restrained expansion strain estimation method. From the results of this regression analysis, it can be concluded that the correlation between the estimation results and the laboratory experiment results is relatively high. To increase confidence in the proposed estimation method, this study also evaluates restrained expansion strain using data from series V and VI of previous studies. The estimation results indicate that the correlation level between the results of the FE analysis and the experimental results for series V is 0.9758 (97.58%), while the correlation level for series VI is 0.9569 (95.69%). Based on the results of the two analyses, it is clear that the reduction factor equation used to calculate the effective free strain is suitable input for FE analysis. A comparison of the expansion strain between experimental and FE analysis results was conducted to understand the reliability of the estimation results of restrained expansion strain of expansive concrete with prism specimens. This study investigates several factors that influence the expansion of expansive concrete using prism specimens in restrained conditions. The influence of the reinforcement ratio, effects of amount of expansive additive, effects of amount of binder, effects of curing conditions, and effects of amount of fly ash are investigated.

(a) Series I to IV moist curing   (b) Series I to IV sealed curing

(c) Series V sealed curing   (d) Series VI moist curing
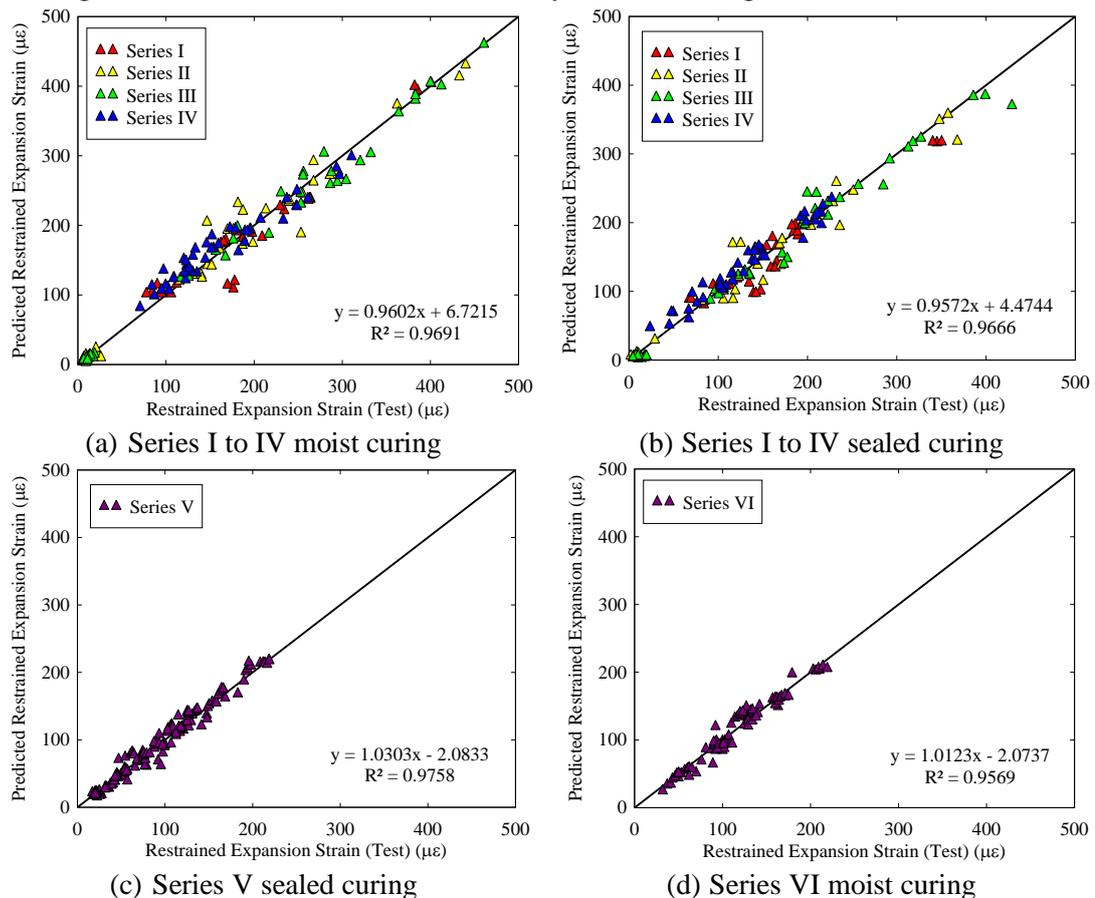
Figure 3.10 Restrained expansion strain comparison between test and FE analysis

3.4.3   **Influence of reinforcement ratio**

The reinforcement ratio is one of the major factors affecting the level of expansion of concrete under restraint. **Figure 3.11** shows the results of the restrained expansion strain test

and the estimation results derived from the FE analysis. This study utilized three different ratios of reinforcement including 0.35 %, 0.79 %, and 1.13 %. This section shows the result for each series with 30 kg/m3 of expansive additive both in moist and sealed curing. Both estimation and laboratory test results show a similar pattern of restrained expansion strain. The results show that a reinforcement ratio increase causes the restrained expansion strain to decrease.

(a) EA30B280 moist curing

(b) EA30B280 sealed curing

(c) EA30B340 moist curing

(d) EA30B340 sealed curing

(e) EA30B380 moist curing
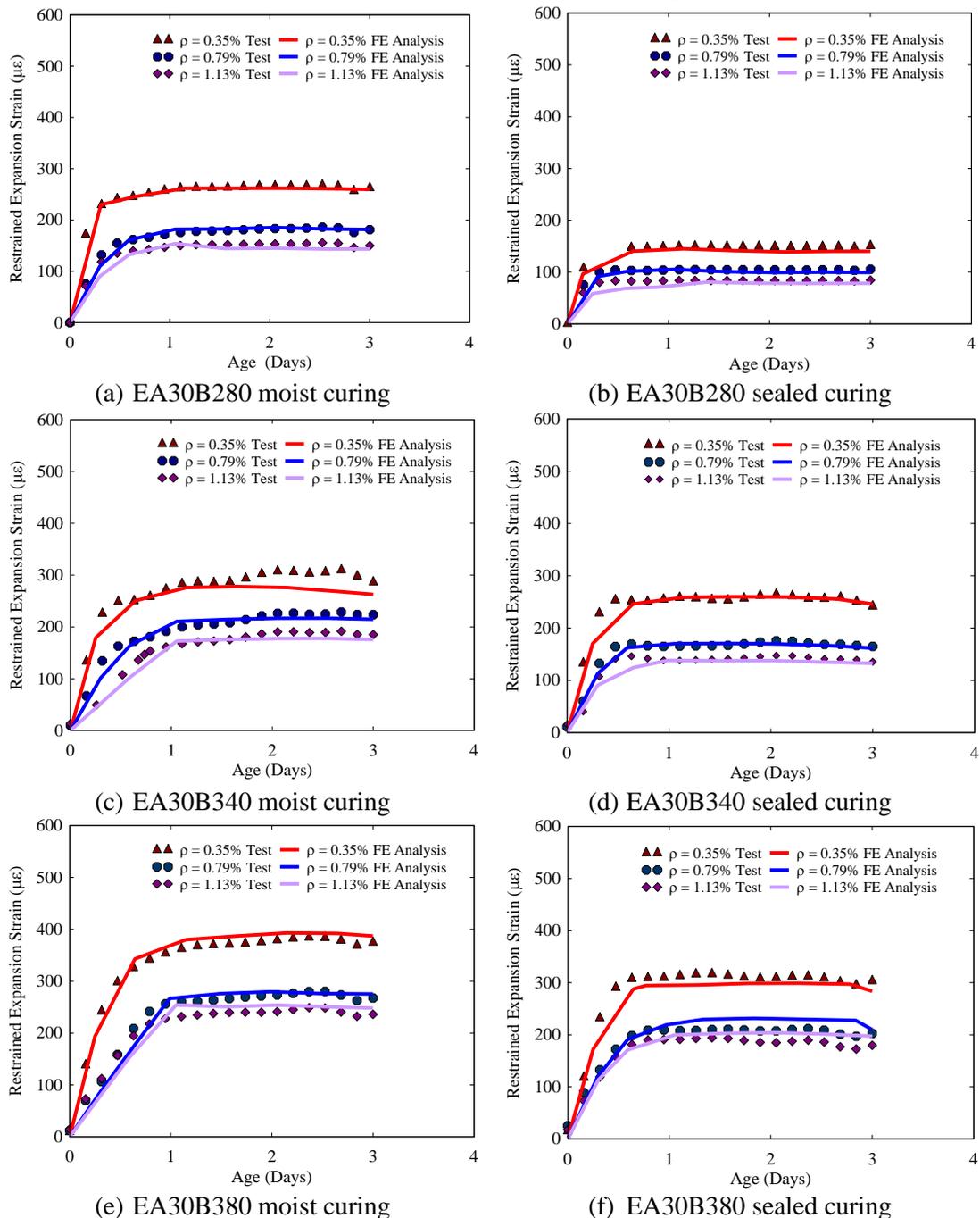
(f) EA30B380 sealed curing

Figure 3.11 Restrained expansion strain comparison between test and FE analysis of expansive concrete specimens with different reinforcement ratios

In restrained specimens, an increase in the reinforcement ratio causes an increase in the compressive stress during the expansion process. When the process of expansion occurs, the

expansive product expands in multiple directions. As the reinforcement ratio increases, the area near the rebar reinforcement produces a larger compressive creep. Thus, causing an increase in the degree of restraint. As a result of this compressive creep causes the level of restrained expansion strain is reduced. In addition, due to the high degree of restraint, the possibility of expansive product entering the pores during the expansion process is also higher. Consequently, the restrained expansion strain decreased despite using the same amount of expansive agent and binder. This pattern of restrained expansion strain also occurs during moist and sealed curing, so it can be concluded that the reinforcement ratio is one of the main factors that influence the levels of restrained expansion strain. The comparison results of the FE analysis and the experimental reveal similar restrained expansion patterns for various reinforcement ratios throughout the whole series. In addition, the estimation results for the entire series of reinforcement ratio variations matched well with the experimental results. Therefore, it can be concluded that this method for estimating expansion strains can be used to estimate restrained expansion strains with varying reinforcement ratio ranges. However, it is necessary to consider the reinforcement ratio employed, as the reinforcement ratio in this study only varies up to 8.0%.

3.4.4 Influence of amount of expansive additive

In both free and constrained conditions, the amount of expansive additive plays an important role in the expansion procedure. **Figure 3.12** shows the results of restrained expansion strain with various amounts of expansive additive but using the same reinforcement ratio. The results of the study indicate that as the amount of expansive additive increases, so does the amount of expansion produced. This is due to the increasing amount of expansive additives resulting in a rise in the production of expansive products. The estimation results from FE analysis show a similar restrained expansion strain pattern as the experimental results. It can be concluded that the estimation method based on FE analysis in this study can be used to estimate the restrained expansion strain with various amounts of expansive additive. In this study, the expansive additive amount ranges from 0 kg/m^3 to 40 kg/m^3. It is not advised to use more than 40 kg/m^3 of expansive additive because it can drastically reduce the compressive strength of concrete.

(a) B280 moist curing   (b) B280 sealed curing

(c) B340 moist curing   (d) B340 sealed curing

(e) B380 moist curing   (f) B380 sealed curing
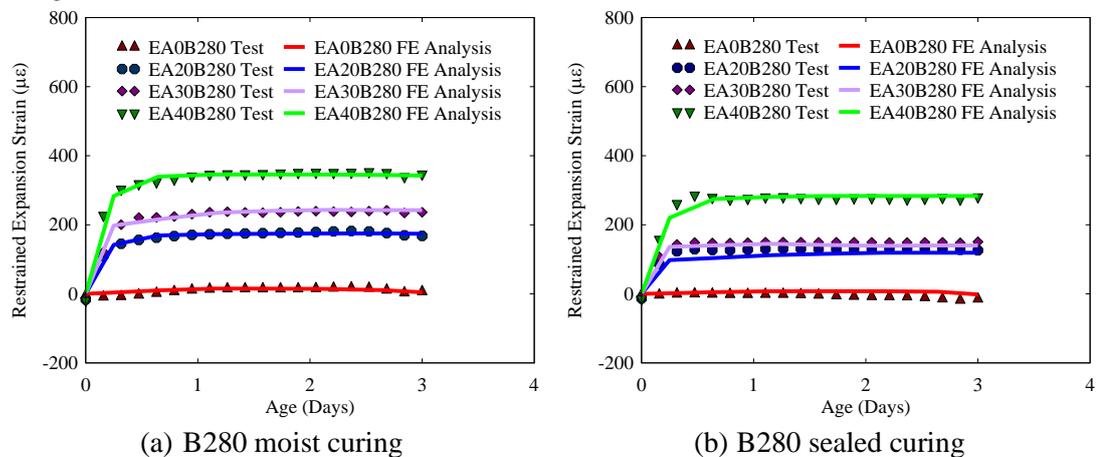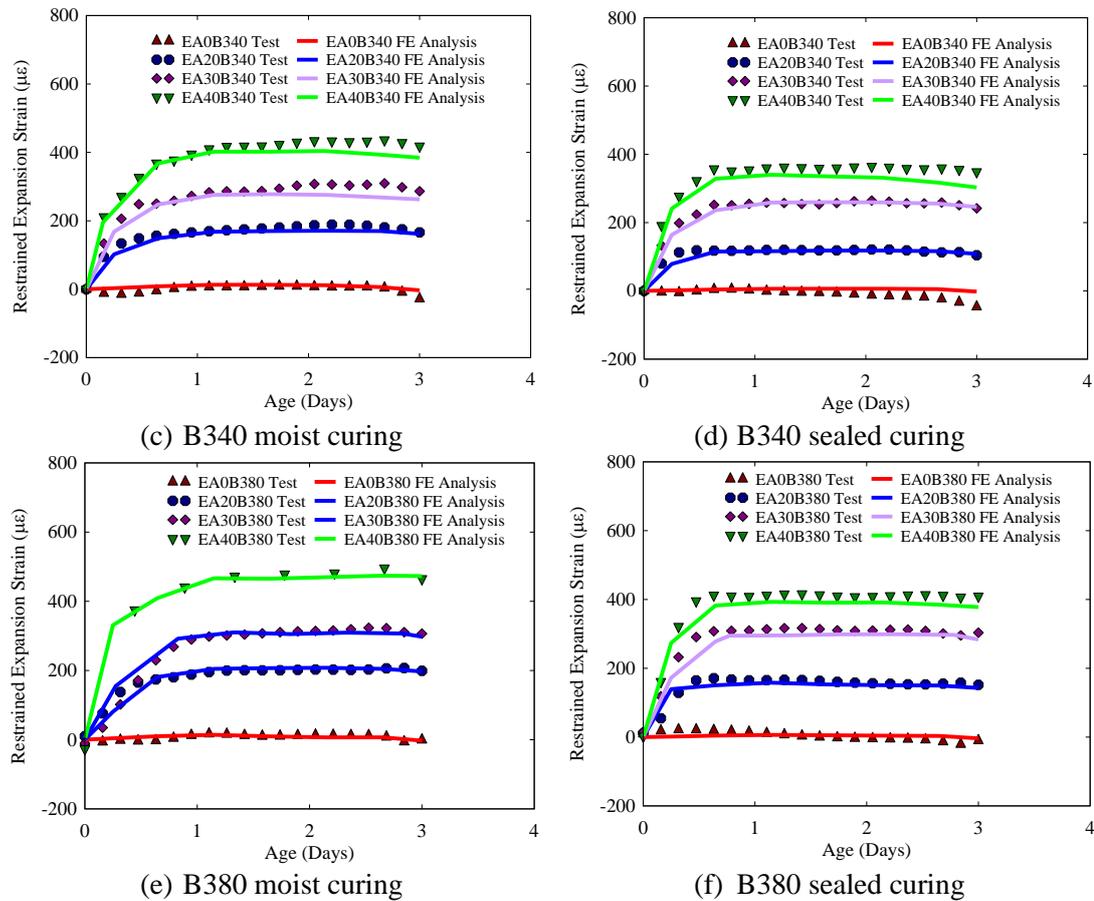
Figure 3.12 Restrained expansion strain of expansive concrete specimens with different amount of expansive additive

3.4.5 Influence of binder content

In addition to the amount of expansive additive, the amount of binder also influences the level of restrained expansion strain in expansive concrete. **Figure 3.13** shows the result of restrained expansion strain with different binder content. This study employs various binder amounts, including 280 kg/m^3, 340 kg/m^3, and 380 kg/m^3.

(a) Moist curing   (b) Sealed curing
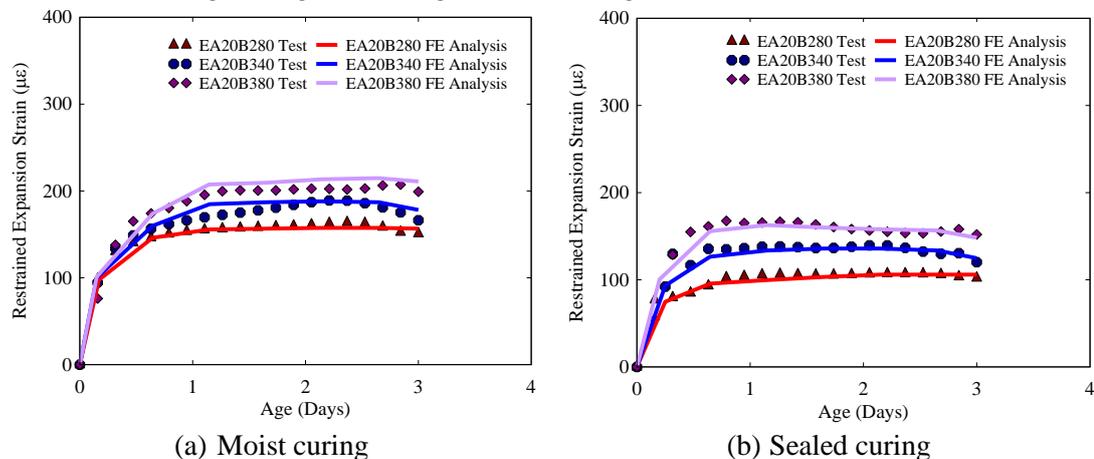
Figure 3.13 Restrained expansion strain of expansive concrete specimens with different amount of binder

The FE analysis and experimental results showed that the restrained expansion strain increased as the amount of binder was increased. This is because expansion occurs mainly in the paste part of concrete. Thus, as the number of binders in expansive concrete increases, so does the paste content. The estimation results of the FE analysis also show that the restrained expansion strain obtained is compatible with the experimental results even though using different binder contents.

3.4.6 Influence of curing conditions

This study also investigates the effect of curing conditions on restrained expansion strain for expansive concrete. The curing conditions checked were the type of curing and curing temperature. **Figure 3.14** shows the results of restrained expansion strain with different types of curing, namely moist and sealed curing. The experimental results and FE analysis show that moist curing always produces a higher level of restrained expansion than sealed curing. Due to the ability of moist curing to maintain the moisture of the concrete throughout the hydration process, the expansion process is optimized. This FE analysis results exhibit the same pattern as the experimental results. Therefore, it can be concluded that the FE analysis is sufficient to estimate the restrained expansion strain for various curing types.

(a)   EA30B280

(b)   EA40B280

(c)   EA30B380

(d)   EA40B380
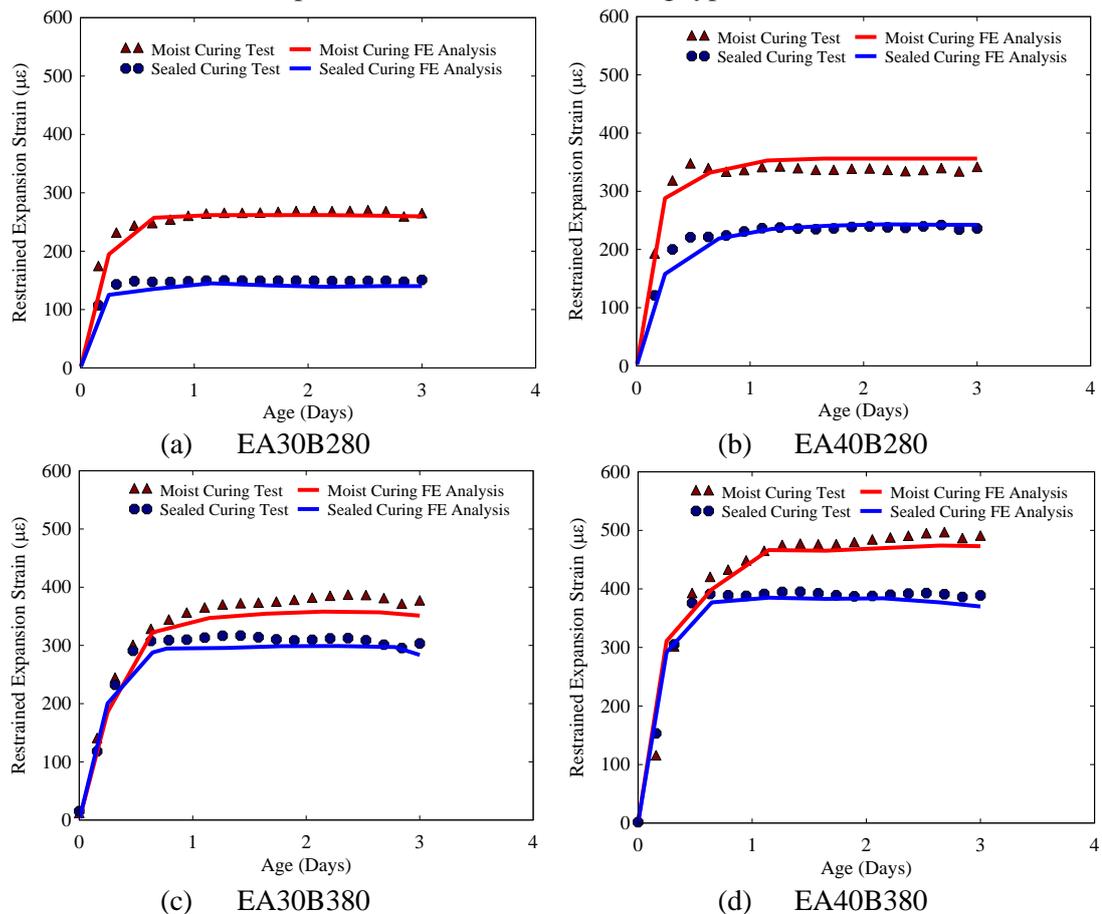
Figure 3.14 Restrained expansion strain of expansive concrete specimens with different curing conditions

3.4.7 Influence of curing temperature

Figure 3.15 shows the effects of different curing temperatures on the expansion strain under restraint. In this study, the curing temperatures were 28 °C, 35 °C, and 40 °C. **Figure 3.15a** and **Figure 3.15b** shows the results of specimens using the amount of expansive additive 30 kg/m3, the amount of binder 280 kg/m^3, and a reinforcement ratio of 1.13%. While **Figure 3.15c** and **Figure 3.15d** shows the results of restrained expansion strain with the amount of expansive additive 30 kg/m^3, amount of binder 380 kg/m^3, and reinforcement ratio of 0.79%. The experimental results showed that the restrained expansion strain increased along with increased curing temperature. This is because the curing temperature accelerates the expansion process to be faster even though the expansive concrete is in restraint condition. In addition, the high temperature accelerates the hydration process, but the low rigidity of the concrete allows the expansive product to expand more freely, leading to enhanced degree of expansion at a high curing temperature. The results of the FE analysis demonstrated that both the curing type and the various curing temperatures resulted in a restrained expansion strain that was highly consistent with the experimental results. Thus, it can be concluded that this estimation method can predict restrained expansion strain under various conditions, including moist and sealed curing and curing temperatures ranging from 28 to 40 °C.

(a) EA30B280ρ1.13 moist curing

(b) EA30B280ρ1.13 sealed curing

(c) EA30B380ρ0.79 moist curing

(d) EA30B380ρ0.79 sealed curing
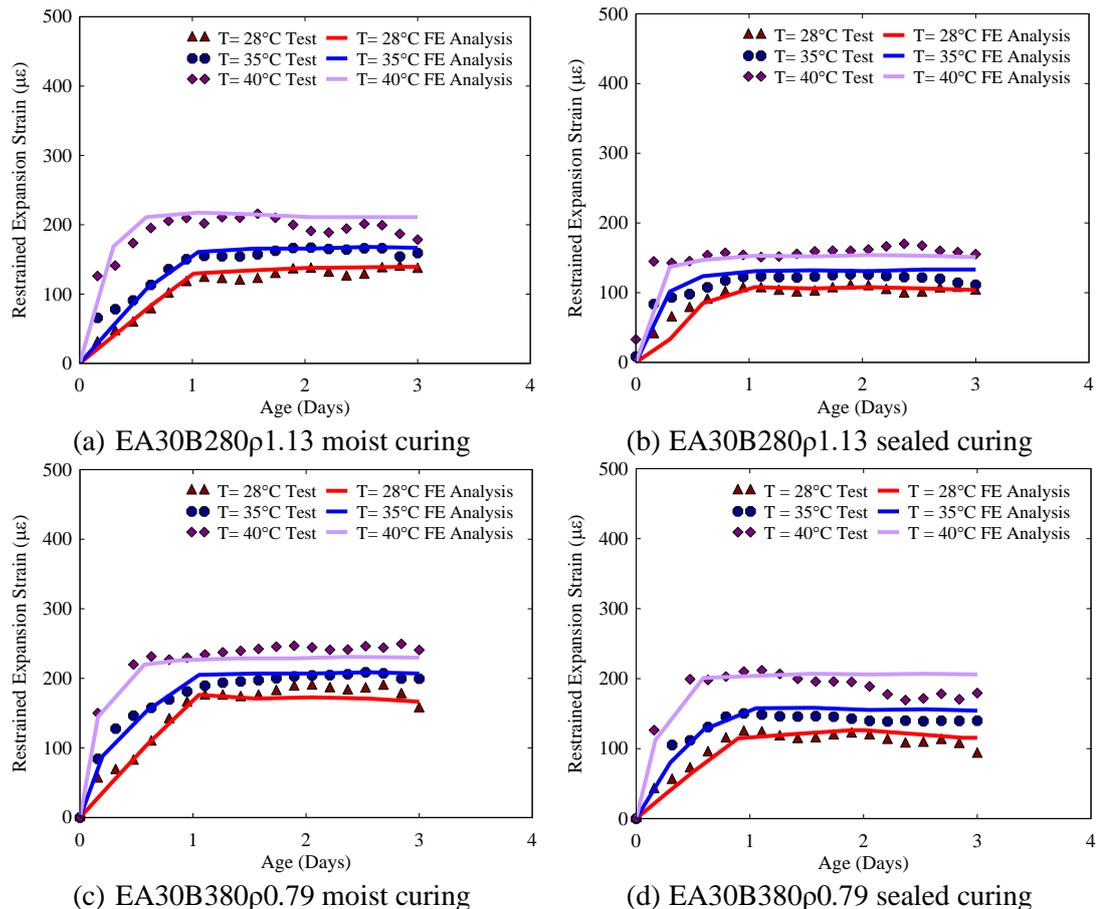
Figure 3.15 Restrained expansion strain of expansive concrete specimens with different curing temperatures

3.4.8 Influence of amount of fly ash

In recent years, fly ash in concrete has become commonplace. The use of fly ash can help reduce heat in the concrete during the hydration process. The effect of using fly ash on the level of restrained expansion strain can be seen in **Figure 3.16** for series V and **Figure 3.17** for series VI. **Figure 3.16** and **Figure 3.17** show the comparison results for series V and VI. It should be noted that the test results in series V and VI were not used to establish the reduction factor in **Eq. 3.15** but were intended to validate the proposed equation and analysis. Experimental results and FE analysis indicate that the level of restrained expansion strain increases as fly ash content in expansive concrete rises. This is because fly ash contains calcium oxide, which can cause expansion strain during the hydration process.

(a) Without fly ash   (b) With fly ash
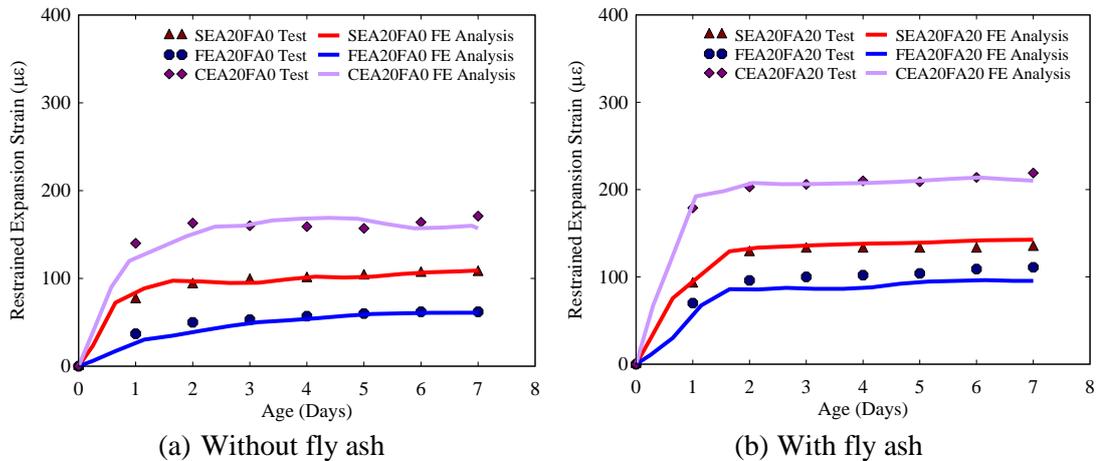
Figure 3.16 Restrained expansion strain comparison between test and FE analysis for
Series V ($\rho = 0.79\%$)

It can be seen from the figures that the test results of mixtures in series V and VI with various fly ash replacement percentages, types of expansive additive (SEA, FEA, CEA, and HEA), and restraining steel ratios can also be well simulated. The proposed reduction factors will be used for analysis and design purposes, including the required dosage of expansive additive.

(a) 20% fly ash replacement   (b) 30% fly ash replacement
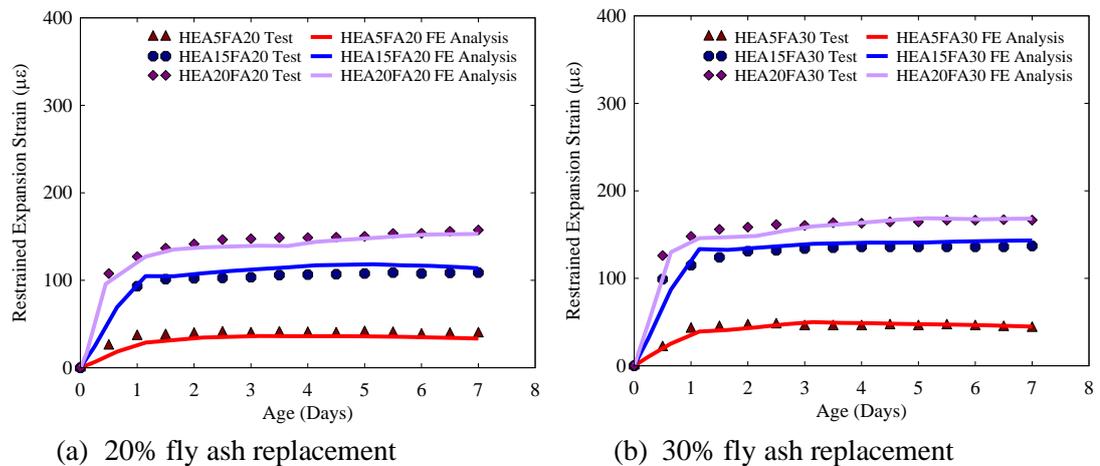
Figure 3.17 Restrained expansion strain comparison between test and FE analysis for
Series VI ($\rho = 1.57\%$)

3.5 Conclusions

This study can draw several conclusions based on the estimation of restrained expansion strain for reinforced expansive concrete.

a) Restrained expansion strain increases when the amount of expansive additive, binder content, fly ash content, water to binder ratio, and curing temperature increases.

b) A large reinforcement ratio causes the restrained expansion strain to be reduced. This is because the reinforcing bar causes compression stress during the expansion.

c) Results of FE analysis of restrained expansion overestimate the test results if the loss of ability to produce expansion due to void filling of expansive products and compression creep is not considered. This loss of ability to produce expansion in restrained expansive concrete is considered by introducing a reduction factor to determine effective free expansion strain from the free expansion strain.

d) The reduction factor equation considers several factors, including binder content, expansive additive dosage, fly ash content, water to binder ratio, reinforcement ratio, curing temperature, and type of curing.

e) The use of effective free strain from our proposed equations, as input in FE analysis, can accurately predict the restrained expansion strain of the tested expansive concrete specimens.

References

[1] K. Huang, X. Shi, D. Zollinger, M. Mirsayar, A. Wang, and L. Mo, "Use of MgO expansion agent to compensate concrete shrinkage in jointed reinforced concrete pavement under high-altitude environmental conditions," *Constr. Build. Mater.*, vol. 202, pp. 528–536, 2019, doi: 10.1016/j.conbuildmat.2019.01.041.

[2] Eriksson & Fritzson, *Crack Control of Extended Concrete Walls*. Sweden: Chalmers University of Technology, 2014.

[3] M. Al-gburi, *Restraint Effects in Early Age Concrete Structures*, no. September. Sweden: Lulea University of Technology, 2015.

[4] N. D. Van, E. Kuroiwa, J. Kim, H. Choi, and Y. Hama, "Influence of restrained condition on mechanical properties, frost resistance, and carbonation resistance of expansive concrete," *Materials (Basel).*, vol. 13, no. 2136, pp. 1–16, 2020.

[5] Y. Tsuji, "Methods of estimating chemical prestress and expansion distribution in expansive concrete subjected to uniaxial restraint," *Concr. Libr. JSCE*, vol. 4, no. 3, pp. 131–143, 1984.

[6] L. Wang *et al.*, "Pore structural and fractal analysis of the effects of MgO reactivity and dosage on permeability and F-T resistance of concrete," *Fractal Fract.*, vol. 6, no. 113, pp. 1–17, 2022, doi: 10.3390/fractalfract6020113.

[7] V. Semianiuk, V. Tur, M. F. Herrador, and M. Paredes G., "Early age strains and self-stresses of expansive concrete members under uniaxial restraint conditions," *Constr. Build. Mater.*, vol. 131, pp. 39–49, 2017, doi: 10.1016/j.conbuildmat.2016.11.008.

[8] M. Wyrzykowski, G. Terrasi, and P. Lura, "Expansive high-performance concrete for chemical-prestress applications," *Cem. Concr. Res.*, vol. 107, pp. 275–283, 2018, doi: 10.1016/j.cemconres.2018.02.018.

[9] L. Wang, C. Shu, T. Jiao, Y. Han, and H. Wang, "Effect of assembly unit of expansive agents on the mechanical performance and durability of cement-based materials," *Coatings*, vol. 11, no. 6, pp. 1–10, 2021, doi: 10.3390/coatings11060731.

[10] J. Han, D. Jia, and P. Yan, "Understanding the shrinkage compensating ability of type K expansive agent in concrete," *Constr. Build. Mater.*, vol. 116, pp. 36–44, 2016, doi: 10.1016/j.conbuildmat.2016.04.092.

[11]   R. Dumaru, W. Saengsoy, and S. Tangtermsirikul, "Effect of restraining and curing conditions on expansion and shrinkage of expansive concrete," *Proc. 2020 Int. Multi-Conference Adv. Eng. Technol. Manag.*, pp. 165–170, 2020.

[12]   C. Xu, H. Chengkui, and Z. Peng, "Expansive behaviors of self-stressing concrete under different restraining conditions," *J. Wuhan Univ. Technol. Mater. Sci. Ed.*, vol. 26, no. 4, pp. 780–785, 2011, doi: 10.1007/s11595-011-0310-5.

[13]   X. S. Qu, Y. Deng, G. J. Sun, Q. Liu, and Q. Liu, "Eccentric compression behaviour of rectangular concrete-filled steel tube columns with self-compacting lower expansion concrete," *Adv. Struct. Eng.*, vol. 25, no. 3, pp. 491–510, 2022, doi: 10.1177/13694332211054228.

[14]   G. Peiwei, X. Shao-yun, C. Xiong, L. Jun, and L. Xiao-lin, "Research on autogenous volume deformation of concrete with MgO," *Constr. Build. Mater.*, vol. 40, pp. 998–1001, 2013, doi: 10.1016/j.conbuildmat.2012.11.025.

[15]   X. Lei, H. Chengkui, and L. Yi, "Expansive performance of self-stressing and self-compacting concrete confined with steel tube," *J. Wuhan Univ. Technol. Mater. Sci. Ed.*, vol. 22, no. 2, pp. 341–345, 2007, doi: 10.1007/s11595-005-2341-2.

[16]   American Concrete Institute Committee, *ACI 223R-10 Guide for the use of shrinkage compensating concrete*. Farmington Hills: American Concrete Institute, 2010.

[17]   Japan Society of Civil Engineers Committee, *JSCE No. 23: Recommended practice for expansive concrete*, no. 23. Tokyo: Concrete Library of JSCE, 1994.

[18]   F. W. Lu, S. P. Li, and G. Sun, "Nonlinear equivalent simulation of mechanical properties of expansive concrete-filled steel tube columns," *Adv. Struct. Eng.*, vol. 10, no. 3, pp. 273–281, 2007, doi: 10.1260/136943307781422271.

[19]   W. Huang, Z. Fan, P. Shen, L. Lu, and Z. Zhou, "Experimental and numerical study on the compressive behavior of micro-expansive ultra-high-performance concrete-filled steel tube columns," *Constr. Build. Mater.*, vol. 254, no. 119150, pp. 1–10, 2020, doi: 10.1016/j.conbuildmat.2020.119150.

[20]   L. Xu, J. Pan, and X. Yang, "Mechanical performance of self-stressing CFST columns under uniaxial compression," *J. Build. Eng.*, vol. 44, no. 103366, pp. 1–14, 2021, doi: 10.1016/j.jobe.2021.103366.

[21]   S. H. Myint, G. Tanapornraweekit, and S. Tangtermsirikul, "Prediction of restrained expansion and shrinkage strains of reinforced concrete specimens by using finite element analysis," in *Lecture Notes in Civil Engineering*, 2021, vol. 101, pp. 1849–1859. doi: 10.1007/978-981-15-8079-6_170.

[22]   H. Prayuda, R. Dumaru, G. Tanapornraweekit, S. Tangtermsirikul, W. Saengsoy, and K. Matsumoto, "Estimation of restrained expansion strain of reinforced expansive concrete considering mixture and curing conditions," *Constr. Build. Mater.*, vol. 322, no. 126386, pp. 1–15, 2022, doi: 10.1016/j.conbuildmat.2022.126386.

[23]   J.-X. Zhang, H.-M. Lyu, S.-L. Shen, and D.-W. Hou, "Investigation of crack control of underground concrete structure with expansive additives," *J. Mater. Civ. Eng.*, vol. 33, no. 1, pp. 1–8, 2021, doi: 10.1061/(asce)mt.1943-5533.0003528.

[24]   X. Y. Jing, X. H. Liu, and X. Zhang, "Thermal stress compensation of MgO concrete in construction of high arch dams in cold areas," *Adv. Mater. Res.*, vol. 852, no. February 1994, pp. 427–431, 2014, doi: 10.4028/www.scientific.net/AMR.852.427.

[25]   P. Sutthiwaree, *A study on behavior and improvement of expansion of concrete with expansive additive and design method*. Pathum Thani: Sirindhorn International Institute of Technology, Thammasat University, 2014.

[26]   D. T. Nguyen, *Expansion Behaviors and Prediction of net expansion of concrete with hyper expansive additive*. Sirindhorn International Institute of Technology, Thammasat University, 2010.

[27]   ASTM International, *C150/C150M-16: Standard specification for portland cement*,

ASTM Inter. West Conshohocken: ASTM International, 2015. doi: 10.1520/C0150.

[28] Thailand Standards Association, *TIS 2135-2545: Coal fly ash for use as an admixture in concrete*. Bangkok: Thailand Industrial Standard, 2003.

[29] ASTM International, *ASTM C618-19: Standard specification for coal fly ash and raw or calcined natural pozzolan for use in concrete*. West Conshohocken: ASTM International, 2019. doi: 10.1520/C0618-19.2.

[30] ASTM International, *ASTM C33/C33M-18: Standards specification for concrete aggregates*. West Conshohocken: ASTM International, 2018. doi: 10.1520/C0033.

[31] ASTM International, *ASTM C494/C949M-19: Standard specification for chemical admixtures for concrete*. West Conshohocken: ASTM International, 2019.

[32] ASTM International, *ASTM C878/C878M-03: Standard test method for restrained expansion of shrinkage-compensating concrete*. 2015.

[33] LSTC, *LS-DYNA keyword user's manual volume II*, vol. I. California: Livermore Software Technology Corporation, 2017.

[34] CEIB, *CEB Bulletin No. 213/214: CEB-FIP model code 90*. Lausanne: Thomas Telford Services, 1990.

[35] LSTC, *LS-DYNA keyword user's manual volume II: material models*, vol. II. LIVERMORE SOFTWARE TECHNOLOGY CORPORATION (LSTC), 2018.

[36] Y. D. Murray, *Users manual for LS-DYNA concrete material model 159*, no. May. Virginia, 2007.

[37] Y. Murray, A. Abu-Odeh, and R. Bligh, "Evaluation of LS-DYNA Concrete Material Model 159," *Rep. No. FHWA-HRT-05-063*, no. May, p. 206, 2007.

[38] H. Jiang and J. Zhao, "Calibration of the continuous surface cap model for concrete," *Finite Elem. Anal. Des.*, vol. 97, pp. 1–19, 2015, doi: 10.1016/j.finel.2014.12.002.

[39] L. E. Schwer and Y. D. Murray, "Continuous surface cap model for geomaterial modeling: A new LS-DYNA material type," *7th Int. LSDYNA Users Conf.*, no. 2, pp. 35–50, 2002.

[40] B. Abdelwahed, B. Belkassem, and J. Vantomme, "Reinforced concrete beam-column inverted knee joint behaviour after ground corner column loss-numerical analysis," *Lat. Am. J. Solids Struct.*, vol. 15, no. 10, pp. 1–15, 2018, doi: 10.1590/1679-78254515.

[41] M. Bermejo, J. M. Goicolea, F. Gabaldón, and A. Santos, "Impact and explosive loads on concrete buildings using shell and beam type elements," *3rd Int. Conf. Comput. Methods Struct. Dyn. Earthq. Eng.*, no. May, pp. 1–14, 2011.

[42] R. M. Brannon and S. Leelavanichkul, "Survey of four damage models for concrete," 2009.

[43] O. Mkrtychev, M. Dudareva, and M. Andreev, "Verification of the reinforced concrete column bar model based on the test results," *MATEC Web Conf.*, vol. 251, pp. 1–6, 2018, doi: 10.1051/matecconf/201825104014.

[44] Y. Parfilko, *Study of damage progression In CSCM Concretes Under repeated impacts*. Rechester Institute of Technology, 2017.

[45] S. Paudel, G. Tanapornraweekit, and S. Tangtermsirikul, "Numerical study on seismic performance improvement of composite wide beam-column interior joints," *J. Build. Eng.*, vol. 46, no. September 2021, pp. 1–26, 2022, doi: 10.1016/j.jobe.2021.103637.

[46] Y. Wu, J. E. Crawford, and J. M. Magallanes, "Performance of LS-DYNA concrete constitutive models," in *12th International LS-DYNA Users conference*, 2012, no. 1, pp. 1–14.

[47] E. Cadoni, M. Dotta, D. Forni, G. Riganti, and H. Kaufmann, "Experimental and numerical analysis of the dynamic behaviour in tension of an armour steel for applications in defence industry," *EPJ Web Conf.*, vol. 94, pp. 1–6, 2015, doi: 10.1051/epjconf/20159405004.

[48] F. Duddeck, M. Bujny, and D. Zeng, "Topology optimization methods based on

nonlinear and dynamic crash simulations," *11th Eur. LS-DYNA Conf.*, pp. 1–13, 2017.

[49]   S. A. Ranjha, R. W. Bielenberg, R. Faller, S. Rosenbaugh, J. D. Reid, and C. Stolle, "Modeling and simulation of PCB cover plate for large open joints," *15 th Int. LS-DYNA Users Conf.*, pp. 1–13, 2018.

[50]   M. Roth and S. Kolling, "Crash and vibration analysis of rotors in a roots vacuum booster," *7th Eur. LS-Dyna Conf.*, pp. 1–10, 2009.

[51]   M. Vogler, S. Kolling, and A. Haufe, "A constitutive model for polymers with a piecewise linear yield surface," *LS-DYNA Anwender Forum*, vol. 6, no. 1, pp. 275–276, 2007, doi: 10.1002/pamm.200610118.

[52]   LSTC, *Basic tutorials: LS-DYNA/LS-Prepost ex.2 tensile test*, vol. 31. Livermore Software Technology Corporation, 2011.

[53]   T. B. T. Nguyen, R. Chatchawan, W. Saengsoy, S. Tangtermsirikul, and T. Sugiyama, "Influences of different types of fly ash and confinement on performances of expansive mortars and concretes," *Constr. Build. Mater.*, vol. 209, pp. 176–186, 2019, doi: 10.1016/j.conbuildmat.2019.03.032.

[54]   N. D. Van, H. Choi, and Y. Hama, "Modeling early age hydration reaction and predicting compressive strength of cement paste mixed with expansive additives," *Constr. Build. Mater.*, vol. 223, pp. 994–1007, 2019, doi: 10.1016/j.conbuildmat.2019.07.290.

CHAPTER 4

ESTIMATION OF RESTRAINED EXPANSION AND SHRINKAGE BEHAVIOR OF EXPANSIVE CONCRETE STRUCTURES

4.1 Introduction

Expansive concrete made with expansive cement or expansive additive has been widely used in various civil constructions in various countries. Expansive concrete is ideally suited for constructions with thin structures and large surface areas. Additionally, expansive concrete is suitable for structures directly exposed to the environment. This is because these structures have a high possibility of cracking due to shrinkage. Previous research indicates that expansive concrete has been used to construct in various structures, including bridge girders, dams, pavements, concrete walls, industrial floors, slabs on grade, beams, and foundations [1]–[10]. Based on this investigation, it can be concluded that expansive concrete effectively prevents shrinkage cracking in concrete at an early age. In addition, several factors that significantly impact the level of expansion can be determined, such as the degree of restraint, curing conditions, mix proportion, and exposure environment. During the design stage, it is necessary to consider the variables that influence the level of expansion of expansive concrete to produce sufficient structures resistant to shrinkage cracking.

ACI 223R-10 [11] and JSCE No. 23 [12] require measuring the restrained expansion strain on a laboratory scale using prism specimens during process design. The purpose of these measurements is to estimate the expansion level by considering the effects of the reinforcement ratio on the concrete. One factor that affects the expansion level in expansive concrete is the degree of restraint. A structure with a high degree of restraint produces low restrained expansion, while a structure with a low degree of restraint produces more restrained expansion. Generally, rebar reinforcement is considered an internal restraint, while neighboring structures and friction are considered external restraints. As a result of the complexity of the actual structure, laboratory measurements of restrained expansion cannot be used to make accurate predictions compared with actual conditions. In addition, the exposure environment has a significant impact on the degree of expansion, whereas laboratory testing can be conducted in a controlled environment, which does not represent the environment in the actual structure. The estimation of restrained expansion strain provided in the current standards is insufficient to represent the actual conditions in expansive concrete structures. Therefore, it is necessary to conduct more extensive research in order to produce a precise estimation method to account for the influence of the configuration of the structure on the restrained expansion strain. The quantity of the expansive additive used for the expansive concrete structure must be calculated accurately. A significant decrease in compressive strength can result from using a large amount of expansive additive, leading to overexpansion and microcracking in the concrete [13]–[15].

Developing a comprehensive estimation method necessitates complex and expensive procedures, as precise measurements of the actual structure must be taken, which requires considerable time, effort, and cost. Finite element (FE) analysis is one method commonly used to predict the performance of civil infrastructure. The estimation of the level of expansion in expansive concrete has also been carried out by several previous researchers, both on the experimental scale [16]–[20] and on the actual structure scale [21], [22]. Estimation of restrained expansion strain using FE analysis is anticipated to expedite the design process for

expansive concrete without the need for direct experiments, thereby reducing design time. In addition, using FE analysis allows for the estimation of restrained expansion strain to represent the actual condition of the structure. Several studies applied experimental free expansion strain as an input in FE analysis to investigate the strain behavior of expansive concrete [20], [21]. Based on these studies, the FE analysis using free expansion strain as input always overestimates the actual restrained expansion strain of the expansive concrete.

This study estimates the restrained expansion strain in expansive concrete using the measured free expansion strain as input to FE analysis. However, the expansion mechanism in free conditions behaves differently than in restricted conditions for expansive concrete. The influence of expansive products on the pore structure of expansive concrete depends on the amount of expansive additive, the expansive agent reactivity, and the restrained conditions [23], [24]. There is no restraining stress in expansive concrete under free conditions, so a larger expansion strain is observed than in expansive concrete under restrained conditions [15], [25]. During the initial hydration process, the expansive agent can react rapidly with water to produce large amounts of expansive products. However, the expansive product does not change much the pore structures since there is no restraining compressive stress on expansive concrete with free conditions [24], [26]–[28]. In the case of expansive concrete under restraint conditions, some losses of expansion can occur in restrained expansive concrete due to the effects of pores filling by expansive products and compression creep during the early expansion under restraint. Under restraining stress, a portion of the expansive products is forced to enter the voids in concrete, reducing the ability to produce expansion. Also, compression creep does not occur in the free expansion concrete as the free expansion causes no compressive stress. On the other hand, the restraint causes compressive stress in the expanding concrete, so compression creep arises in the restrained expansion concrete at an early age [25], [29]. As most of the FE models are at a macroscopic level, the concrete pores and pore filling of the expansive product during the expansion cannot be simulated. Therefore, the effective free expansion strain is required to be one of the inputs in FE analysis to estimate the expansion of expansive concrete under restraint. With this expansion mechanism, the free expansion strain cannot be used directly as input to the FE analysis. Some reduction factor is required to produce an effective free expansion strain that considers the effect of reducing the pore structure due to restraint and compressive creep.

Chapter 3 discussed the equation of reduction factor generated through lab tests. In this chapter, the reduction factor equation will be used to calculate the effective free expansion strain, which can then be used to estimate the level of expansion in the actual expansive concrete structure. This investigation involves measuring the strain on the actual structure and estimating the strain using FE analysis with effective free strain as an input. Measurements on the actual structure are carried out on several types of structures, namely slabs on grade, slabs on beam, slabs on pile, and water tank walls. Strain measurement is carried out on normal and expansive concrete to estimate the effectiveness of expansive concrete in preventing shrinkage cracking. In addition, this measurement can examine the effect of the degree of restraint and the direction of the strain based on the configuration of the structures. This research aims to produce a comprehensive estimation method for expansive concrete structures by considering the main factors that affect the level of expansion in actual structures. Besides, this research is expected to prove that the reduction factor equation to generate effective free strain can be used to estimate the level of expansion under restraint conditions.

4.2 Field investigation

4.2.1 Scope of the study

This study investigates the early age strain behavior of four types of actual structures, including slabs on grade, slabs on beam, slabs on pile, and water tank walls. Each structure has different mix proportion and measurement objectives. The general information and purpose of the measurement for each structure are shown in **Table 4.1**. In general, the purpose of this measurement is to study the effect of the effectiveness of the expansive agent, the effect of the degree of restraint (internal and external), and the effect of strain direction. In the slabs on grade and slabs on beam, there are two different construction sites, whereas the slab on pile and water tank wall uses only one measurement location with multiple structural components. The expansive agent dosage in this study was based on JSCE. No. 23 states that the amount of expansive additive used to prevent shrinkage cracking should not exceed 30 kg/m^3. The compressive strength will decrease significantly if the amount of expansive additive used exceeds 30 kg/m^3 [12]. This study used two types of expansive additive (EA), namely a calcium sulfoaluminate (C-S-A) and a combination of calcium oxide (CaO) with calcium sulfoaluminate (C-S-A + CaO) based expansive agents.

Table 4.1 General information of the investigated structures

Structures		Amount of EA (kg/m^3)	Type of Expansive Agent	Purpose of measurement
Slab on Grade Site 1	SG-1-NC	-	-	- effect of type of expansive agent.
	SG-2-EA	20	C-S-A	- effect of internal restraint.
	SG-3-EA	25	C-S-A + CaO	- effect of strain direction.
Slab on Grade Site 2	SG-4-EA	30	C-S-A + CaO	- effect of dimension of the structures
	SG-5-EA			- effect of strain direction.
Slab on Beam Site 1	SB-1-NC	-	-	- effect of type of expansive agent.
	SB-2-EA	25	C-S-A + CaO	- effect of internal and external restraint.
	SB-3-EA	20	C-S-A	- effect of strain direction.
Slab on Beam Site 2	SB-4-NC	-	-	- effect of type of expansive agent.
	SB-5-EA	30	C-S-A + CaO	- effect of internal and external restraint.
Slab on Pile	SP-1-NC	-	-	- effect of type of expansive agent.
	SP-2-EA	30	C-S-A + CaO	- effect of internal and external restraint.
Water Tank Wall	WT-1-EA	30	C-S-A + CaO	- effect of dimension of the structures.
	WT-2-EA			- effect of internal and external restraint.

In addition, to analyze the strain behavior of expansive concrete structures, several specimens were tested for concrete compressive strength and length change in free conditions (no restraint). The compressive strength and free strain results will be used as input in the FE analysis. Length change measurement was carried out based on ASTM C157 [30] using prism specimens, while the compressive strength test was carried out according to ASTM C39 [31]. The compressive strength was performed on the cube specimens (100 x 100 x 100 mm^3) at 3, 7, and 28 days. Specimens for length change were demolded 8 ± 2 hours after casting. However, the length change measurements of the specimens were carried out simultaneously according to the measurement of the structure at the construction site. Specimens were placed at the construction site during the measurement period to ensure that the condition of the specimens remained the same and accurately reflected the field circumstances.

4.2.2 Materials and mix proportions

Binders used in this experiment consist of an Ordinary Portland Cement (OPC) type I according to ASTM C150 [32], a class 2b fly ash according to TIS 2135 [33] from Mae Moh

power plant, and class 2a fly ash from BLCP power plant, Thailand, and two types of expansive additive (EA) namely a calcium sulfoaluminate (C-S-A) and a combination of calcium oxide (CaO) with calcium sulfoaluminate (C-S-A + CaO) based expansive agents. Mae Moh fly ash was used in the slabs on grade at construction site 1, slabs on beam, and water tank walls, while BLCP fly ash was used for slabs on grade construction site 2 and slabs on pile. This study did not evaluate the influence of fly ash on the degree of expansion and shrinkage strain. The chemical compositions of all binders used in this study are shown in **Table 4.2**. Three different mix proportions were used in slabs on grade at construction site 1: SG-1-NC without expansive additive, SG-2-EA with C-S-A based expansive additive, and SG-3-EA with C-S-A + CaO based expansive additive. The same type of C-S-A + CaO-based expansive additive was used for the slabs SG-4-EA, SG-5-EA, slabs on beam in construction site 2 (SB-5-EA), slabs on pile (SP-2-EA), and water tank walls (WT-1-EA and WT-2-EA). The slabs on beam were cast in 3 different mix proportions, SB-1-NC used normal concrete, SB-2-EA used a combination of CaO and C-S-A based expansive agent concrete, and SB-3-EA used C-S-A based expansive agent concrete. **Table 4.3** shows the concrete mix proportions for casting all structures in this study.

Table 4.2 Chemical compositions of binders

Binder	SiO_2	Al_2O_3	Fe_2O_3	CaO	MgO	SO_3	K_2O	Na_2O	SrO	MnO
OPC	19.60	5.40	3.30	63.20	1.40	2.90	0.60	0.20	-	-
FA (Mae Moh)	36.18	20.21	13.89	18.74	2.69	3.74	1.14	2.29	-	-
FA (BLCP)	34.52	17.22	14.01	22.61	3.16	3.11	2.12	2.00	-	-
EA (C-S-A)	1.93	5.03	1.22	69.47	1.04	17.70	0.05	0.01	0.02	0.03
EA (C-S-A + CaO)	2.45	5.21	0.19	61.85	0.60	25.80	-	-	-	0.11

Table 4.3 Concrete mix proportions used for casting the structures.

Structures		OPC (kg)	FA (kg)	EA (kg)	Class of FA	Water (kg)	Fine Agg (kg)	Coarse Agg (kg)	Type D (g)	Type F (g)
Slab on grade site1	SG-1-NC	270	30	-	2b (Mae Moh)	190	840	1100	1090	500
	SG-2-EA	250	30	20						900
	SG-3-EA	245	30	25						1200
Slab on grade site 2	SG-4-EA	256	64	30	2a (BLCP)	180	820	1100	880	1200
	SG-5-EA									
Slab on beam site 1	SB-1-NC	226	54	-	2b (Mae Moh)	185	930	1040	791	1600
	SB-2-EA	201	54	25					800	1700
	SB-3-EA	206	54	20					791	1600
Slab on beam site 2	SB-4-NC	252	64	-	2b (Mae Moh)	190	880	1040	1256	500
	SB-5-EA	222	64	30					1175	1500
Slab on pile	SP-1-NC	320	80	-	2a (BLCP)	180	810	1070	880	1200
	SP-2-EA	290	80	30						
Water Tank Wall	WT-1-EA	179	171	30	2b (Mae Moh)	175	820	1070	505	1600
	WT-2-EA									

4.2.3 Information of investigated structures
4.3.2.1 Slabs on grade

Several construction projects carried out strain investigations on actual expansive concrete structures. Field investigations of slabs on grade were conducted for construction site 1 in Pathum Thani Province and construction site 2 in Saraburi Province. **Figure 4.1** shows the plan view and site condition of the slabs on grade at construction site 1. Measurement on

construction site 1 was conducted on three identical slabs with dimensions of $12.80 \times 4.80 \times 0.15$ m (length $\times$ width $\times$ thickness). The measurement in slabs on grade at construction site 1 was conducted to investigate the effects of the type and amount of expansive additive and the effects of internal restraint in transverse and longitudinal directions. The SG-1-NC slab was cast with normal concrete (without expansive additives), whereas SG-2-EA and SG-3-EA slabs were cast with expansive concrete with varying types and dosages of expansive additives, SG-2-EA used C-S-A type, and SG-3-EA use CaO + C-S-A type.
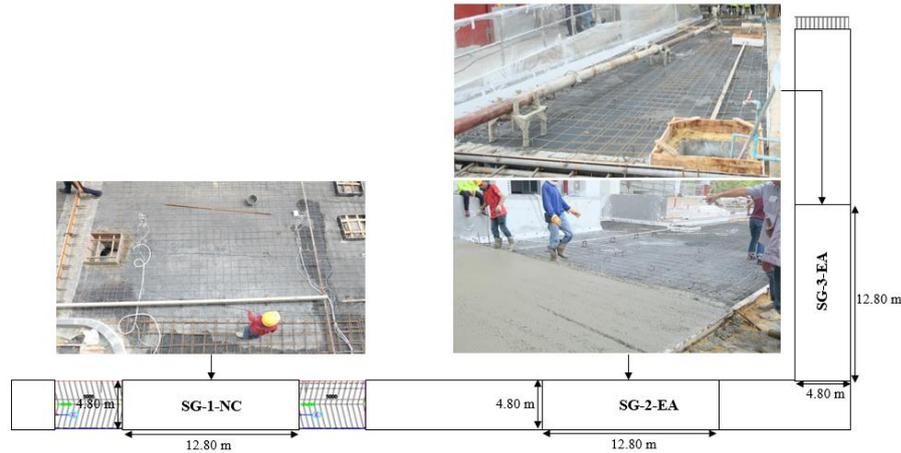

Figure 4.1 Plan view and site conditions of the investigated slabs on grade 1 at construction site 1

Uniaxial foil strain gauges with the vinyl coating (120 mm gauge length with 120 Ω) were applied to measure strain in concrete, while foil strain gauges with 5 mm gauge length and 1.4 mm gauge width were used to measure the strain of the steel rebars. Strain measurements with varying durations for each structure depend on the equipment and construction site conditions. Data is generally recorded using a data logger every 30 minutes for 28 to 90 days. In addition, it should be noted that construction work is still ongoing during the measurement process, causing noise and damage to the results in some locations. However, the obtained strain results were sufficient to include the overall objectives of the measurements.

In the slab on grade at construction site 1, two measurement locations were selected for each slab. **Figure 4.2** shows the installation location of strain gauges in each slab for SB-1-NC, SB-2-EA, and SB-3-EA. Deformed bar mesh having a diameter of 6 mm and a spacing of 200 mm was provided for longitudinal (parallel to the slab length) and transverse (parallel to the slab width) directions. Deformed bars with a diameter of 25 mm and a spacing of 300 mm were installed at the edge of each slab as the dowels. The installation of strain gauges in slabs on grade is separated into two locations: near the center of the span and near the end of the slab near the expansion joint. The installation of strain gauges at the center of the span is divided into two layers, with the first layer located in the mid-depth position (7.5 cm from the top surface) and the second in the top steel layer (3.5 cm from the top surface) (see **Figure 4.3**). At the measurement locations near the center of the span (locations 1, 3, and 5) close to the steel layer, each strain gauge is installed in longitudinal and transverse directions. While at the mid-depth layer, it is only installed in the longitudinal direction. Strain gauges are only installed on the top steel layer (3.5 cm from the top surface) in the longitudinal direction at installation locations near expansion joints (locations 2, 4, and 6).
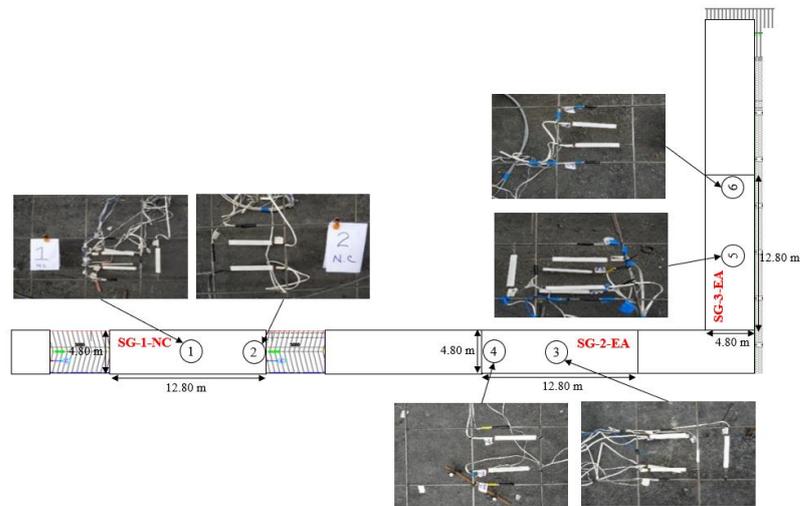
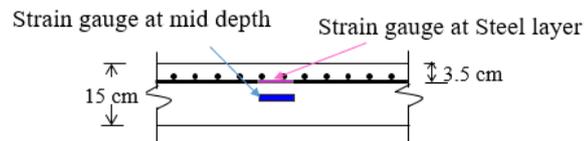**Figure 4.2** Measurement locations for slabs on grade at construction site 1

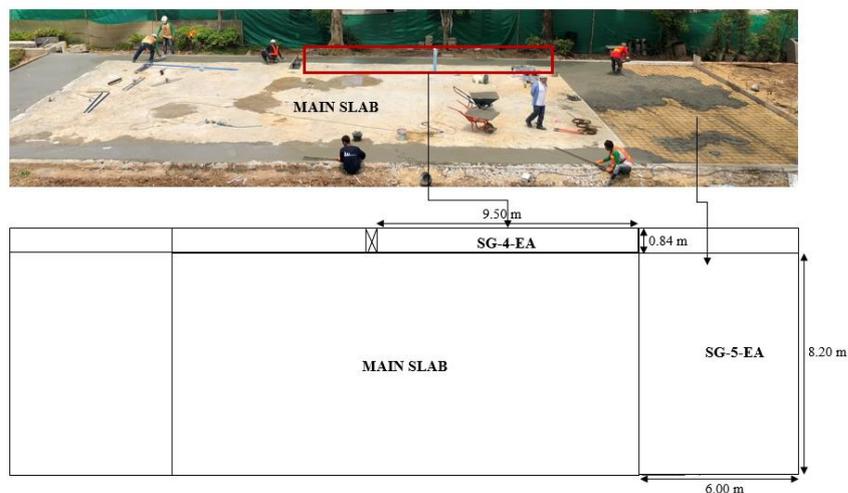**Figure 4.3** Position of strain gauge for slab on grade at construction site 1

Figure 4.4 Plan view and site condition of the investigated slabs on grade 2 at construction site 2

The plan view and site condition of the investigated slabs on grade at construction site 2 can be seen in **Figure 4.4**. The measurements were conducted on two slabs with different dimensions (SG-4-EA and SG-5-EA) cast with the same mix proportion. The dimensions of the SG-4-EA were $9.5 \times 0.84 \times 0.12$ m, and the SG-5-EA were $6.00 \times 8.2 \times 0.12$ m (length $\times$ width $\times$ thickness). This measurement was intended to investigate the effects of structure dimension on the expansion rate of expansive concrete. SG-4-EA and SG-5-EA were cast simultaneously using the same expansive agent (CaO + C-S-A based).

Figure 4.5 shows the installation location of strain gauges for slabs on grade at construction site 2. At this location, there are two slabs with different dimensions (SG-4-EA

and SG-5-EA) but using the same mix proportion. In SG-4-EA, there are 8 strain gauge installation locations in the longitudinal and transverse directions on the top steel layer (3.5 cm from the top of the surface). In addition, concrete strain gauges were installed at mid-depth (6 cm from the top of the surface) at locations 2, 5, and 8 along the longitudinal direction. Strain gauges are installed at five locations in SG-5-EA, from location 9 to location 13. The strain gauges were installed on the top steel layer in longitudinal and transverse directions. Rebar reinforcement used for slabs on grade at construction site 2 was the same as construction site 1, 6 mm diameter rebar mesh with 200 mm spacing, installed in longitudinal and transverse directions.
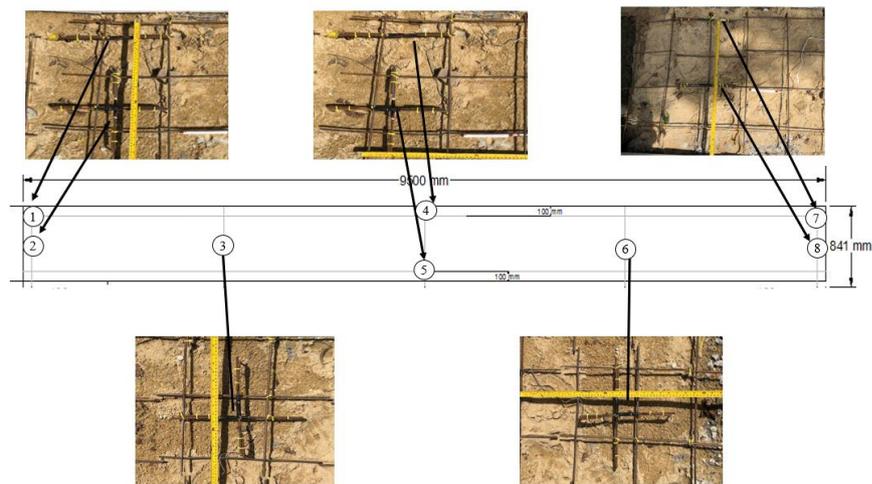
(a) SG-4-EA
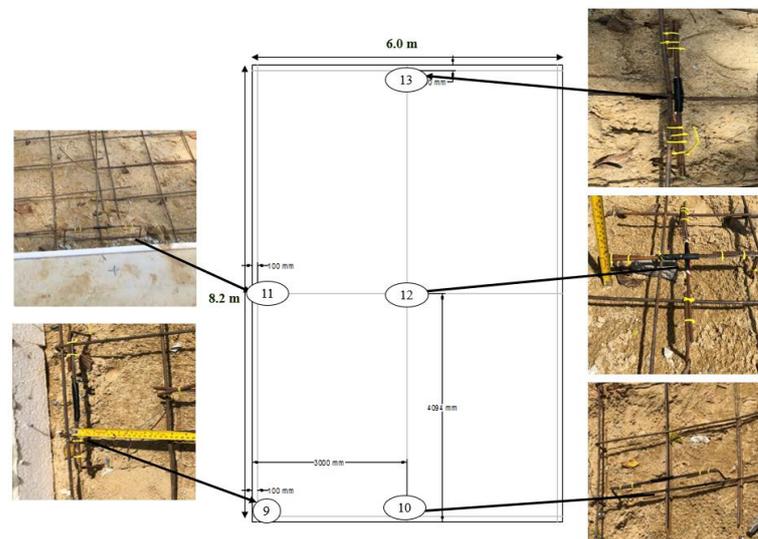
(b) SG-5-EA

Figure 4.5 Measurement locations for slabs on grade at construction site 2

4.3.2.2 Slabs on beam

The ground slabs of a building (slabs on beam and foundation) were also chosen to study the effectiveness of expansive additive dan the effect of restraint conditions. Strain monitoring was carried out at several locations and in different measurement directions to determine the effect of the degree of restraint on the level of expansion and shrinkage strain. The expansion and shrinkage strain levels depend highly on the structure configuration, degree

of internal and external restraint, and mix proportion. Reinforcing bars in these slabs on beam provided internal restraint, while the base friction between the slabs and sub-base, adjacent structural members, and footings provided external restraint. Direct field monitoring of the slabs on beam structure is carried out at two locations: the ground slab of the industrial building (construction site 1) and the ground slab of the educational building (construction site 2).
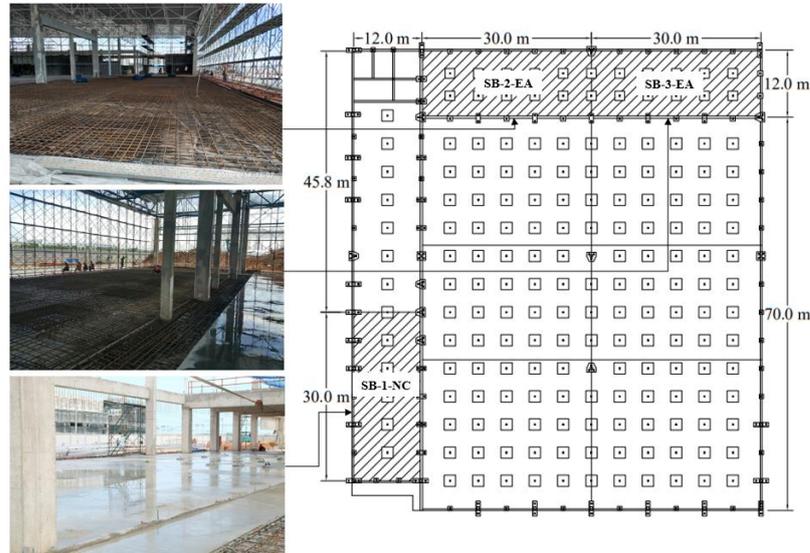

Figure 4.6 Plan view and site condition of the investigated slab on beam at construction site 1

Three identical slabs on beam at construction site 1 were selected for the strain investigation, as shown in **Figure 4.6**. Each slab has dimensions of $30 \times 12 \times 0.25$ m (length $\times$ width $\times$ thickness). The measurement of slab on beam at construction site 1 focuses on investigating the effectiveness of expansive additives and the effect of internal restraint (rebar reinforcement) and external restraint (perimeter beams, columns, and pile caps). The SB-1-NC slab was cast with normal concrete (without expansive additives). While the SB-2-EA and SB-3-EA slabs were cast with expansive concrete using different types and dosages of expansive additives (CaO + C-S-A based for SB-2-EA and C-S-A based for SB-3-EA).

Concrete strain gauges were installed in the longitudinal (along the slab length) and transverse (along the slab width) directions at all measured locations of the top steel layer (0.035 m from the top surface) and mid-depth (0.125 m from the top surface). For slab SB-1-NC, strain gauge location 1 was in between the two adjacent footings in the longitudinal direction of the slab. Location 2 was 70 cm away from the longitudinal perimeter beam. Location 3 was 70 cm from the transverse perimeter beam. Location 4 was 70 cm away from transverse and longitudinal perimeter beams (see **Figure 4.7a**). For SB-2-EA, strain gauge location 5 was 70 cm from the transverse perimeter beam. Location 6 was between two adjacent footings with thermocouples installed in this location. Location 7 was in the middle of the adjacent perimeter beam and footings (see **Figure 4.7b**). Measurement locations for SB-3-EA were selected to be the same as SB-1-NC, except that there was no measurement at the slab corner. Therefore, location 8 was between the perimeter beam and footings. Location 9 was in the middle of two footings, and location 10 was 70 cm away from the adjacent parameter beam (see **Figure 4.7c**). Additionally, concrete strain gauges were installed in longitudinal and transverse directions for all measurement locations in the slabs on beam.
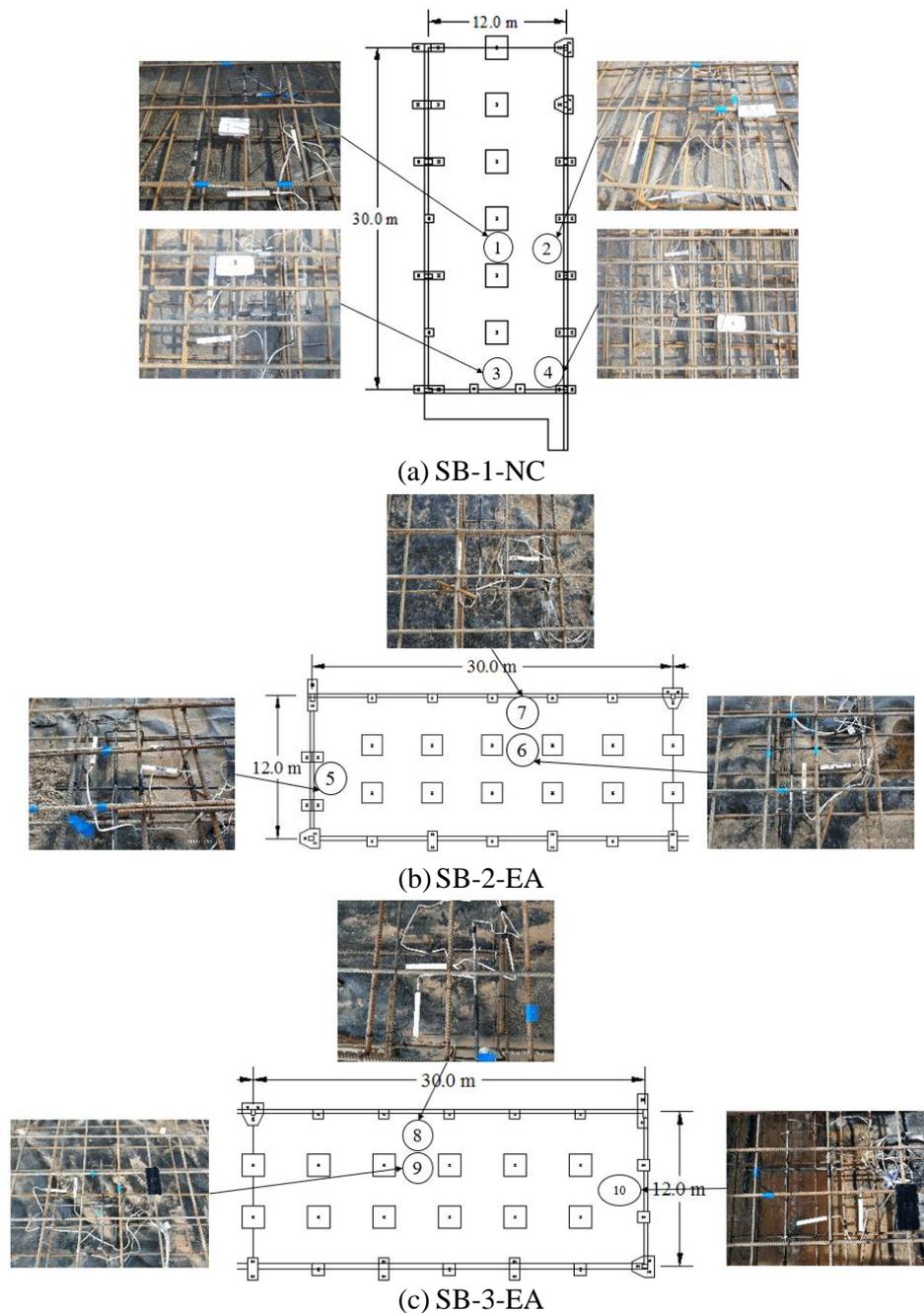
(a) SB-1-NC

(b) SB-2-EA

(c) SB-3-EA

Figure 4.7 Measurement locations for slabs on beam at construction site 1

Figure 4.8 shows the plan view and site condition of the investigated slabs on beam at construction site 2. There are two different cast slabs in this construction site 2, SB-4-NC used normal concrete, and SB-5-EA used expansive concrete with CaO + C-S-A type. This measurement aims to determine the effectiveness of the expansive additive and the effect of restraint conditions on the expansion and shrinkage of actual structures. SB-4-NC dimension is $11.5 \times 11.5 \times 0.25$ m, while SB-5-EA is $15.5 \times 11.5 \times 0.25$ m (length $\times$ width $\times$ thickness). In this structure, the rebar reinforcement is assumed as internal restraint, while adjacent structural members such as beams, columns, and pile caps are assumed as external restraint.
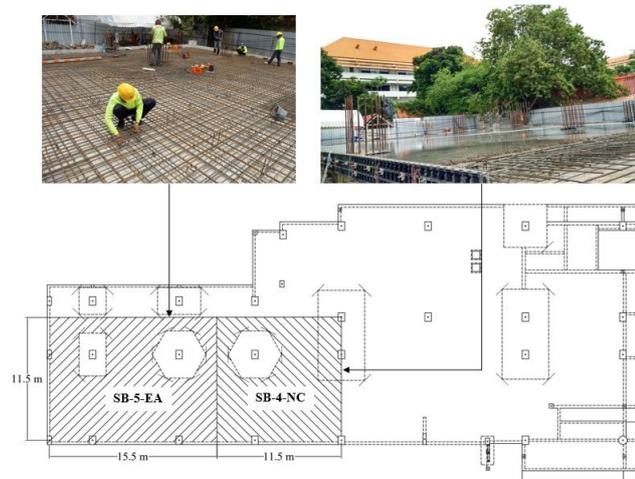
Figure 4.8 Plan view and site condition of slab on beam at construction site 2

The location of the strain gauges installation for slab on beam at construction site 2 can be seen in **Figure 4.9**. Strain gauges are installed at 6 different places on each slab, locations 1 to 6 for expansive concrete and 7 to 12 for normal concrete. Concrete strain gauges are installed at each point in the mid-depth of the slab (12.5 cm from the top surface). Strain gauges are also installed in two directions at each point, the longitudinal (X direction) and transverse (Y direction). This slab on beam investigates the effects of mix proportions, internal restraint, external restraint, and strain direction. Consequently, the location of the installed strain gauges corresponds with the objective of this measurement.
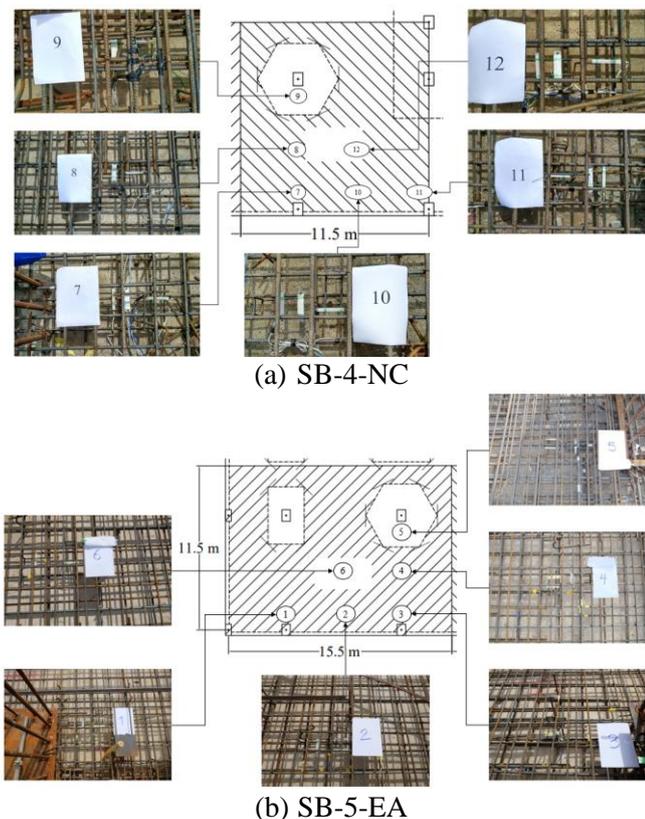

(a) SB-4-NC

(b) SB-5-EA

Figure 4.9 Measurement locations for slabs on beam at construction site 2

4.3.2.3 Slabs on pile

Field investigations were also carried out on slabs on pile structures with a plan view and site conditions, as shown in **Figure 4.10**. The measurements were conducted in 2 different slabs, normal concrete for SP-1-NC and expansive concrete for SP-2-EA. The purpose of this field investigation is to monitor the expansion and shrinkage behavior of the slab on pile due to the influence of internal and external restraint. Rebar reinforcement is considered internal restraint in this structure, while beams, columns, and piles are considered external restraint. In addition, this study also investigates the effectiveness of the expansive additive on the level of expansion, which used CaO + C-S-A based expansive agent. The dimension of the slab is $38.50 \times 27.775 \times 0.25$ m for SP-1-NC and $42.45 \times 27.775 \times 0.25$ m (length $\times$ width $\times$ thickness) for SP-2-EA.
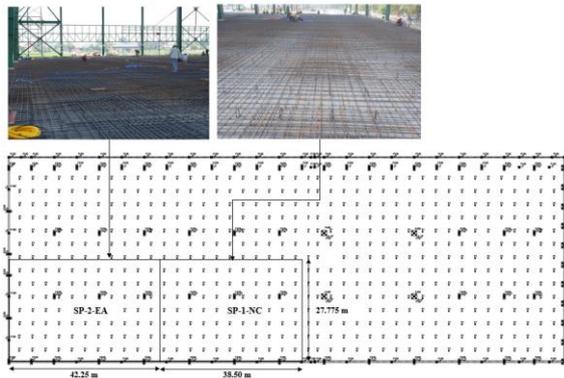

Figure 4.10 Plan view and site condition of the investigated slabs on pile
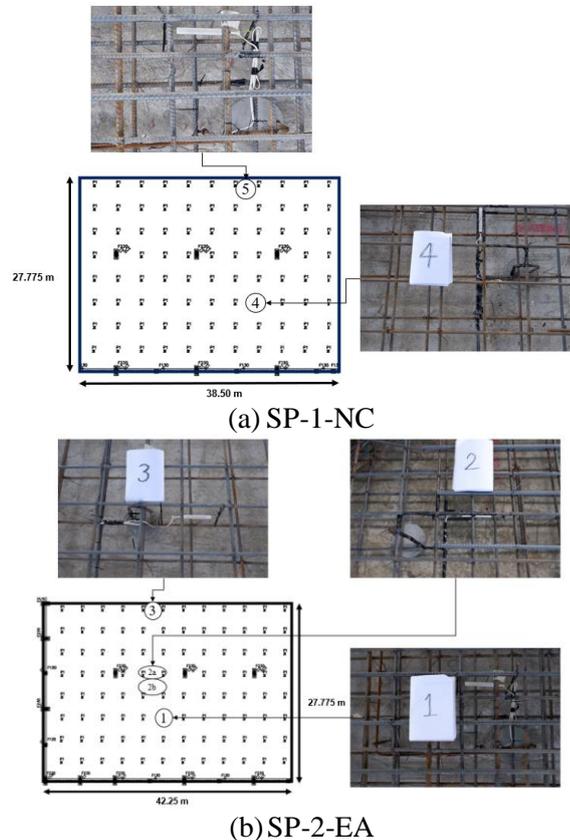

(a) SP-1-NC

(b) SP-2-EA

Figure 4.11 Measurement locations for slabs on pile

Strain gauge installation locations for each location on the slabs on pile can be seen in **Figure 4.11**. In normal concrete (SP-1-NC), all strain gauges are installed at mid-depth or 12.5 cm from the top surface. At location 4, the strain gauge is installed in longitudinal and transverse directions, while location 5 is only installed in the transverse direction. Location 4 is above the pile caps, while location 5 is close to the edge of the measured slab. The strain gauge installation in expansive concrete (SP-1-EA) consists of 3 locations, location 1 is directly above one of the pile caps, location 2 is divided into two installation locations, which 2a is between two pile caps, and location 2b is just above the slab. At locations 1 and 2, strain gauges for longitudinal and transverse directions are installed. The last strain measurement location on SP-2-EA is location 3, which is only installed for the transverse direction near the edge of the measured slab. The measurements at location 3 are intended to determine the impact of the construction step on the adjacent slab.

4.3.2.4 Water tank walls

The plan view and site condition of the studied water tank wall structure can be seen in **Figure 4.12**. Strain measurements were conducted on two side walls cast with the same mix proportion but different dimensions, i.e., $8.4 \times 3.05 \times 0.25$ m for the east wall (WT-1-EA) and $6.2 \times 3.05 \times 0.25$ m for the north wall (WT-2-EA) (length × height × thickness). This measurement aimed to investigate the geometry of structure, effects of restraint, and effects of construction steps. The total height of the wall, which included the thickness of the base slab and top slab was 3.05 m, while the net height was 2.65 m. This water tank wall structure was located on the rooftop of a building with a base slab elevation of 32.7 m above the ground. The casting process of the water tank wall was divided into three steps. The first step was the casting of the base slab, followed by the casting of the wall structure, and the top slab was cast 21 days after the wall casting was completed.
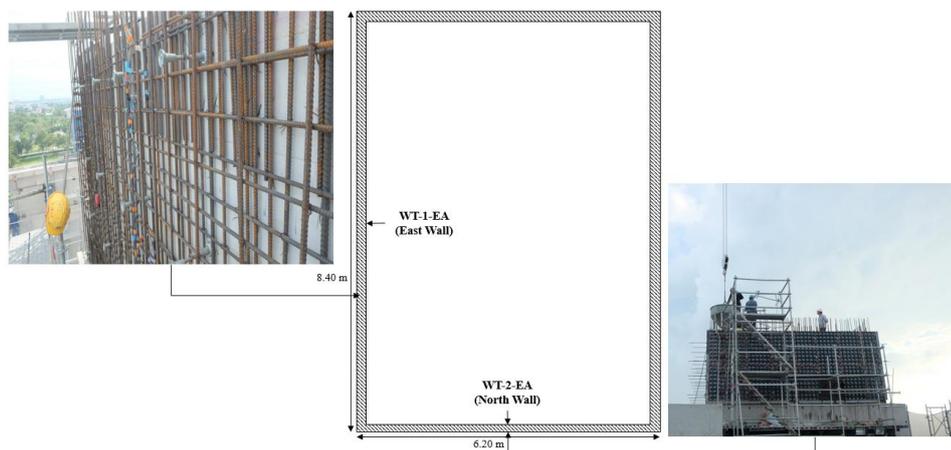
Figure 4.12 Plan view and site condition of the investigated water tank walls

For the rooftop water tank walls, the strain gauges were installed at four locations on the east wall (WT-1-EA) and three locations on the north wall (WT-2-EA), as shown in **Figure 4.13**. The influence of internal and external restraints incorporated in the structure was considered by analyzing the strain at each location. The strain gauges were installed in the horizontal and vertical directions for each measurement location. Because this structure was directly exposed to sunlight and different rebar reinforcement size were used, strain gauges

were also installed on the inner and outer faces at some measured locations of the water tank walls. In WT-1-EA (east wall), strain gauges at locations 1 and 2 were in the middle span of the wall, while at locations 3 and 4, they were in 1/4 from the total length of the wall. Locations 1 and 3 were 1.3 m below the top surface of the wall, while locations 2 and 4 were 0.5 m above the bottom surface of the wall. All measured locations for WT-2-EA (north wall) were in the middle of the wall span. Location 5 was 1.3 m below the top slab, location 6 was 0.5 m above the bottom slab, and location 7 was 0.5 m below the top slab.
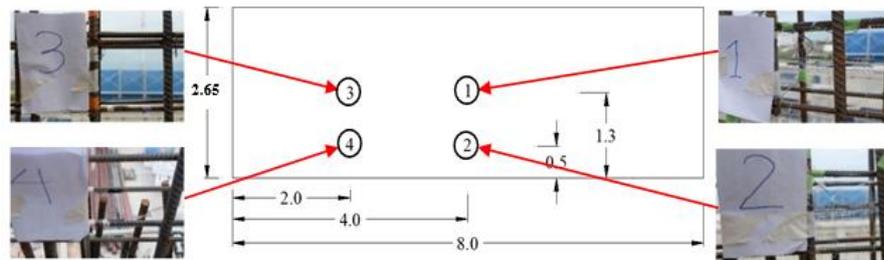
(a) WT-1-EA (East wall)
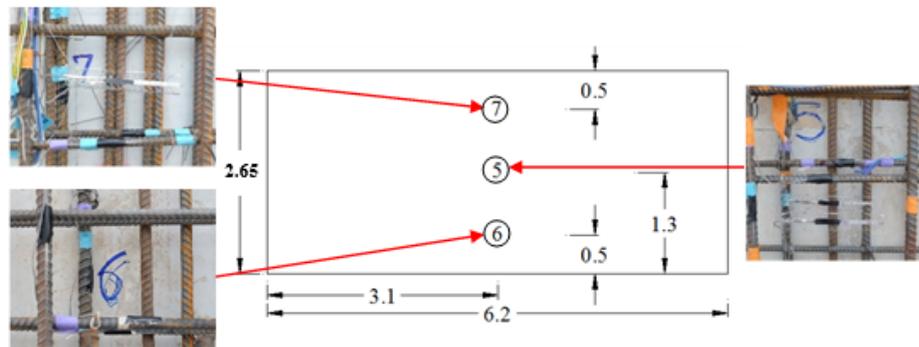
(b) WT-2-EA (North wall)

Figure 4.13 Measurement locations for water tank wall

Table 4.4 summarizes the dimensions of all structures, the reinforcement ratio, and the focused study in each investigated structure. In the slabs on grade, both construction sites 1 and 2 employ the same rebar size but different reinforcement ratios due to the difference in thickness of the slabs in these two sites. Deformed bar mesh (P6-200) was provided for longitudinal (parallel to the slab length) and transverse (parallel to the slab width) directions at the top layer of the slab, which are 0.035 m from the top surface for slab on grade at construction 1 and 0.006 m from the top surface for slab on grade at construction site 2. For the slabs on beam at construction site 1, the same bar size and spacing for top and bottom layer rebar reinforcement were applied (DB12-250), resulting in the same reinforcement ratio for all slabs (SB-1-NC, SB-2-EA & SB-3-EA) in both longitudinal and transverse directions. For the slab on beam at construction site 2, the rebar sizes DB16-200 were applied both in SB-4-NC and SB-5-EA in the longitudinal and transverse directions, resulting in the same reinforcement ratio for these two structures. The same reinforcement ratio also appeared in slabs on pile. DB16-175 mm was applied in longitudinal and transverse directions at the top and bottom surfaces of slabs on pile. The water tank wall employed the same rebar sizes for the horizontal direction on the inner and outer faces (DB12-250), but different rebar size was applied in the vertical direction, which is DB16-250 for the outer face and DB20-125 for the inner face.

Table 4.4 Summaries of geometry and reinforcement information for each investigated structure.

Structures		Dimension (l × w × t) (m)	Rebar Information (mm) Longitudinal / Horizontal*	Transverse / Vertical*	Reinforcement Ratio (%) Longitudinal / Horizontal*	Transverse / Vertical*
Slab on Grade site1	SG-1-NC	12.80 × 4.80 × 0.15	P6-200	P6-200	0.09	0.09
	SG-2-EA	12.80 × 4.80 × 0.15	P6-200	P6-200	0.09	0.09
	SG-3-EA	12.80 × 4.80 × 0.15	P6-200	P6-200	0.09	0.09
Slab on Grade site 2	SG-4-EA	9.50 × 0.84 × 0.12	P6-200	P6-200	0.11	0.11
	SG-5-EA	6.00 × 8.20 × 0.12	P6-200	P6-200	0.11	0.11
Slab on Beam site 1	SB-1-NC	30.0 × 12.0 × 0.25	DB12-250 (top & bottom)	DB12-250 (top & bottom)	0.36	0.36
	SB-2-EA	30.0 × 12.0 × 0.25	DB12-250 (top & bottom)	DB12-250 (top & bottom)	0.36	0.36
	SB-3-EA	30.0 × 12.0 × 0.25	DB12-250 (top & bottom)	DB12-250 (top & bottom)	0.36	0.36
Slab on Beam site 2	SB-4-NC	11.5 × 11.5 × 0.25	DB16-200 (top & bottom)	DB16-200 (top & bottom)	0.80	0.80
	SB-5-EA	15.5 × 11.5 × 0.25	DB16-200 (top & bottom)	DB16-200 (top & bottom)	0.80	0.80
Slab on Pile	SP-1-NC	38.5 × 27.8 × 0.25	DB12-175 (top & bottom)	DB12-175 (top & bottom)	0.96	0.96
	SP-2-EA	42.4 × 27.7 × 0.25	DB12-175 (top & bottom)	DB12-175 (top & bottom)	0.96	0.96
Water Tank Wall	WT-1-EA	8.40 × 3.05 × 0.25	DB12-150 (outer & inner)	DB16-250 (outer) DB20-125 (inner)	0.54	
	WT-2-EA	6.20 × 3.05 × 0.25	DB12-150 (outer & inner)	DB16-250 (outer) DB20-125 (inner)	0.54	

4.3 Finite element analysis

4.3.1 Geometry and boundary conditions

4.3.1.1 Slabs on grade

An example of three-dimensional geometry and boundary conditions for the FE model of slabs on grade is shown in **Figure 4.14**. The slab on grade modeling employs three layers of solid elements, with the bottom layer representing the base soil, the middle layer representing the sub-base soil, and the top layer representing the main concrete slab. The slabs on grade FE models utilize the typical geometry but different dimensions and boundary that are customized based on the actual structure conditions. The reinforcement rebar in this analysis consists of the main rebar, the dowel, and the dowel connection. Base, sub-base, and concrete slab components are defined as solid elements, while all reinforcement and dowel components are defined as beam elements. The mesh size employed in this investigation varies based on the configuration of each case of the structure. However, the main slab employs a minimum of 5-layer meshing in the vertical direction (z-direction), while the other direction adjusts based on the meshing size in the vertical direction.

In this FE analysis, the boundary conditions are fixed in all directions (x, y, and z) at the bottom surface of the base structure. It is assumed that the contact surface between the base and sub-base structure is the tied contact surface to the surface. While the contact surface between the concrete slab and the sub-base surface has friction with a friction coefficient of 1.50 [34]. The bond stress relationship between concrete and reinforcement is assumed to be

perfect bonding using beam in solid tools. It should be noted that the boundary condition depends on site conditions, some structures have formwork or adjacent structural members that may affect the expansion process. In this case, the formwork elements are also modeled in this analysis using a configuration that adapts to field conditions to produce reliable and efficient results.
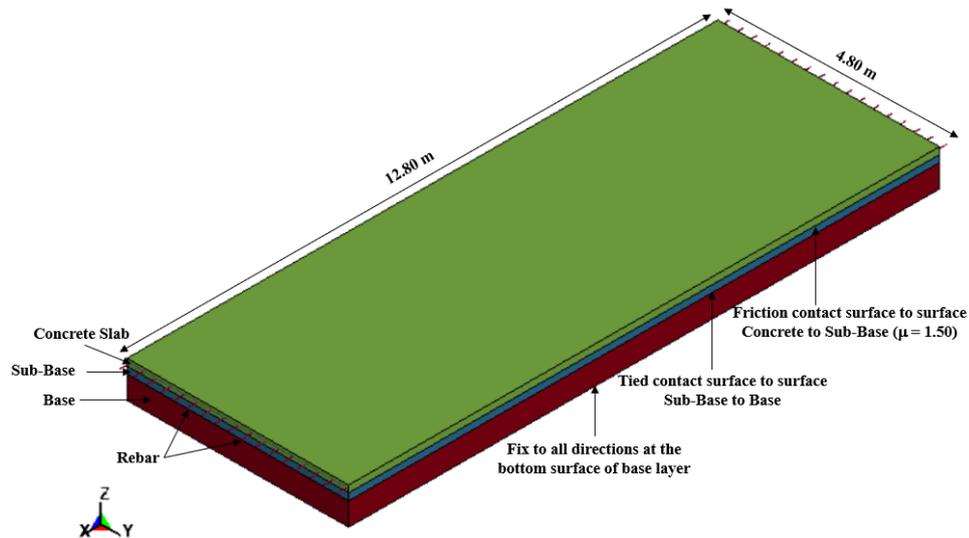

Figure 4.14 An example of a three-dimensional finite element model of slab on grade

4.3.1.2 Slabs on beam

FE analysis modeling for slabs on beam was carried out on two types of slabs with different construction sites. **Figure 4.15** shows a typical slab on beam FE model for a slab at construction site 1, while **Figure 4.16** shows slabs on beam FE model at construction site 2. The slabs on beam at construction site 1 have nearly identical dimensions and structural configuration, but their mix proportion is different. Meanwhile, the slab on beam at construction site 2 consists of two types of slabs with different mix proportions, namely normal and expansive concrete. In this analysis, the concrete part is defined as a solid element, and rebar reinforcement is defined as a beam element.
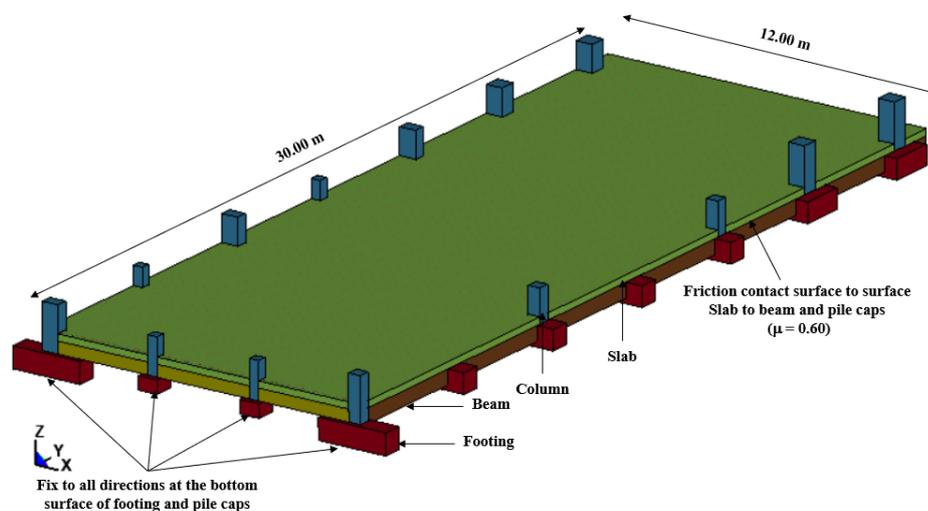

Figure 4.15 Three-dimensional FE model of slab on beam at construction site 1
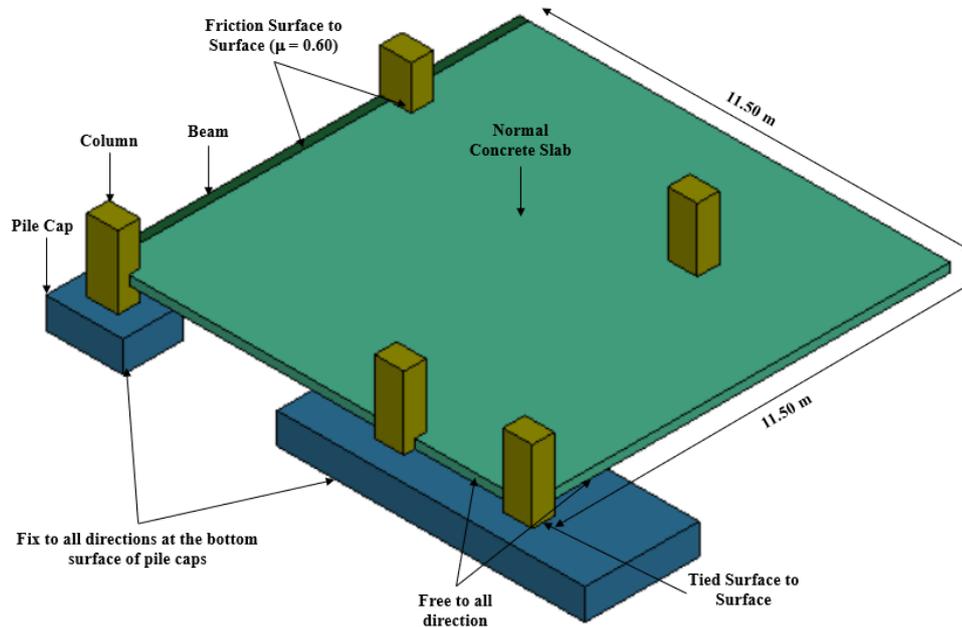
Figure 4.16 Three-dimensional FE model of slab on beam at construction site 2

In slabs on beam modeling, the fixed conditions in the x, y, and z directions are set on the bottom surface of pile caps and footing. As a result of the complex structural configuration, the slab-on-beam model is divided into multiple elements, producing more contact surfaces between each element. However, in structural members cast simultaneously or considered to have no effect on the results of expansion and shrinkage strain investigations, the contact between members assumed as tied surface to surface, such as the contact between the footing and column and the beam and column or footing. Meanwhile, the contact between adjacent structural members and the investigated slab employs a friction contact surface-to-surface with a friction coefficient that must be applied. The bond relationship between concrete and reinforcement is assumed to be perfect bonding by using beams in solid tools.

4.3.1.3 Slabs on pile

Figure 4.17 show an example of three-dimensional modeling of slabs on pile. The slabs on pile have a similar modeling concept to the slabs on beam structures. In this model, solid elements represent concrete components, while beam elements represent rebar reinforcement components. The structure configuration used for this modeling is based on the actual structure's conditions. The boundary conditions also adjust based on the actual condition of the structures, so it is expected to produce strain changes that match the results of field investigations. Fixed conditions in x, y, and z directions are applied to the bottom surface of pile caps and footings. On the main slab surface directly related to adjacent structural members, friction contacts are utilized due to the condition of the other structural members, which were cast long before the slab casting process was cast. While the bond relationship between rebar and concrete is assumed to be perfectly bonded.
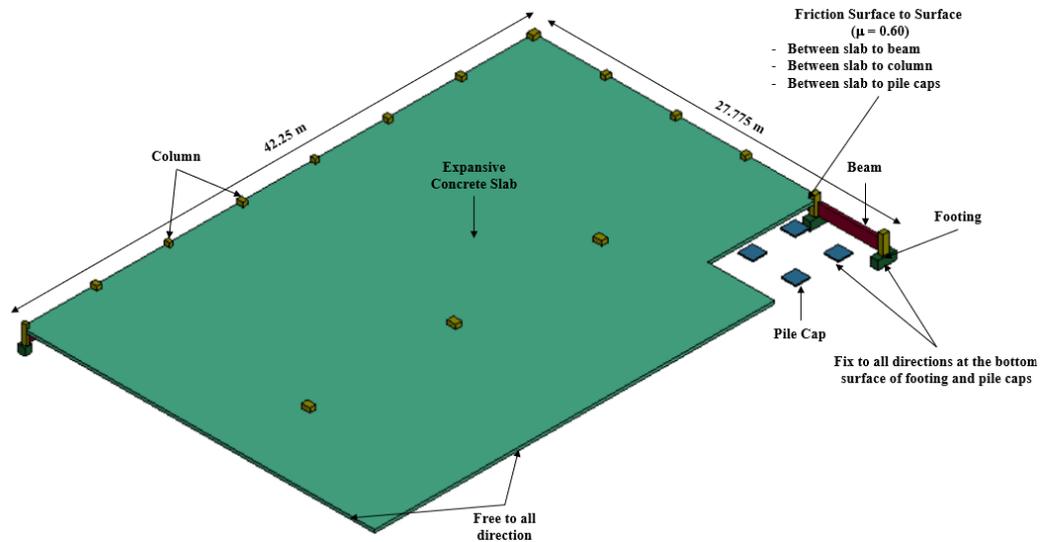
Figure 4.17 An example of a three-dimensional finite element model of slab on pile

4.3.1.4 Water tank wall

Figure 4.18 shows the three-dimensional model for the water tank wall structure. It should be noted that the water tank wall structure was constructed in several steps. This step of construction can affect the level of expansion and shrinkage strains in the walls. The bottom slab was cast before casting all the wall segments. All walls were cast simultaneously, while the top slab was cast 21 days after the whole walls had been cast. Because the top part of the walls has lower restraint than the bottom during early ages due to time difference in step-construction, the expansion at the top of the wall can be higher than that at the bottom, resulting in a non-uniform level of expansion. To solve this step of the construction issue, a construction stage tool was used in the LS Dyna model, which involved running the model without a top slab for 21 days, and the top slab was added afterward until the running was completed. Fixed boundaries at the x, y, and z directions were applied on beams connected to the columns. Surface to surface friction contact was applied to simulate contact behavior between the main walls and top slab. Tied surface to surface contact was applied for other connections between each pair of structural parts.
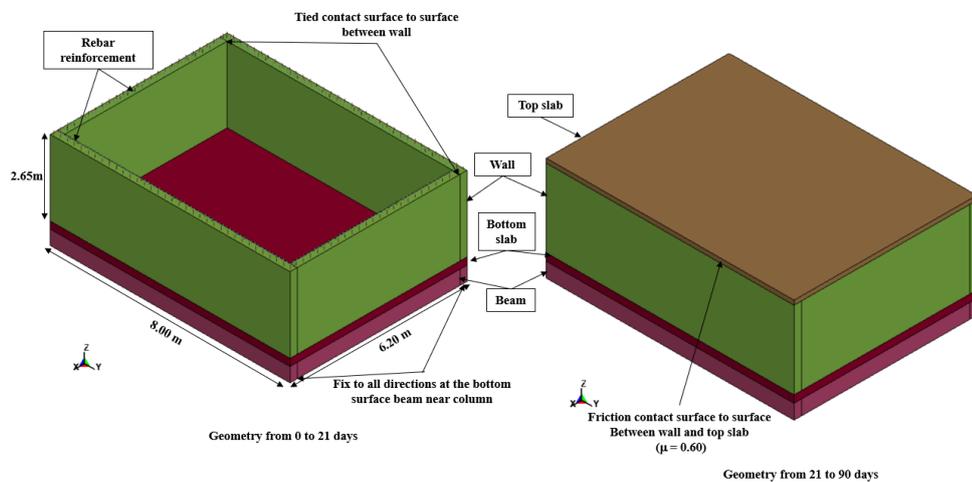

Figure 4.18 Three-dimensional finite element model of the water tank walls

4.3.2 Materials models

According to the conditions and configurations of each structure, various types of material models are utilized in the FE modeling of the expansive concrete structure. However, the main material model used in this analysis is material for concrete in the investigated elements (main slabs for slab on beam, slabs on grade, and slabs on pile and main wall for water tank wall). In addition, the material model used in this analysis is also for rebar reinforcement and thermal expansion. In this study, a continuous surface cam model (CSCM) or MAT 159 is used to describe the properties of main concrete and Mat Add Thermal Expansion to investigate the expansion and shrinkage strain. While material piecewise linear plasticity or MAT 024 is employed for rebar reinforcement. This subchapter does not discuss MAT 024 and Mat add thermal expansion because it has been thoroughly explained in the material properties subchapter for FE analysis of prism specimens. In addition, for other structural components such as columns, beams, pile caps, footing on slabs on beam and slabs on pile, sub-base, and base in slab on grade, Elastic Materials or MAT 001 will be used.

The material continuous surface cap model (CSCM) or MAT 159 was first developed to simulate concrete structures for the National Cooperative Highway Research Program of The United States Department of Transportation [35]. There are three types of independent failure in the MAT 072R3 material mode: maximum failure, yield failure, and residual failure surface. However, the transition between the failure surface and hardening cap in this model material is continuous or smooth [35]–[37]. MAT 159 is one of the material models offered by the Ls Dyna and is widely utilized for concrete materials subject to various loading. The ability to automatically generate the input parameters of the material model based on the concrete strength is one of the benefits of this material model. Only general concrete properties data, such as mass density, Poisson's ratio, compressive strength, maximum aggregate size, and rate effect, are required to generate concrete parameters.
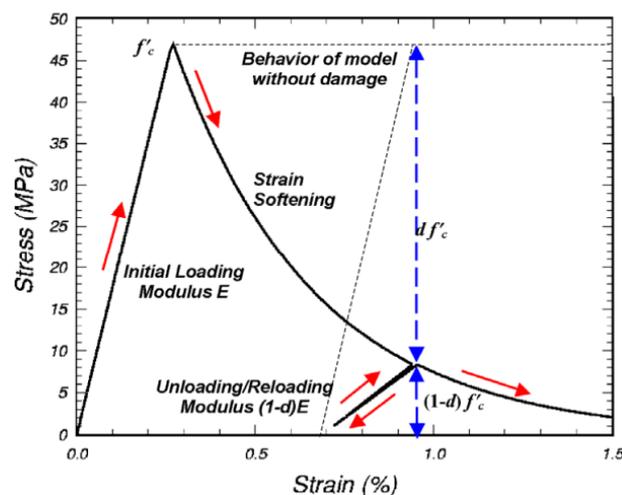
Figure 4.19 Illustration of generate results of concrete properties for MAT 159 [35]

This material model generates the stress-strain behavior of concrete based on the CEB FIB standard [38]. **Figure 4.19** illustrates the stress-strain relationship generated by the LS-Dyna based on uniaxial compressive strength. The benefits of this material model for generating concrete behavior based on uniaxial compressive strength make it simple for users to analyze the behavior of reinforced concrete structures under different loading conditions. In addition,

this model material can generate strain softening behavior after post-peak in concrete using the quadratic fitting equations regression analysis. However, this CSCM material model is highly dependent on the compressive strength of concrete, and it is difficult to define the behavior of certain types of concrete based on the compressive strength. Therefore, this material model also provides space for users to define more complete concrete material properties according to the condition of the concrete. Users need to input fracture energy, torsion, and triaxial compression behavior [35], [39]. For a comprehensive explanation utilizing MAT 159, various previous case studies utilizing this material model have been conducted [36], [40]–[45].

The other material model used to define adjacent structural members is elastic material or MAT 001. This material model is an anisotropic hyperplastic material and can be used for beam, shell, and solid elements. The input parameters for MAT 001 consist of mass density, young modulus, Poisson's ratio, and bulk modulus (for fluid option) [46]. Strain investigation is not conducted on this portion of the structure, but the stiffness and restraint from the adjacent structure can affect the level of expansion and shrinkage in the investigated element, so MAT 001 with an appropriate meshing size will produce a stiffness that is reliable and can be compared to the results of the actual structures.

4.3.3 Determination of Free Expansion and Free Shrinkage

Length change in free conditions is one of the inputs used in FE analysis to estimate the expansion and shrinkage strain level for expansive concrete structures. In each case of an investigated structure in this study, length change in free condition specimens and compressive strength were measured for properties as the input in FE modeling. This length change measurement refers to the ASTM C157 standard with prism specimens measuring $75 \times 75 \times 285$ mm3. During the measurement process, all specimens were placed on the construction site so that the results of the FE analysis would be comparable to the actual condition. In addition, apart from experiments, the free expansion and shrinkage strain of expansive concrete can also be predicted using an approach method that previous researchers have developed. The prediction of expansion was developed by [47], and the prediction of free shrinkage strain was developed by [48].

4.3.4 Effective Free Strain for Expansive Concrete

As explained previously, the free expansion strain from the test results cannot be used directly as an input in the FE analysis due to the difference in expansion mechanism between free and restrained conditions for expansive concrete. Therefore, it is necessary to reduce the free expansion strain so that the free expansion used has considered the effect of loss of expansion due to expansion product entering the pores and compression creep. The effective free expansion strain is the free expansion strain that considers the effect of expansion loss due to the restraint effect. Later, this effective free expansion strain will be used as the main input for predicting the restrained expansion strain in expansive concrete structures. **Equation (3.19)** can be used to determine the effective free expansion strain of expansive concrete. The value of the reduction factor is derived from the results of the regression analysis conducted based on the experimental data. However, this equation has never been used to predict restrained expansion strain in actual structures accurately. Consequently, one of the contributions of this study is to validate the equation of the reduction factors that the author has developed so that it can be utilized in the estimation of the effective free expansion strain.

It should be noted that in **Equation (3.19)** only considers the influence of the reinforcement ratio as a restraint that affects the expansion process. In actual structures, the effect of adjacent structural members is also one of the factors affecting the degree of expansion in expansive concrete. To estimate the level of expansion in actual structures, **Equation (3.19)** to determine effective free strain has not been able to account for the influence of adjacent structural members. In order to identify the effective free expansion strain in the simulation of the actual structure, two different types of equations are used. **Equation (3.19)** is applied to regions far from the influence of adjacent structural members, while **Equation (4.1)** is used for areas located close to adjacent structures.

$$\varepsilon_{\text{eff, free}} = (\phi_i \times \varepsilon_{\text{free}}) \, \phi_e \qquad\qquad (4.1)$$

Where $\varepsilon_{\text{eff, free}}$ is the effective free strain (μ), ϕ_i is the reduction factor caused by internal restraint, ϕ_e is the reduction factor caused by external restraint, and $\varepsilon_{\text{free}}$ is measured free expansion strain of the unrestrained expansive concrete (μ).

In Equation (4.1), the reduction factor is classified into two parts: internal and external restraints. To calculate the reduction factor caused by internal restraint (ϕ_i) using the formulas presented in chapter 5, and to calculate the reduction factor produced by external restraint (ϕ_e) in this study using the efficiency obtained from the simulation of FE analysis. The concept of effective free strain application adjusts to the conditions and configuration of each existing structure.

Application of effective free strain in simulation to estimate the level of expansion and shrinkage strain in expansive concrete structures based on the type of investigated structure. This occurs as a result of the influence of the different degree of restraint in each structure. On slab on grade, the main external restraint is friction on the bottom slab. It is considered that the ensuing friction is an external restraint that can impact the level of expansion. **Figure 4.20** illustrates an example of how to apply the reduction factor while modelling slab on grade expansive concrete. Because the reinforcement ratio is the same for all tested slabs on grade structures, the reduction factor from internal restraint (ϕ_i) is applied uniformly to the entire slab area. Meanwhile, the application of the reduction factor due to external restraint (ϕ_e) is divided into several parts as shown in **Figure 4.20**. At the end of the slab using ϕ_e with a larger value, this is due to the effect of friction is smaller at the edge area of the slab, while in the middle of the span using a smaller ϕ_e resulting in a smaller effective free strain. Due to the increased frictional effect in the middle of the span, a smaller ϕ_e is used.
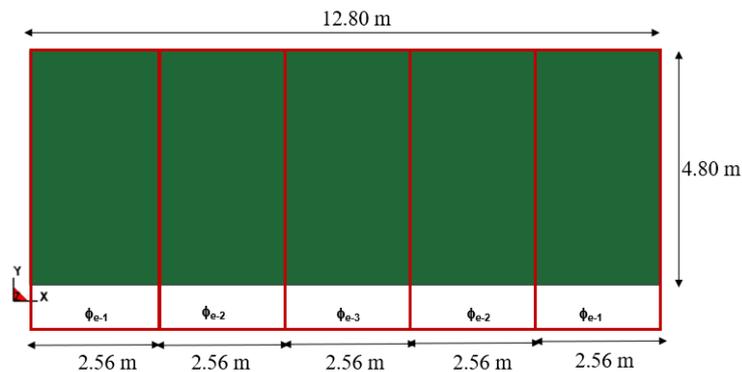

Figure 4.20 Illustration of application of reduction factor ϕ_e for slab on grade

On slabs on beam and slabs on pile structures, various reduction factors are used between spots near to neighboring structures and those far away. **Figure 4.21** shows illustrative examples of the application of different reduction factors for slab on beam. **Figure 4.21a** shows the overall view of the slab on beam structure, including the locations of adjacent structures. **Figure 4.21b** shows areas that are far from neighboring structures or are unaffected by restraint from neighboring structures. In the area shown in **Figure 4.21b**, the effective free strain employed in **Equation (3.19)** solely accounts for the effects of internal restraint and rebar reinforcement. While **Figure 4.21c** shows the area affected by neighboring structures. The area used in this simulation is dependent on the structures configuration and the generated stress distribution results. This area applies the reduction factor in **Equation (4.1)** by taking the influence of external restraint into account. Similar simulations were performed on slab on pile structures, with the distribution of effective free strain divided into two locations: locations close to neighboring structures using effective free strain from **Equation (4.1)** and locations far from neighboring structures using effective free strain from **Equation (3.19)**.
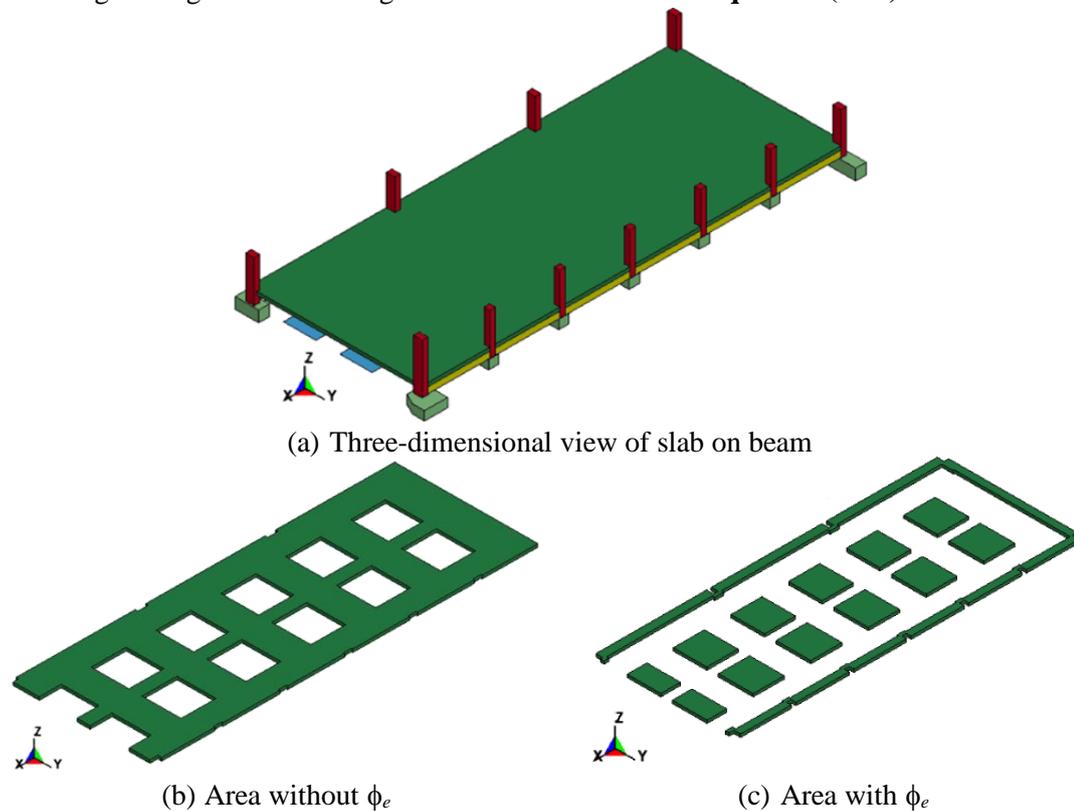

(a) Three-dimensional view of slab on beam

(b) Area without ϕ_e (c) Area with ϕ_e

Figure 4.21 Illustration of application of reduction factor ϕ_e for slab on beam

On the water tank wall, a different reduction factor is used between parts that are near to the neighboring structure and those that are far away. As previously described, the bottom part of the water tank wall is directly connected to the bottom slabs and beams. As a result, the area is subject to the effect of adjacent structures, which might affect the expansion process. **Figure 4.22** shows sites where an additional reduction factor (ϕ_e) is applied due to external restraints. while at the top of the wall, only a reduction factor (ϕ_i) is used since the expansion process at the top of the wall is unaffected by adjacent structures.
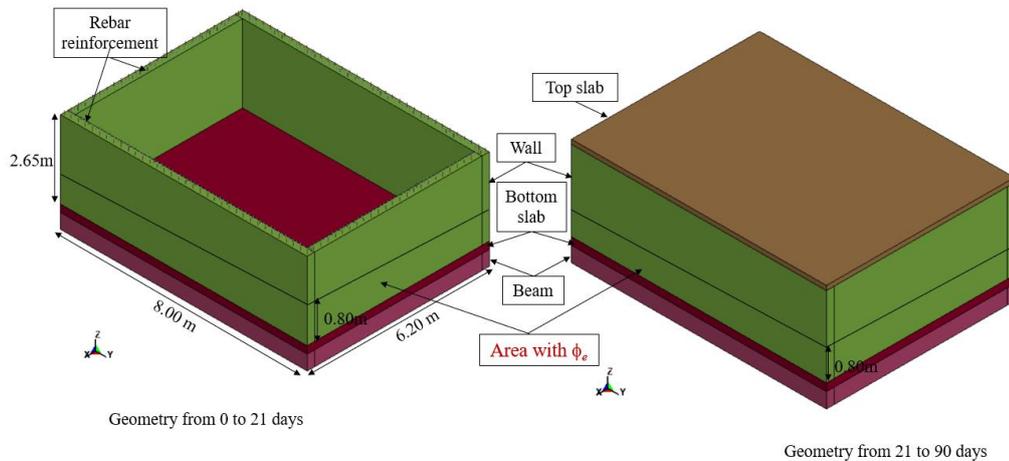
Figure 4.22 Illustration of application of reduction factor ϕ_e for water tank wall

4.4 Results and discussions

After completing the experiment on restrained expansion behavior in expansive concrete, the research expanded on to investigate the behavior of expansion and shrinkage strain in reinforced concrete structures made with expansive concrete. This study discusses the result of field investigations conducted on four different types of reinforced expansive concrete structures, including slabs on grade, slabs on beam, slabs on pile, and water tank walls. The expansion and shrinkage behavior of each structure in response to various influencing factors is investigated. This field investigation aims to investigate the behavior of an expansive additive that is directly applied to actual structures. Through this investigation, it is expected that the behavior of expansive concrete in actual reinforced concrete structures will be studied systematically.

In addition to field investigations, this research estimates the behavior of expansion and shrinkage strains in expansive concrete structures using FE analysis. The FE analysis used conceptually similar to the method used to estimate the restrained expansion strain for prism specimens. For the estimation of restrained expansion behavior for reinforced concrete structures, the effective free strain through reduction factor equation is used as input in FE analysis, whereas for shrinkage parts, the free shrinkage strain through direct measurement without reduction factor is used. This analysis also aims to evaluate the accurateness of the previously developed reduction factor equation in predicting the amount of restrained expansion for the actual expansive concrete structure. Therefore, FE analysis investigations must be carried out to prove that this restrained expansion strain estimation method can be applied to actual structures.

This chapter discusses the expansive concrete properties used as inputs in the FE analysis, such as the compressive strength and free strain test results (expansion and shrinkage). In addition, this chapter discusses the outcomes of the reduction factor and effective free strain calculations utilized as inputs for the FE analysis. The results of the investigation and estimates of restrained expansion and shrinkage strain in actual structures are presented in this chapter. This discussion will evaluate the efficacy of expansive concrete in preventing shrinkage cracking and the influence of the type of expansive additive. In addition, there were discussions regarding the effects of internal and external restraints on the expansion rate. This chapter will also discuss the effect of the exposure environment on the expansion and shrinkage behavior.

4.4.1 Compressive strength

The compressive strength of concrete was tested on unconfined specimens of each structure at 1, 3, 7, and 28 days of age. The average of three specimens was used to calculate the compressive strength of concrete for each proportion. The compressive strength of concrete for each investigated structure is presented in **Table 4.5**. This compressive strength is one of the inputs used in the FE analysis to define the material properties of concrete. This investigation indicates that the amount of expansive material influences the compressive strength of concrete. The compressive strength of concrete gradually decreases with the increase of the amount of expansive additives as cement replacement materials. Compressive strength decreases because the formation of pores and micro-cracks are generated due to large expansion.

Table 4.5 Compressive Strength for all structures

Type of Structures		Compressive Strength (MPa)			
		1 Day	3 Days	7 Days	28 Days
Slab on Grade site 1	SG-1-NC	9.37	12.54	16.74	23.43
	SG-2-EA	8.22	12.12	14.86	20.31
	SG-3-EA	8.96	12.24	16.08	19.22
Slab on Grade site 2	SG-4-EA & SG-5-EA	12.64	20.45	26.81	37.10
Slab on Beam site 1	SB-1-NC	17.32	19.88	34.43	35.23
	SB-2-EA	13.55	15.57	28.11	26.37
	SB-3-EA	16.31	18.8	26.80	32.28
Slab on Beam site 2	SB-4-NC	12.40	21.57	25.03	30.05
	SB-5-EA	12.32	18.67	23.38	29.18
Slab on Pile	SP-1-NC	23.44	43.23	56.68	73.09
	SP-2-EA	19.23	39.65	51.27	65.04
Water Tank Wall	WT-1-EA & WT-2-EA	20.33	22.42	24.16	28.93

4.4.2 Strain in free condition

Concrete length change with time in free conditions is usually employed as input in FE analysis to estimate the length change of concrete under restrained conditions. Therefore, it is necessary to observe the length change of each mix proportion using a prism specimen. Several examples of free strain test results for each structure are shown in **Figure 4.23**. The free strain from the prism specimen cannot be used directly as an input to the FE analysis due to the difference in the expansion mechanism between free and restrained concrete. Therefore, it is necessary to reduce the value of the free expansion strain using the reduction factor equation, referred to as effective free strain. **Figure 4.23** also shows the results of the reduced free strain for several selected structures. Normal concrete and expansive concrete produce a reduction factor of 1.00, indicating that there is no need to reduce the free expansion strain or that free strain is equivalent to effective free strain. This effective free strain is used as input to the FE analysis to estimate the strain under restraint for reinforced concrete structures.

The summary of the reduction factor used for each structure in this study can be seen in **Table 4.6**. A reduction factor of 1.00 is applied for all slab on grade structures based on calculation results for normal and expansive concrete (SG-1-NC to SG-5-EA). Reduction factors of 0.81 for SB-2-EA & SB-5-EA and 0.83 for SB-3-EA are applied to obtain the effective free strain in slab on beam, while the SB-1-NC and SB-4-NC used reduction factor 1.00 because this structure did not use the expansive additive. A reduction factor of 0.72 is used

for SP-2-EA and a reduction factor of 0.78 of used for all water tank wall structures (WT-1-EA and WT-2-EA).

Table 4.6 Reduction factor caused by internal restraint (ϕ_i) for each structure

Slab on Grade		Slab on Beam		Slab on Pile		Water Tank Wall	
ID	(ϕ_i)	ID	(ϕ_i)	ID	(ϕ_i)	ID	(ϕ_i)
SG-1-NC	1.00	SB-1-NC	1.00	SP-1-NC	1.00	WT-1-EA	0.78
SG-2-EA	1.00	SB-2-EA	0.81	SP-2-EA	0.72	WT-2-EA	0.78
SG-3-EA	1.00	SB-3-EA	0.83				
SG-4-EA	1.00	SB-4-NC	1.00				
SG-5-EA	1.00	SB-5-EA	0.81				

(a) Free strain for slab on grade
(b) Free strain for slab on beam
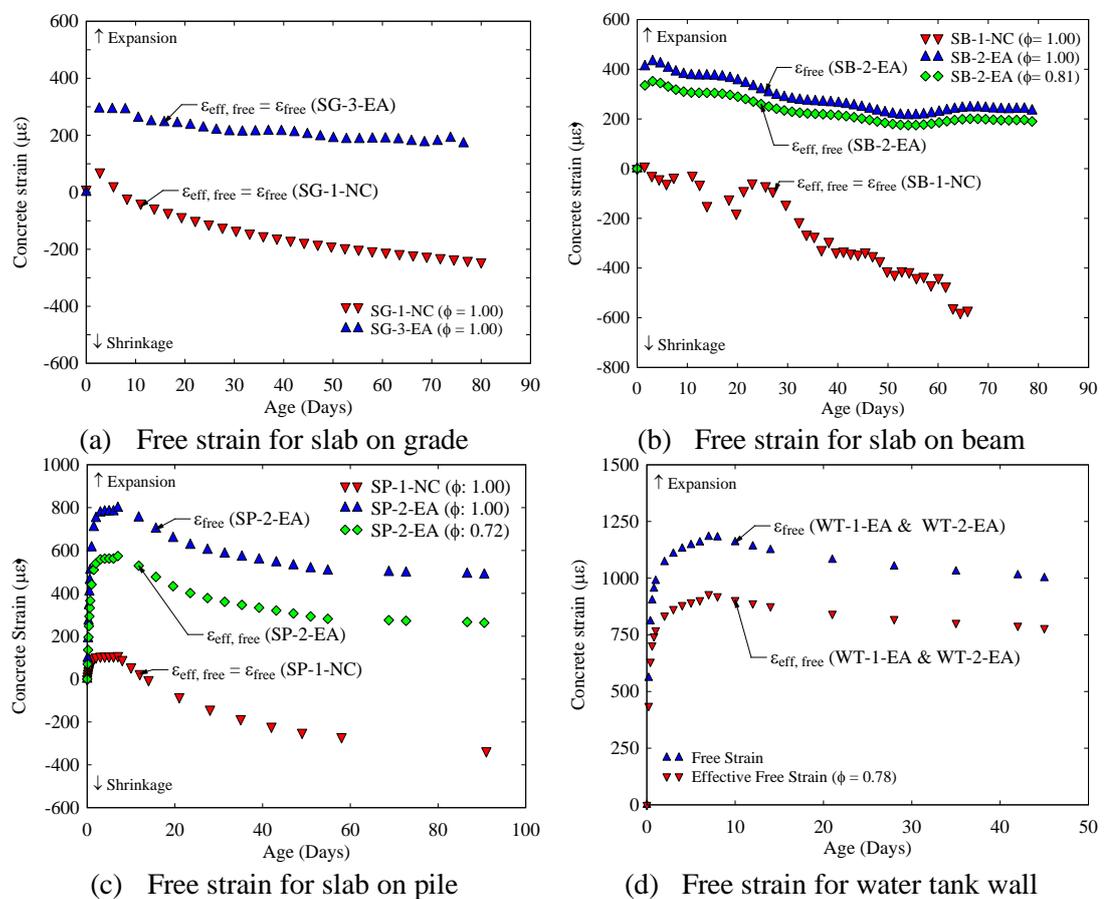(c) Free strain for slab on pile
(d) Free strain for water tank wall

Figure 4.23 Expansion and shrinkage strain in free condition specimen

In addition, this simulation also uses a reduction factor (ϕ_e) caused by external restraint. **Table 4.7** shows the results of the estimated reduction factor (ϕ_e) used for each structure. The slab on grade uses different reduction factor for several locations, this is due to the influence of friction which may be different for each investigated structure. While for slab on beam, slab on pile and water tank wall apply reduction factor (ϕ_e) in areas adjacent to other structural members.

Table 4.7 Reduction factor caused by external restraint (ϕ_e) for each structure

Slab on Grade				Slab on Beam		Slab on Pile		Water Tank Wall	
ID	(ϕ_{e-1})	(ϕ_{e-2})	(ϕ_{e-3})	ID	(ϕ_e)	ID	(ϕ_e)	ID	(ϕ_e)
SG-1-NC	1.00	1.00	1.00	SB-1-NC	1.00	SP-1-NC	1.00	WT-1-EA	0.92
SG-2-EA	1.00	0.97	0.95	SB-2-EA	0.91	SP-2-EA	0.95	WT-2-EA	0.92
SG-3-EA	1.00	0.97	0.95	SB-3-EA	0.95				
SG-4-EA	1.00	1.00	1.00	SB-4-NC	1.00				
SG-5-EA	1.00	1.00	1.00	SB-5-EA	0.95				

4.4.3 Effectiveness of expansive concrete

The effective free strain can be used as a simulation input to estimate the restrained expansion and shrinkage strain of expansive concrete structures after calculating the reduction factor. In this study, strain measurements on actual structures and FE analysis were conducted on four types of structures, including slabs on grade, slabs on beam, slabs on pile, and water tank walls. This chapter discusses the effects of various factors on the expansion and shrinkage strains of expansive concrete structures. The discussion focuses on the effect of the type and amount of expansive additive, the effects of internal and external restraint, the effect of the structure dimensions and strain direction measurement, and the effect of the exposure environment. In addition, to determine the effectiveness of expansive concrete, this chapter also shows the results of damage pattern shrinkage cracking of normal and expansive concrete structures.

The concrete mix proportion is an important factor affecting the expansion and shrinkage of expansive concrete structures. This study investigates the effect of the type and amount of expansive additive on the behavior of expansion and shrinkage strain in order to investigate the effects of mix proportion. To determine the effectiveness of the expansive concrete, investigations were also conducted on structures made of normal concrete to compare the effect of the amount of expansive additive. The structure chosen to investigate the effect of the type and amount of expansive additive were slabs on grade at construction site 1, slabs on beam at construction sites 1 and 2, and slabs on pile. The presented results are the strain comparisons of the same measurement location for each structure.
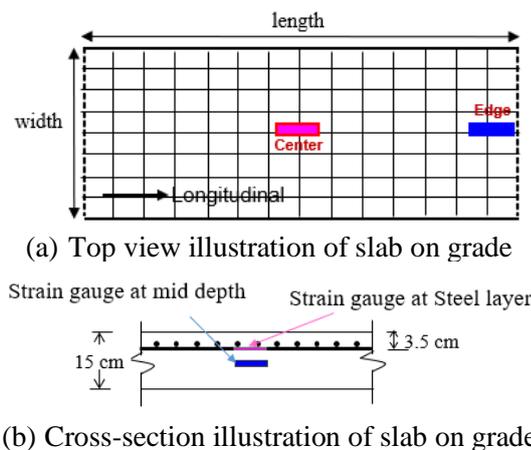

(a) Top view illustration of slab on grade

(b) Cross-section illustration of slab on grade

Figure 4.24 Investigated location for slab on grade at construction site 1 (SG-1-NC, SG-2-EA, & SG-3-EA)

The effect of the type and amount of expansive additive on slab on grade was investigated at two different locations for each slab, including at the center and the edge of the

slab. This investigation was carried out on SG-1-NC (normal concrete), SG-2-EA (C-S-A based expansive agent), and SG-3-EA (C-S-A + CaO based expansive agent). In addition, studies regarding the effect of this mix proportion were conducted only in the longitudinal direction for the strains at the steel layer, locations 1, 3, and 5 (slabs at the center) and locations 2, 4, and 6 (slabs at the edge). **Figure 4.24** illustrates the investigation location for a slab on grade at construction site 1.

Figure 4.25 shows the investigation results on the actual structure compared with the estimation from FE analysis for slab on grade at construction site 1. **Figure 4.25a** shows the results of the investigation at the center of the slab, while **Figure 4.25b** shows the results of the investigation at the edge of the slab. It should be noted that there are some missing data for slab on grade at the early ages of measurement due to the disruption of the data logger. Field investigation and FE analysis of the slabs on grade indicate that expansive concrete mixtures (SG-2-EA and SG-3-EA) produce higher expansion strain than normal concrete (SG-1-NC), both at the center and at the edge of the slab. The higher level of expansion of expansive concrete is certainly influenced by the amount of expansive additive used. This expansion strain is one of the advantages obtained from the use of expansive agents in order to prevent shrinkage cracking. However, the total shrinkage of the normal concrete and the subsequent shrinkage after expansion of the expansive concrete are equivalent.

In addition, this investigation also shows that SG-2-EA produces a higher level of restrained expansion strain than SG-3-EA at the same measured location. Even though, in terms of the amount of expansive additive, SG-2-EA used the amount of expansive additive of 20 kg/m^3 while SG-3-EA used 25 kg/m^3 with the same total amount of binder. The difference in the level of expansion strain between SG-2-EA and SG-3-EA, as determined by field investigations is approximately 70-100 µε. The difference in restrained expansion strain is due to the different types of expansive additives used between the two slabs. SG-2-EA used C-S-A based expansive agent, while SG-3-EA used C-S-A + CaO-based expansive agent. It can be concluded that the type of expansive agent significantly affects the expansion strain.
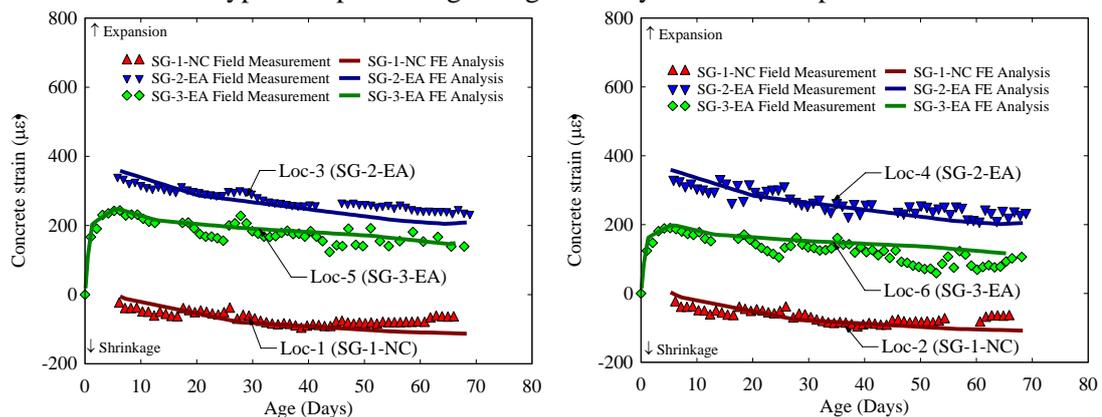

(a) At the center of the slab	(b) At the edge of the slab

Figure 4.25 Strain investigation in longitudinal direction for slab on grade at construction site 1 with the different mix proportion

Investigations on the influence of the type and amount of expansive additive were also carried out on the slabs on beam at both construction site 1 and construction site 2. The slabs on beam at construction site 1 employ two types of expansive additives, namely C-S-A + CaO based expansive agent for SB-2-EA and C-S-A based expansive agent for SB-3-EA. The

amount of expansive agent used for slab on beam at construction site 1 is 25 kg/m^3 for SB-2-EA and 20 kg/m^3 for SB-3-EA. Two measurement locations were selected for each slab to investigate the effect of mix proportion on strain behavior. **Figure 4.26** illustrates the investigated location to determine the effectiveness of expansive concrete. For each slab, strain measurements were taken at the same place, depth, and measured direction. Investigations were carried out between the two adjacent footings and near the transverse perimeter beam.
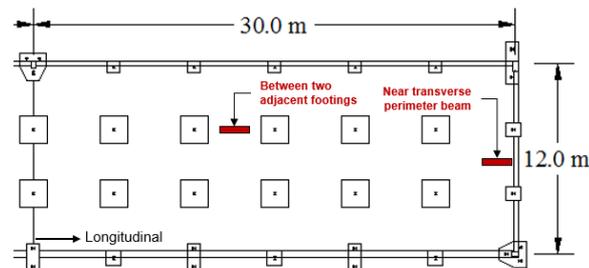
Figure 4.26 Investigated location for slab on beam at construction site 1 (SB-1-NC, SB-2-EA, & SB-3-EA)

Figure 4.27 shows the results of field investigations and FE analysis regarding the effect of mix proportion on expansion and shrinkage behavior for slab on beam at construction site 1. By using the exact measurement location for each slab, it was determined that expansive concrete produces a higher level of restrained expansion strain than normal concrete at the early age of the concrete. This is due to the amount of expansive additive used in expansive concrete. In addition, the investigation of the slab on beam at construction site 1 revealed that the SB-3-EA produced a larger amount of restrained expansion than the SB-2-EA, both at the investigated location near the transverse perimeter beam and between two adjacent footings. The difference in expansion is due to the type of expansive agent utilized, with C-S-A-based expansive agent (SB-3-EA) being more effective in producing expansive products.
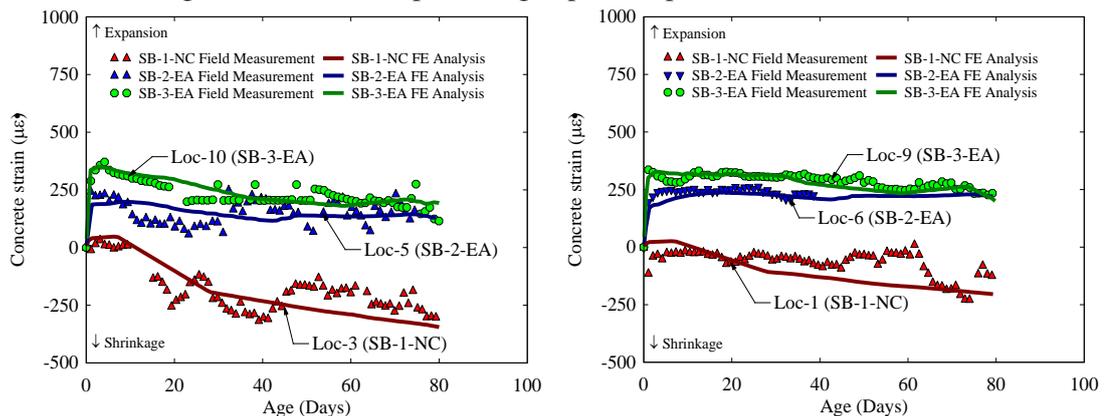
(a) Near transverse perimeter beam   (b) Between two adjacent footings

Figure 4.27 Longitudinal strain in slabs on beam at construction site 1 with different mix proportions

In addition to slabs on beam at construction site 1, slabs on beam at construction site 2 were also used to investigate the effect of mix proportion on strain behavior (SB-4-NC & SB-5-EA). In the slab on beam at construction site 2, only two types of concrete are employed, including normal concrete (SB-4-NC) and expansive concrete with C-S-A + CaO-based

expansive agent (SB-5-EA). The amount of expansive agent used for SB-5-EA is 30 kg/m3. Investigations were carried out at two locations for each slab, namely between two columns (locations 8 and 4) and near the beam and column (locations 11 and 1). **Figure 4.28** illustrates the investigation location for both normal and expansive concrete. The strain investigated for the slab on beam at construction site 2 is at the mid-depth of concrete (concrete strain) in the transverse direction.
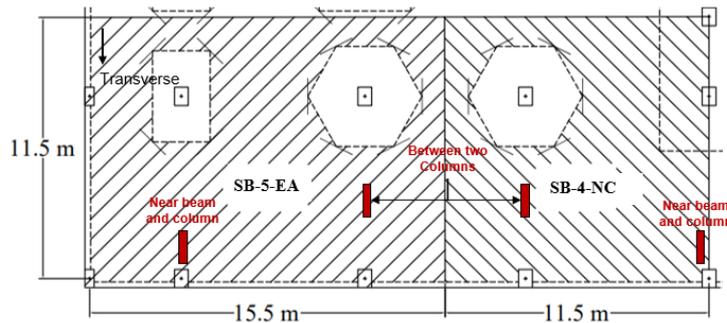

Figure 4.28 Investigated location for slab on beam at construction site 2 (SB-4-NC & SB-5-EA)

Figure 4.29 shows the results of the investigation and FE analysis conducted on the slab on beam at construction site 2 to determine the effect of the mix proportion on the expansion and shrinkage behavior. The results at two different locations shows that expansive concrete produces larger expansion products than normal concrete. This is because the amount of expansive additive is sufficient to produce a significant level of restrained expansion strain. This investigation also revealed no significant difference between the shrinkage of normal and expansive concrete after expansion. To prevent shrinkage cracking, expansive concrete effectively reduces the tensile strain.
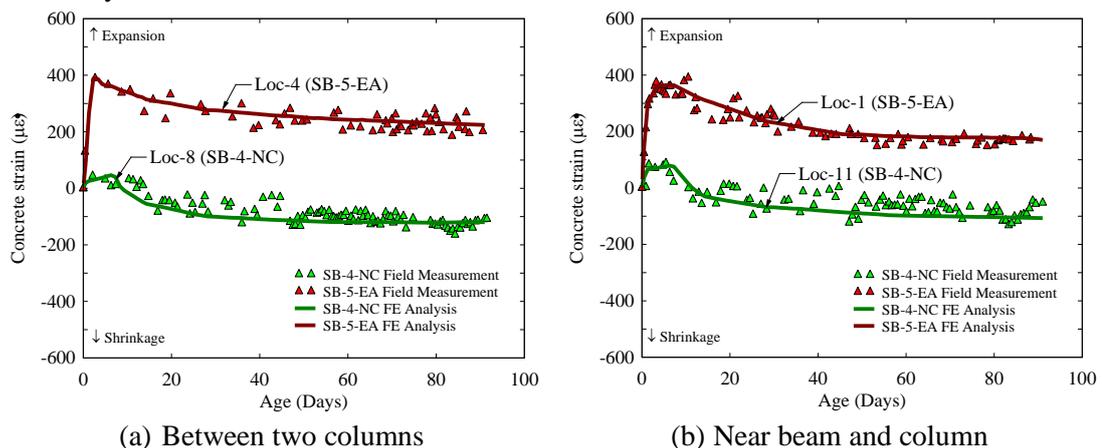
(a) Between two columns　　　　　(b) Near beam and column

Figure 4.29 Transverse strain in slabs on beam at construction site 2 with different mix proportions

The effect of mix proportion can also be investigated in slab on pile structures (SP-1-NC and SP-2-EA). **Figure 4.30** shows the investigation locations for slab on pile structures for normal (SP-1-NC) and expansive concrete (SP-2-EA). This measurement was taken at the top of the pile caps (locations 4 and 1) and near the edge of the slab (locations 5 and 3). Strain in the transverse direction was conducted near the edge of the slab, while longitudinal strain

direction was conducted near the top of pile caps. For slabs on pile with expansive concrete, C-S-A based expansive agent is used with a total amount of 30 kg/m^3.
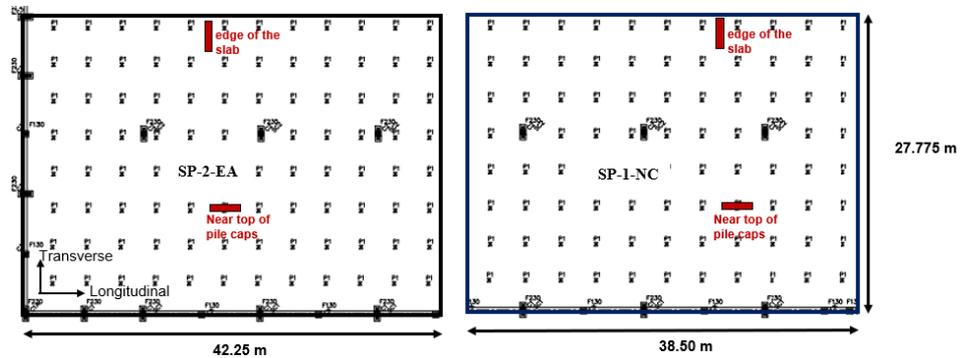

Figure 4.30 Investigated location for slab on pile (SP-1-NC & SP-2-EA)

Figure 4.31 shows the results of the investigation and FE analysis on the effectiveness of expansive concrete in the slab on pile structure. From the strain behavior, it can be concluded that the level of restrained expansion in expansive concrete is much larger than normal concrete. All cases investigated structures show that expansive concrete is effective in producing the level of restrained expansion at the early age of the concrete. In addition, it can be concluded that the shrinkage produced after maximum expansion in expansive concrete does not significantly differ from normal concrete. With two different types of expansive agents used in this study, it can also be concluded that C-S-A-based expansive agent always produces higher level of expansion than C-S-A + CaO-based expansive agent.
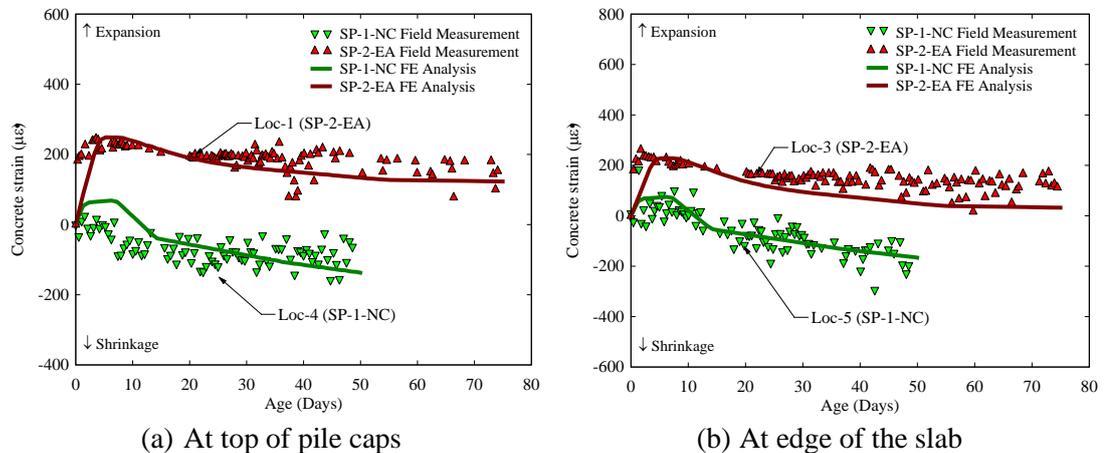

(a) At top of pile caps

(b) At edge of the slab

Figure 4.31 Strain investigation in slabs on pile with different mix proportions

Based on the overall results of investigations regarding the effect of mix proportions such as type and amount of expansive additive on various types of structures, it appears that the estimation results could produce very similar and reliable strain behavior compared to strain behavior of actual structures. The strain behavior from the FE analysis for all the structures, including the slabs on grade, slabs on beam, and slabs on pile is remarkably consistent with the strain behavior of the actual structure, both for normal and expansive concrete. Thus, it can be concluded that the approach method in this study can be used for estimating restrained expansion and shrinkage strain for normal and expansive concrete structures. In expansive concrete structures with various mix proportions, the restrained expansion can be predicted by

applying the reduction factor to generate the effective free expansion strain as input in FE analysis.

4.4.4 Shrinkage damage pattern

The effectiveness of expansive concrete can also be evaluated by investigating the shrinkage cracking between the structures made with normal and expansive concrete. This study investigated the shrinkage cracking pattern that occurs in several structures. This shrinkage cracking investigation was carried out in field investigations and FE analysis. Investigation of the shrinkage damage pattern on the actual structure was carried out on the slabs on grade at construction site 1 and slabs on pile (normal and expansive concrete), while the slab on beam was only investigated through FE analysis due to inspection of crack patterns were not possible because floor tiles were installed and completed during the early ages. While in slabs on grade at construction site 2 and water tank wall structures were cast with only expansive concrete, the effectiveness of expansive concrete over normal concrete could not be evaluated. **Figure 4.32** shows the result of the field inspection on the pattern of shrinkage cracking on the slabs on grade at construction site 1.
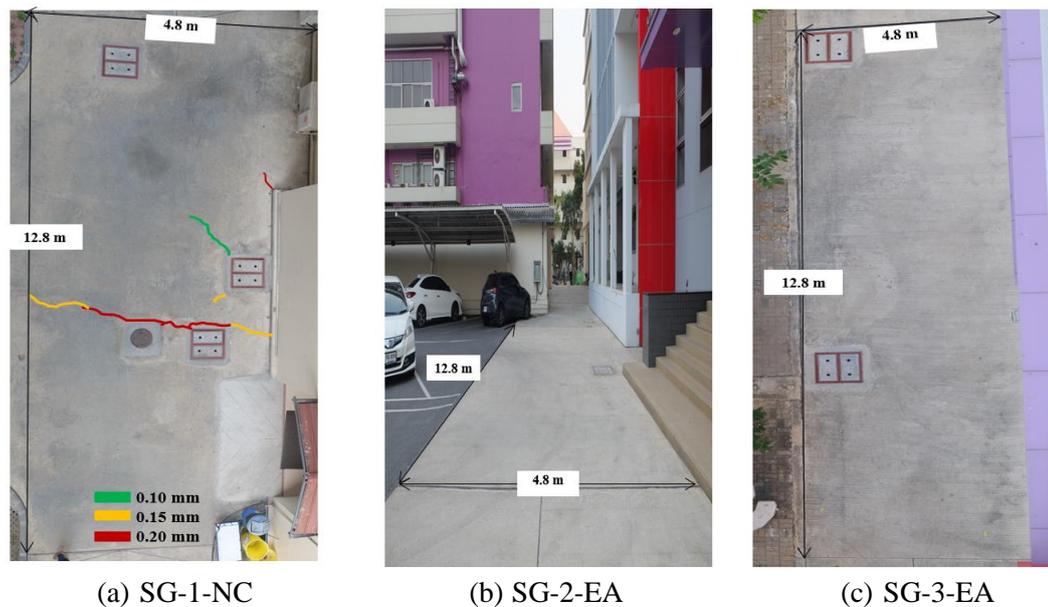
(a) SG-1-NC   (b) SG-2-EA   (c) SG-3-EA

Figure 4.32 Shrinkage cracks from field investigation of the slabs on grade

In the slabs on grade, there are 3 different slabs were used, namely SG-1-NC (normal concrete), SG-2-NA (Expansive concrete with C-S-A based expansive agent), and SG-3-EA (expansive concrete with CaO + C-S-A based expansive agents). This inspection reveals that normal concrete possesses cracks in the transverse direction at the center of the slab, but the expansive concrete structure has no cracks entirely. The crack width is varied from 0.10 to 0.20 mm. The longitudinal direction generates higher stress than the transverse direction due to larger effects of friction. As a result, cracks usually occur in the transverse direction in slabs on grade for normal concrete due to tensile stress. Cracks in normal concrete indicate that the tensile strain is higher than the tensile strain capacity near the crack area. **Figure 4.33** shows damage pattern obtained from FE analysis was investigated using effective plastic strain. Effective plastic strain is a common failure mode for concrete in tension when it is in a plastic

state. Therefore, the effective plastic strain illustrated crack patterns due to shrinkage in the investigated concrete structures. The effective plastic strain is calculated on a scale of 0.00 to 1.00, which means that the tensile strain in the distribution area is zero at 0.00. While an increase in the effective plastic train value indicates an increase in the tensile strain in the concrete, with 1.00 representing cracking.

Based on FE analysis results, it can be seen that SG-1-NC has cracks in the transverse direction located near the center of the slab, while SG-2-EA and SG-3-EA have no cracks. It can be concluded that expansive concrete is effective enough for shrinkage cracking prevention. The maximum total tensile strain in the normal concrete slab was higher than the expansive concrete slab because the normal concrete slab had a relatively much lower early age expansion strain. From the results of the damage pattern based on effective plastic strain from FE analysis, this is comparable to the shrinkage cracking observed from the field investigation for both normal and expansive concrete (compare **Figure 4.32** and **Figure 4.33**). It can be concluded that the results of the FE analysis are very reliable and represent the conditions in the actual structures so that it can be utilized to conduct comprehensive studies on expansive concrete structures.
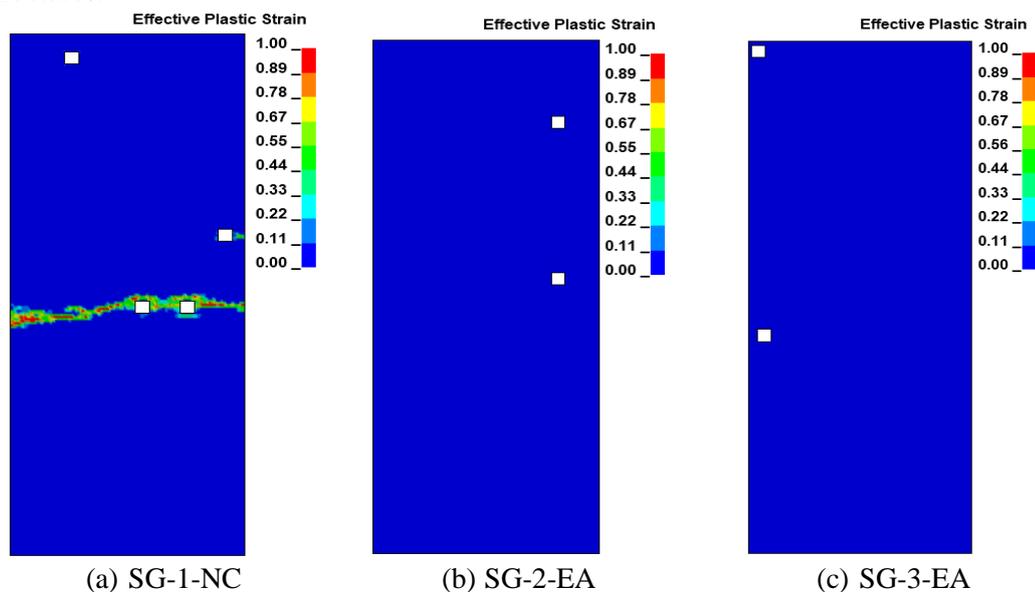

(a) SG-1-NC   (b) SG-2-EA   (c) SG-3-EA

Figure 4.33 Damage patterns in the slabs on grade obtained from FE analysis at 90 days

For slabs on beam both in construction sites 1 and 2, the effectiveness of expansive concrete can also be demonstrated by inspecting shrinkage damage patterns. However, only the effective plastic strain from FE analysis is shown for the slabs on beam since it is not possible to obtain the on-site cracking condition, as explained earlier. The effective plastic strains in the slab on beam at construction site 1 cast with normal concrete indicate the damage (cracking) in the concrete after 90 days due to shrinkage, as shown in **Figure 4.34**. The cause of cracks in SB-1-NC (normal concrete) is restrained shrinkage that exceeds the tensile strain capacity. Cracks dominated near the beam and column and expanded transversely. This indicates that the formation of this failure begins in the area with a high degree of restraint. On the other hand, the expansive concrete slabs on beam (SB-2-EA and SB-3-EA) reveal that cracks only appear near the beam and column, especially in SB-3-EA. This shows that the beam and column areas remain to provide a high degree of restraint. Nevertheless, expansive concrete slabs on beam

produce fewer cracks than normal concrete, so it can be concluded that expansive concrete effectively prevents shrinkage cracking.
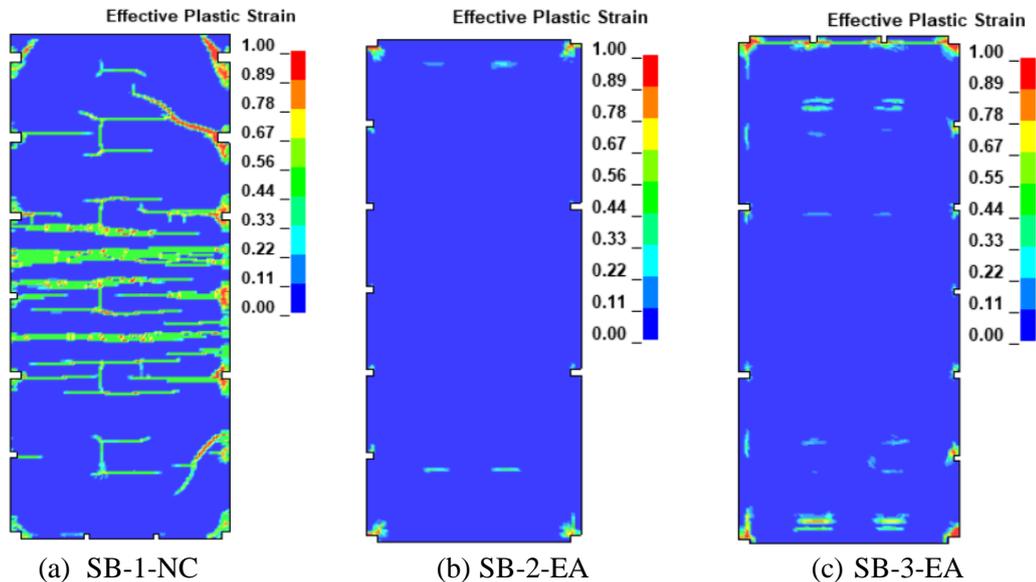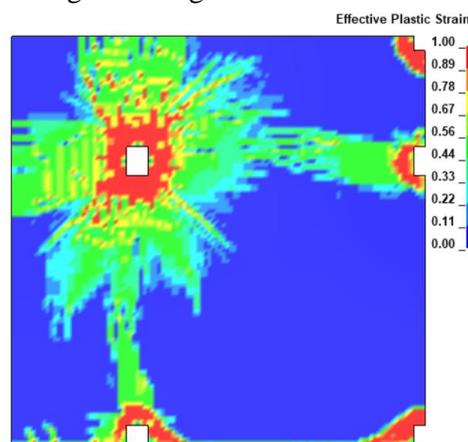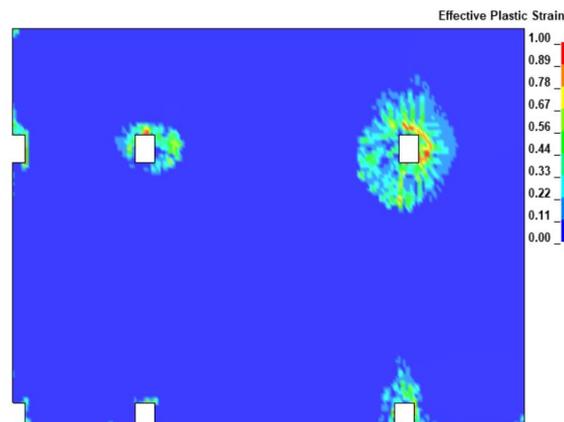

(a) SB-1-NC (b) SB-2-EA (c) SB-3-EA

Figure 4.34 Damage patterns in slabs on beam at construction sire 1obtained from FE analysis at 90 days

The effectiveness of expansive concrete can also be seen in the slabs on beam at construction site 2, both in SB-4-NC (normal concrete) and SB-5-EA (Expansive concrete). **Figure 4.35** shows the effective plastic strain (damage pattern) of slab on beam at construction site 2. In this investigation, no field inspection was conducted because the surface of the slab was finished at an early age of concrete, presenting only the FE analysis results. The results of the effective plastic strain show that the first crack formation begins in the area near the column and adjacent to the pile caps. Based on the damage pattern due to shrinkage in normal concrete, it can be concluded that the area near the crack that occurred probably has a high degree of restraint, producing higher restrained shrinkage strain. The crack continues to spread longitudinally and transversely. On the other hand, significant damage in expansive concrete is seen only in the area near the columns and pile caps. By comparing normal and expansive concrete damage patterns, it is possible to conclude that expansive concrete can significantly reduce the possibility of shrinkage cracking.

(a) SB-4-NC

(b) SB-5-EA

Figure 4.35 Damage patterns in slabs on beam at construction site 2 obtained from FE analysis at 90 days

The inspection of damage patterns due to the effect of expansive additives in overcoming shrinkage cracking prevention can also be observed in slabs on pile structures. The slabs on pile are cast using two different mix proportions, which are normal concrete (SP-1-NC) and expansive concrete (SP-2-EA). As displayed in **Figure 4.36**, field inspections were conducted on both slabs on pile (SP-1-NC & SP-2-EA) as part of this investigation. It should be noted that the area denoted by the blue area cannot be investigated because the surface of the slab has been covered during the early age. This field inspection reveals the damage pattern in the cracks caused by shrinkage occurring in the nearby area of the pile caps and then spreading in the longitudinal and transverse directions. The location of the pile caps is an area with a high degree of restraint, as there is additional reinforcement as the connector between pile caps to the slab. While the slab with expansive concrete shows that the damage occurs at the slab near to column and perimeter beam. The damage in this area occurs as a result of a high degree of restraint due to the restraint effect from the beams and columns.

Figure 4.37 shows the damage pattern on the slab-on-pile results of the FE analysis. The pattern and mechanism of damage to normal and expansive concrete are comparable to the observations of field inspections. Due to the larger restraint in the nearby area of the pile caps, normal concrete is primarily damaged in the vicinity of the pile caps, resulting in a more dominant crack. While damage occurs only in the area adjacent to beams and columns in slabs with expansive concrete, this is due to the influence of external restraint from the beam and column, resulting in a significant degree of restraint in that area. This expansive concrete is sufficient for minimizing damage or cracks in the slabs on pile. In addition, the results of the FE analysis appear to be reliable compared to the field inspections, so the results of FE analysis can be used to predict the behavior of expansive concrete structures accurately.

From the results of field inspections and FE analysis on slabs on grade, slabs on beams, and slabs on piles, it is possible to conclude that expansive concrete is effective in preventing cracking due to shrinkage strain. The results of the FE analysis also confirm the predominance of cracks in normal concrete. On the other hand, expansive concrete has fewer or minor cracks in various structures due to the high degree of restraint. Notably, the results of the FE analysis in this study through damage pattern investigations closely match the results of field investigations on slabs on grade and slabs on pile, indicating the reliability of the investigative

method used to study the behavior of expansive concrete structures. A similar method is implemented on slab on beam, producing comprehensive and reliable strain behavior.
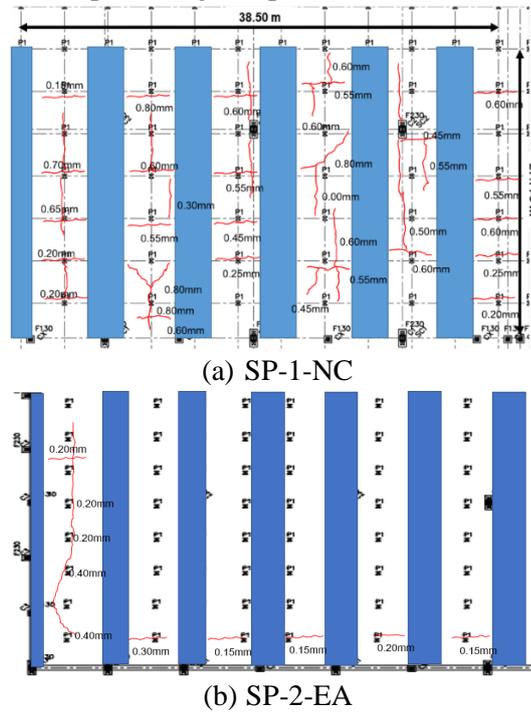

(a) SP-1-NC

(b) SP-2-EA

Figure 4.36 Shrinkage cracks from field investigation of the slabs on pile
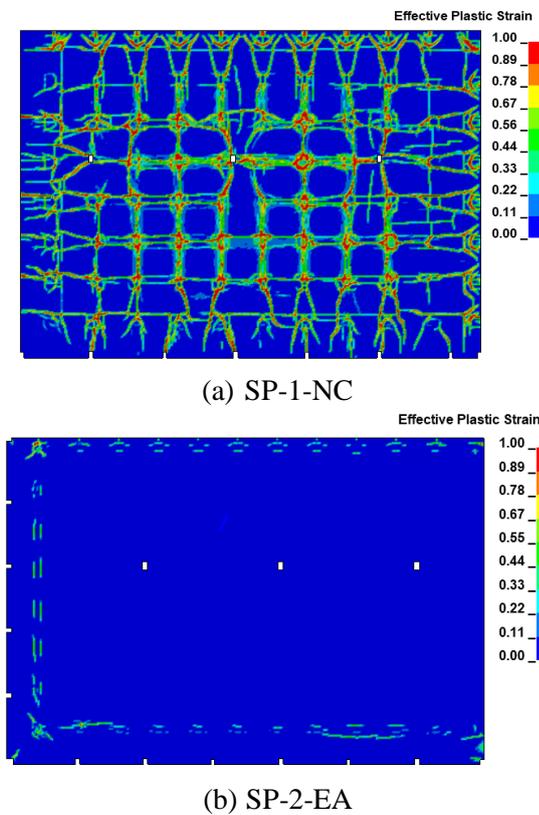

(a) SP-1-NC

(b) SP-2-EA

Figure 4.37 Damage patterns in the slabs on pile obtained from FE analysis at 90 days

4.4.5   Influence of internal restraint

The degree of restraint is one of the most important factors influencing the expansion and shrinkage strain in reinforced concrete structures. For design purposes, measuring the length change of expansive concrete under restraint is recommended. However, the restrained expansion test with a prism specimen does not represent the condition of restrained expansion in actual expansive concrete structures. The length change measurement standard only encompasses a limited range of reinforcement ratios (prism specimen). Meanwhile, the reinforcing ratios in expansive concrete structures vary depending on structure configurations.

Moreover, expansive concrete structures derive their restraint from multiple sources, most notably external restraint. However, the prism specimens only consider internal restraint from the rebar reinforcement. Thus, the level of restrained expansion strain exhibited by the prism specimen is insufficient to represent the level of restrained expansion strain in actual expansive concrete structures. Therefore, FE analysis provides a more comprehensive and better solution for estimating the restrained expansion and shrinkage strains in expansive concrete structures with a broader range of reinforcement ratios and more complex restraint conditions.

This section explores the influence of internal restraint on the expansion and shrinkage of expansive concrete structures. The investigation and FE analysis regarding the effect of internal restraint were conducted on a slab on grade at construction site 1. The longitudinal strain behavior of slabs of grade (SG-2-EA & SG-3-EA) were chosen to investigate the effects of internal restraint on the level of expansion and shrinkage, with the results shown in **Figure 4.38**. The concrete investigation was conducted at the center of the span and at the end of the span near the expansion joint. The total thickness of SG-2-EA and SG-3-EA is 0.15 m, while the main steel layer is located at 0.0035 m from the top surface of the slab. Internal restraint is provided by only rebar reinforcement at the mid-span and by rebar reinforcement, dowels, and dowel connector at the end of the span. All slabs contain the same amount of reinforcement in both the longitudinal and transverse directions. Two measured strain gauges were chosen for each slab to investigate the effects of the level of internal restraint: concrete strain gauges at locations 3 and 4 for SG-2-EA and concrete strain gauges at locations 5 and 6 for SG-3-EA. Locations 3 and 5 are at the mid-span, while locations 4 and 6 are at the end of the span.
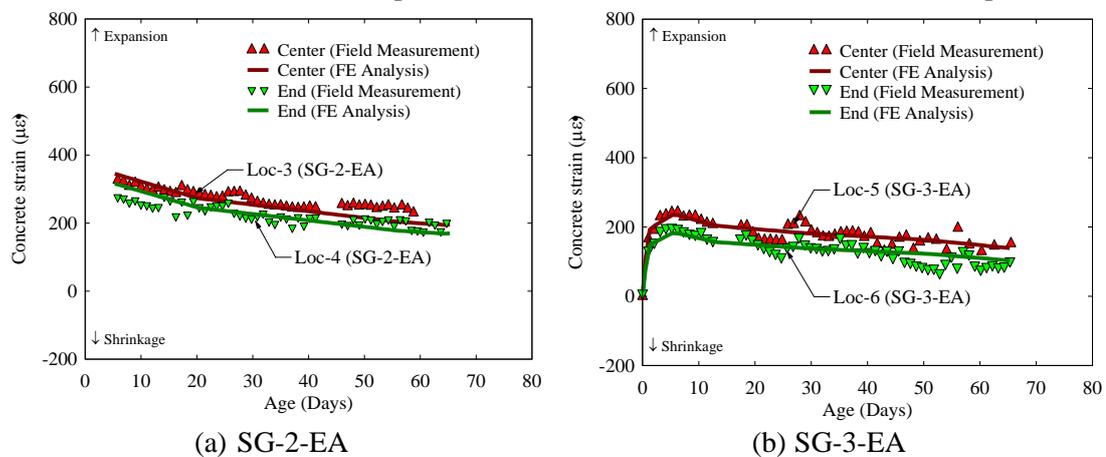

(a) SG-2-EA   (b) SG-3-EA

Figure 4.38 Effects of internal restraint in slabs on grade (construction site 1) in the longitudinal direction

Field investigations and FE analysis results in **Figure 4.38** show that the expansion strain at the end of the slab span is lower than the strain at the center. Low expansion strain near the end of the slab span is caused by the additional internal restraint from the dowel reinforcement. **Figure 4.39** shows the reinforcement details at the end of the slab, showing extra dowel rebars, while there is no additional reinforcement at the mid-span of the slab. The dowel rebars at the end of the slab provide additional restraint in this area compared to the mid-span of the slab. Therefore, the expansion near the joint is lower than at the center of the slab. It can be concluded that a higher degree of restraint causes lower expansion, and the predicted expansion and shrinkage strain results from FE analysis satisfactorily matched with the field measurement.
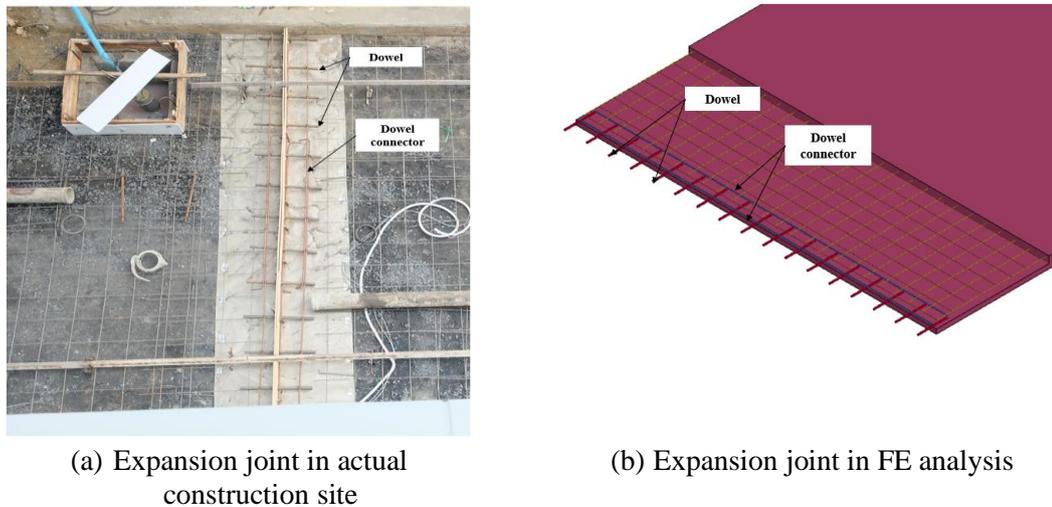

(a) Expansion joint in actual construction site
(b) Expansion joint in FE analysis

Figure 4.39 Expansion joint in slabs on grade structure

The effect of internal restraint on the level of expansion and shrinkage is also demonstrated by comparing the in-plane strain along depth direction in slab on grade. **Figure 4.40** shows the longitudinal strain at mid-depth and steel layer in the slabs SG-2-EA and SG-3-EA in order to investigate the in-plane depth expansion strain. The strain gauges chosen for this investigation are located at location 3 for SG-2-EA and location 5 for SG-3-EA, respectively. The field investigation and FE analysis show that the concrete expansion strain at the mid-depth is higher than that at the steel layer. Due to the high degree of restraint from the rebars, the restrained expansion strain at the steel layer decreases. The mid-depth expansion strain is higher than the expansion strain at the steel layer. This is because the area near the mid-depth has less internal restraint, allowing the expansive agent to produce the expansive product more sufficiently.

Based on the results of field investigations and estimates using FE analysis, it can be seen that the results of this FE analysis corresponded satisfactorily with the field measurement. The results of this FE analysis can estimate the restrained expansion and shrinkage strain for various internal restraint configurations based on the analysis of multiple cases involving the effect of internal restraint. It can be concluded that the estimating method to study the behavior of expansion and shrinkage in reinforced expansive concrete can be applied in various internal restraint configurations.
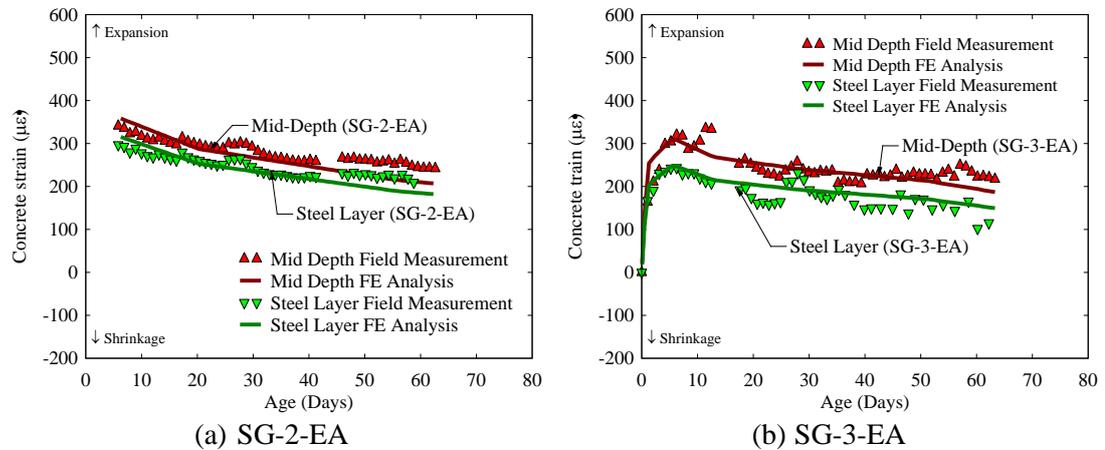
Figure 4.40 Effects of internal restraint in slabs on grade (construction site 1) in the depth direction

4.4.6 Influence of external restraint

The configuration of a structure, including its dimensions and adjacent structures, influences the level of complexity of the structure. The external restraint complexity can affect the level of restrained expansion and shrinkage in expansive concrete structures. Several measured locations were chosen for expansive concrete slabs on beam, slabs on pile, and water tank walls in order to investigate the effect of external restraint on expansion and shrinkage behavior. The effect of external restraint on the restrained expansion and shrinkage rate can be observed from the slabs on beam at construction site 1.

The internal restraint in the slabs on beam at construction site 1 is provided by the rebar reinforcement, while the external restraint is provided by the adjacent structural members such as pile caps, transverse and longitudinal perimeter beams, columns, and footings. On SB-2-EA and SB-3-EA, the effect of external restraint was investigated at several measurement locations. The mid-depth transverse concrete strain was selected to investigate the external restraint effects in the slabs on beam at construction site 1. Two different strain gauge locations for each slab, as shown in **Figure 4.41**. The first strain gauge location is at the center between the two pile caps (location 6 for SB-2-EA and location 9 for SB-3-EA), and the second location is near the longitudinal perimeter beam (location 7 for SB-2-EA and location 8 for SB-3-EA).
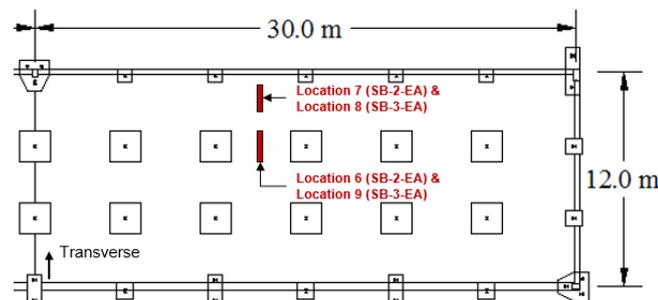

Figure 4.41 Measured location in slabs on beam at construction site 1 to study the effects of external restraint

Figure 4.42 shows the field investigation and FE analysis results for restrained expansion and shrinkage strain for slabs on beam at construction site 1 for selected measured locations. According to the results of strain measurement and FE analysis of SB-2-EA, the

restrained expansion strain in the transverse direction near the longitudinal perimeter beam is less than the strain between two pile caps. This is due to the fact that the measurement of strain was conducted in the transverse direction, where location 7 is very near to the longitudinal perimeter beam, while location 6 is far from that beam. According to this investigation, the degree of restraint near the beam and column area (location 7) is high due to the effect of external restraint provided by the beam and columns, causing the restrained transverse expansion strain to be lower. In the transverse direction, location 6 resulted in higher restrained expansion strain than location 7. This is due to the effect of restraints in this region, particularly in the transverse direction are only internal restraints (reinforcing bars) are provided, while the effect of external restraints may be relatively low. The field measurement and FE analysis results for SB-3-EA exhibit a similar restrained expansion and shrinkage strain pattern. SB-3-EA measurements are taken in the same spot as SB-2-EA measurements. External restraints significantly impact the expansion and shrinkage of reinforced concrete structures.
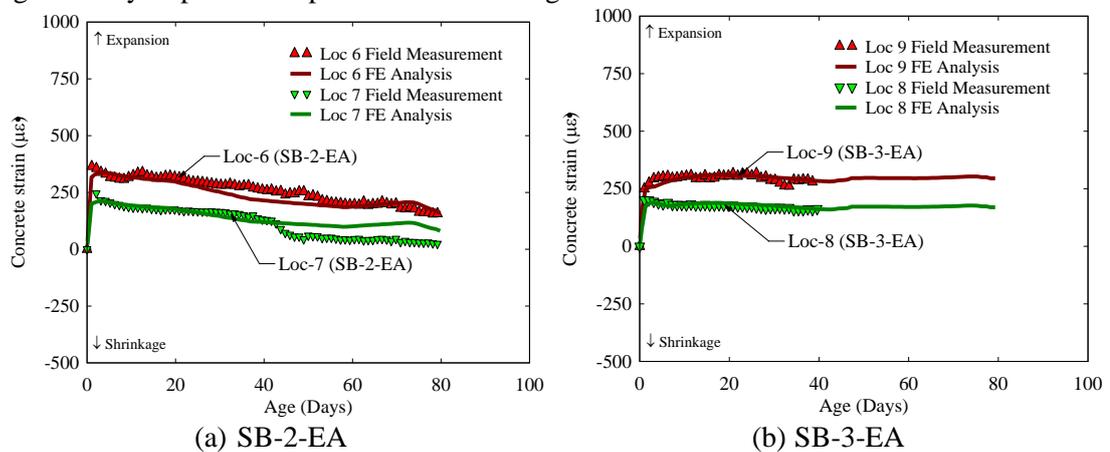

(a) SB-2-EA   (b) SB-3-EA

Figure 4.42 Effects of external restraint in slabs on beam (construction site 1)

The effect of external restraint on restrained expansion and shrinkage strain can also be investigated in slabs on beam at construction site 2. Investigations on slabs on beam at construction site 2 were only carried out on slabs cast with expansive concrete (SB-5-EA). **Figure 4.43** shows the measured location and direction of the strain measurement in order to investigate the effect of external restraint on the rate of expansion and shrinkage. In this investigation, the concrete strain at mid-depth was determined by comparing the strain at locations 2 and 3 in the longitudinal direction. In addition, an investigation was conducted by comparing the concrete strain at locations 4 and 5 along the transverse direction.
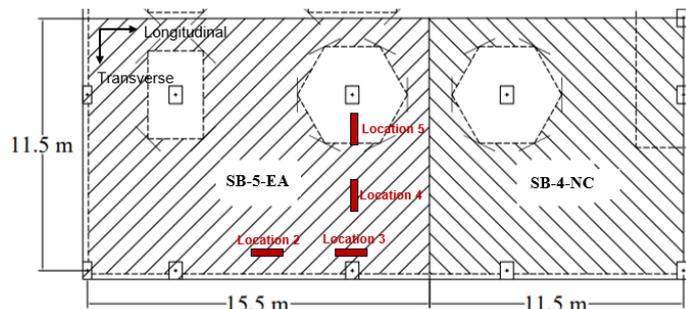

Figure 4.43 Measured location in slabs on beam at construction site 2 (SB-5-EA) to study the effects of external restraint

Figure 4.44 shows the results of the field investigation and FE analysis of the slabs on beams at construction site 2. As seen in **Figure 4.44a**, the strain in the longitudinal direction shows that location 3 produces a larger restrained expansion than location 2. This is due to the influence of internal restraint from the reinforcing bar and external restraint from the effect of friction on the base slab on the restrained expansion at this location (location 2). However, location 3 along the longitudinal direction is near another slab (normal concrete), as this conventional concrete is placed after expansive concrete. Therefore, location 3 has a lower degree of restraint in the longitudinal direction during the expansion process. Consequently, the derivative restrained expansion strain is larger than location 2. **Figure 4.44b** shows that location 4 generates a more significant restrained expansion strain than location 5. This is evidently the case due to location 5 to the column and pile caps in the transverse direction, so the influence of external restraint at location 5 reduces the restrained expansion strain.
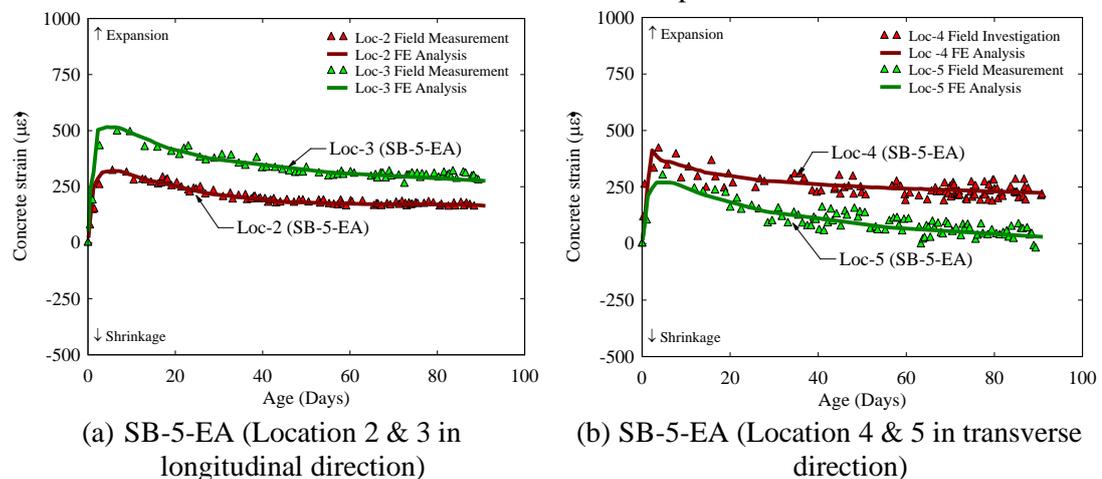

(a) SB-5-EA (Location 2 & 3 in longitudinal direction)

(b) SB-5-EA (Location 4 & 5 in transverse direction)

Figure 4.44 Effects of external restraint in slabs on beam (construction site 2)

Field investigation and FE analysis can also be performed on the slabs on pile (SP-2-EA) to determine the effect of external restraint. The reinforcing bar is considered an internal restraint in these slabs on pile structure, while the column, beam, and pile caps provide the external restraint. Three longitudinal field measurement locations were selected to investigate the effect of external restraint. All measurements were taken at the mid-depth of the slab. The location of the investigation into the effect of external restraint for slabs on pile is displayed in **Figure 4.45**. The first location is located directly above the pile caps, while the second location is divided into two sections, with location 2a located between two pile caps and location 2b located in the center of the slab with less effect from the external restraint.

Figure 4.46 shows the results of the field investigation and FE analysis related to the impact of external restraint on the slabs on pile made with expansive concrete (SP-2-EA). **Figure 4.46a** compares location 1 and location 2b, where FE analysis and field measurements discover that location 2 has a larger expansion strain than location 1. This is because location 1 is directly above the pile caps, where the pile caps provide an external restraint and an additional reinforcing bar as a connector between the pile caps and the slab. Location 2b, on the other hand, is far away from pile caps and other external restraints. At location 2b, only internal restraint (reinforcing bars) and external restraint from friction on the bottom surface of the slab provide restraints. By comparing the restraint conditions at these two locations, it is obvious that location 1 has a higher level of restraint, resulting in less expansion than location

2b. In addition, **Figure 4.46b** compares the results of the strain investigation at locations 2a and 2b for the slabs on pile. The investigation and FE analysis revealed that location 2b showed a larger restrained expansion strain than location 2a. This is because location 2a is between two pile caps, allowing for additional external restraint, and increasing the degree of longitudinal restraint near location 2a. Due to the small effect of external restraint, location 2b produces larger restrained expansion than location 2a.
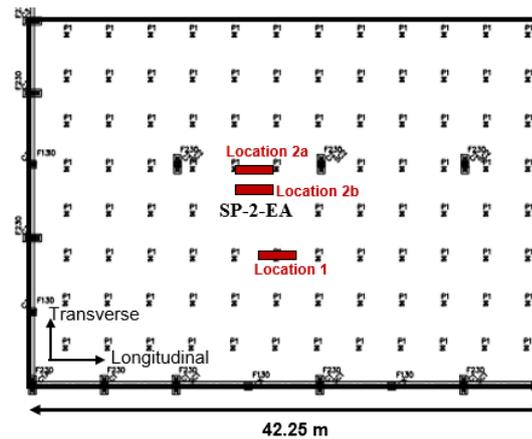

Figure 4.45 Measured location in slabs on pile (SP-2-EA) to study the effects of external restraint

(a) SP-2-EA (Location 1 & 2b)   (b) SP-2-EA (Location 2a & 2b)
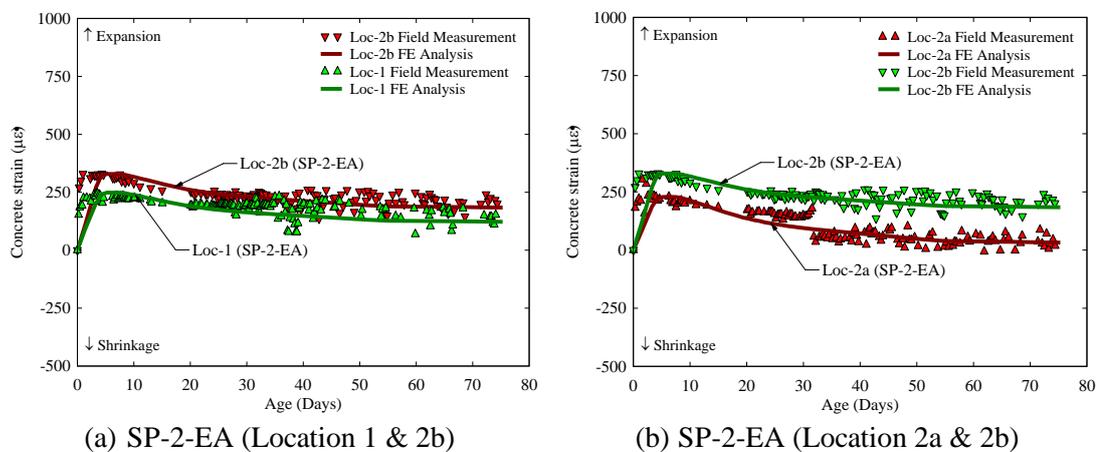
Figure 4.46 Effects of external restraint in slabs on pile

The structure of water tank walls can also be investigated to determine the effect of external restraint on the expansion rate (WT-1-EA and WT-2-EA). The measurement locations on the two water tank wall structures are described in **Figure 4.47**. On each wall, the investigation was conducted by comparing the horizontal measurement location in the middle of the span (1 for WT-1-EA and 5 for WT-2-EA) with the horizontal direction measurement near the bottom slab (location 2 for WT-1-EA and location 6 for WT-2-EA). In this investigation, the bottom and top slabs are assumed to be external restraints, while reinforcing bars are assumed to be internal restraints.

Figure 4.48 shows the results of the investigation and FE analysis regarding the effect of external restraint on the water tank wall. This investigation found that WT-1-EA and WT-2-EA generated a higher restrained expansion strain at the span center (locations 1 and 5) than at

the measurement location near the bottom slab (locations 2 & 6). At the measurement location near the bottom slab, an additional reinforcing bar is connected between the bottom slab and the wall. As a result, the degree of restraint in the area near the bottom part of the wall increases, resulting in a lower restrained expansion strain (locations 2 & 6).
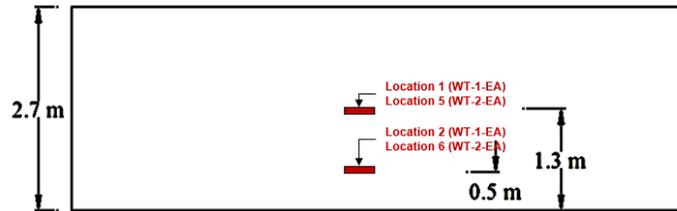

Figure 4.47 Measured location in water tank walls to study the effects of external restraint

Field investigations and FE analysis can be conducted to determine the effect of external restraint on the expansion and shrinkage behavior of expansive concrete structures. External restraint plays a significant role in the expansion and shrinkage behavior of expansive concrete structures, as demonstrated by the research results of this investigation. In areas adjacent to external restraints, such as neighboring structure and friction effect increase the degree of restraint. In areas with a high degree of restraint, the level of restrained expansion is lower than in areas with a low degree of restraint. To mitigate the effects of external restraint, an additional reduction factor (ϕ_e) was utilized in this investigation. Due to the presence of an external restraint, neighboring areas are subjected to increased compressive stress, allowing more expansive product move into the pores. The estimation results from the FE analysis of the effect of external restraint on slabs on beam, slabs on pile, and the water tank walls indicate that the overall location satisfactorily matched the field investigation results. This demonstrates that the method used to estimate the restrained expansion and shrinkage strain in this study is adequate for predicting the behavior of strains with different types of structural configurations.
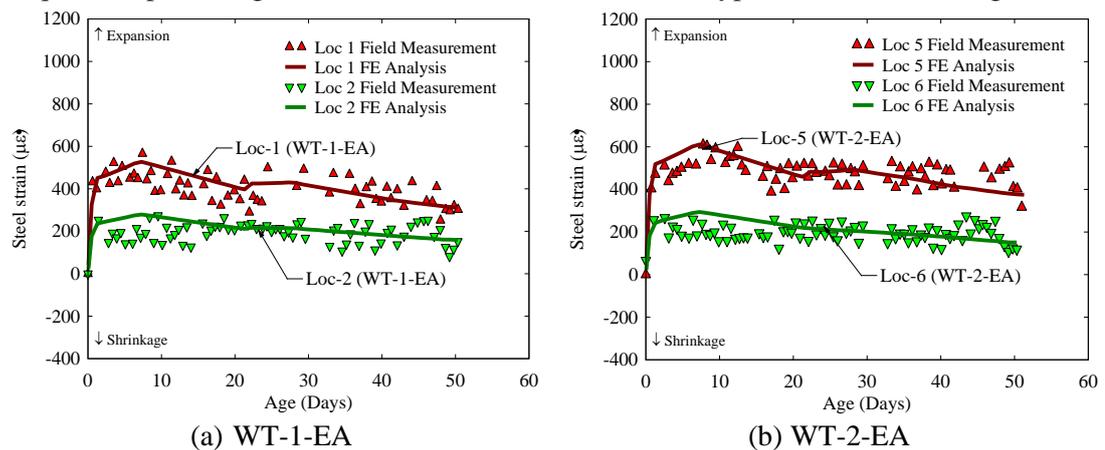

(a) WT-1-EA   (b) WT-2-EA

Figure 4.48 Effects of external restraint in water tank walls

4.4.7 Influence of dimension and direction

In expansive concrete structures, the configuration of the structure, such as dimension and direction of strain, also affects the behavior of restrained expansion and shrinkage strain. A degree of external restraint and strain orientations are typically dependent on the dimensions of the structure and the adjacent structural member. A larger dimension increases the frictional effects at the base slab in slabs on grade. However, due to the effects of adjacent structural

members, the short dimension of slabs on beam structures may result in a high degree of external restraint. To evaluate the complexity of external restraints on expansive concrete structures, it is necessary to conduct expansion strain studies in multiple directions. Slabs on grade at construction site 2, slabs on beam, and water tank walls were chosen to determine the effect of dimensions and strain direction on the level of expansion. The effect of the dimension of the structures on the slab on grade was investigated using two slabs with the same mix proportion but different dimensions (SD-4-EA and SG-5-EA). Location 5 at the edge of the center span was chosen for SG-4-EA and location 12 at the center span was also chosen for SG-5-EA to investigate the effect of the dimensions. **Figure 4.49** shows the results of the investigation and FE analysis by comparing strains at the exact location but in different measurement directions (longitudinal and transverse).

The field measurement results for SG-4-EA and SG-5-EA in **Figure 4.49** appear to fluctuate because construction work occurs during the measurement process, affecting the measured strain. The results of SG-4-EA show a slight difference in expansion and shrinkage strains between the longitudinal and transverse directions. The expansion strain in the transverse direction is slightly lower than the longitudinal expansion strain. This is because the measured location (location 5) in the transverse direction was close to the main slab that had been already cast before this measured slab casting process. The results of SG-5-EA indicate that the strains in the transverse and longitudinal directions are nearly identical. This is because the same reinforcement ratio is used in both directions (longitudinal and transverse). Besides, the length and width of SG-5-EA are not much different, resulting in similar friction effects in both directions. In addition, the measured location at SG-5-EA (location 12) is far away from the main slab, so the main slab does not significantly restrain expansion and shrinkage as in the case of SG-4-EA.
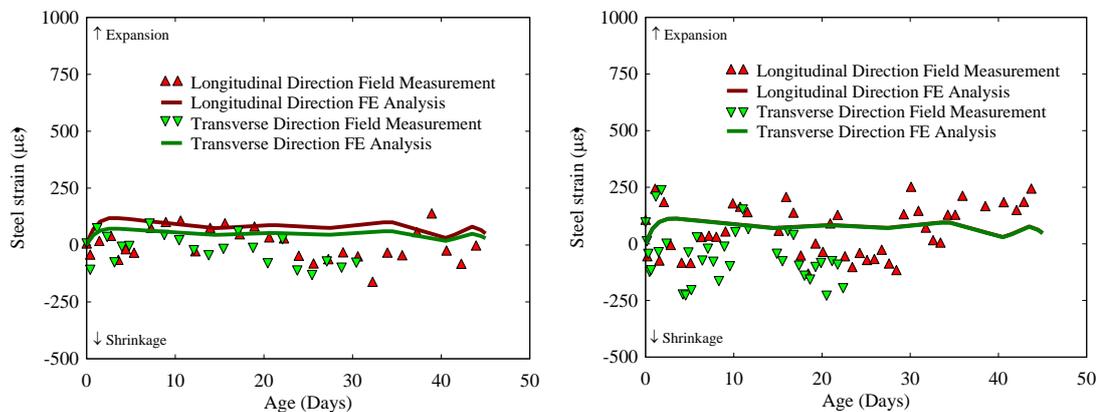
(a) SG-4-EA (Location 5)   (b) SG-5-EA (location 12)

Figure 4.49 Effects of the dimension and strain direction in slabs on grade
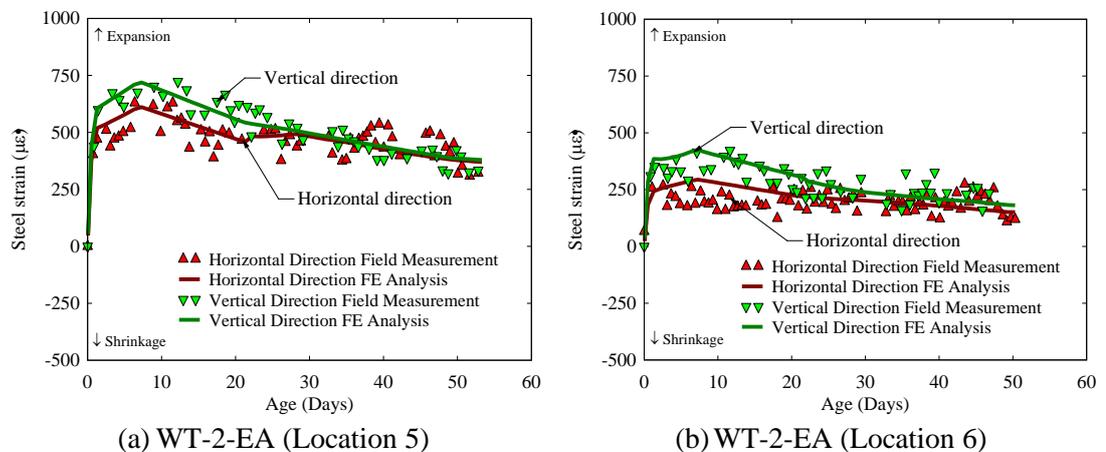
The influence of the dimensions of the structure can also be investigated on the WT-1-EA and WT-2-EA water tank walls. This water tank wall is cast using the same mix proportion but in different dimensions. Measurements were located at the center of the wall (location 1 for WT-1-EA and location 5 for WT-2-EA). At these two locations, measurements were taken on the outer face in the horizontal direction. **Figure 4.50** shows the results of the field investigation and FE analysis concerning the influence of structural dimensions on restrained expansion and shrinkage strain. The results in **Figure 4.50** show that WT-1-EA (strain gauge location 1)

expands less than WT-2-EA (strain gauge location 5), this is due to the effect of different lengths of the east and north wall. The expansion strain in the horizontal direction of WT-2-EA is higher than the strain in WT-1-EA due to the different degrees of restraint caused by the length of the wall. Because WT-2-EA has a shorter span than WT-1-EA, the expansion strain is larger due to lower restraint. It can be concluded that based on field investigation and FE analysis, the structural configuration has significant effects on the level of expansion and shrinkage. The dimensions of the structure also affect the stiffness and degree of restraint, which are crucial factors in determining the level of expansion in expansive concrete structures.
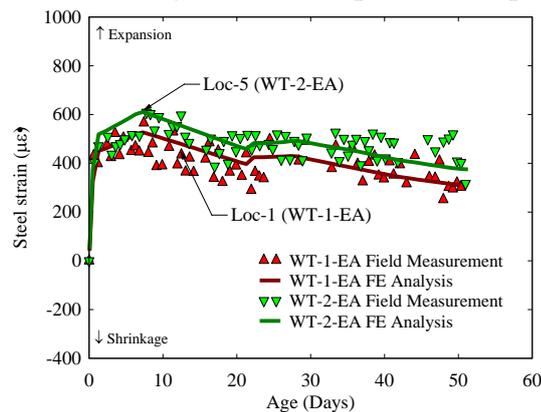

Figure 4.50 Strain comparison between WT-1-EA and WT-2-EA

Strain differences between longitudinal and transverse directions were also studied for slabs on beams at a construction site 1. For the investigation, two distinct locations for SB-3-EA were chosen: location 9 in the center between two pile caps and location 10 near the transverse perimeter beam and columns. The investigation and FE analysis results regarding the effect of strain direction on the degree of expansion for slabs on beam can be seen in **Figure 4.51**. Concrete strain from field investigation and FE analysis in SB-3-EA show that the transverse direction gives higher restrained expansion strain than the longitudinal direction at these two locations (locations 9 and 10). The same reinforcement ratio was used in transverse and longitudinal directions at location 9. However, two pile caps are near that location in the longitudinal direction. These pile caps provide external restraint in the longitudinal direction. As a result, the expansion strain in the longitudinal direction is lower than the transverse expansion strain due to the effects of the position of the pile caps. Under these conditions, it is obvious that the degree of restraint at location 9 in the longitudinal direction is higher than in the transverse direction. Meanwhile, location 10 is very close to the transverse perimeter beam and columns but is in the center of the span in the transverse direction. This configuration implies that the degree of restraint in the longitudinal direction provided by the transverse perimeter beam and columns is high compared to the transverse direction. As a result of field investigation and FE analysis at location 10, it can be concluded that the longitudinal direction produces a lower level of restrained expansion strain than the transverse direction due to the difference in restraint degree between these two directions in this location.

The effects of strain directions in the water tank east wall (WT-2-EA) are demonstrated in **Figure 4.52**. This section discusses the results of steel strain near the outer face in field investigation and FE analysis at several measured locations. Location 5 at the center of the wall and location 6 near the bottom slab were chosen to investigate the strain in different directions.

1) The reduction factor used to determine the free strain can effectively estimate the restrained expansion strain in expansive concrete structures.
2) The level of expansion and shrinkage strains can be estimated by considering various factors affecting the expansion level on expansive concrete structures, such as mix proportion, degree of restraint, and measurement direction.
3) Structures with expansive concrete achieve a higher expansion rate than normal concrete. The level of expansion of the C-S-A-based expansive concrete is higher than the CaO + C-S-A-based expansive concrete.
4) The observed crack pattern indicates that expansive concrete effectively prevents shrinkage cracking, as evidenced by the field investigation and FE analysis.
5) In expansive concrete structures, structural configuration and degree of restraint significantly affect the level of expansion and shrinkage. The area with higher restraint conditions always produced lower restrained expansion strain.

References

[1]   A. I. Zerin, A. Hosoda, S. Komatsu, and H. Ishii, "Full scale thermal stress simulation of multiple span steel box girder bridge evaluating early age transverse cracking risk of durable RC deck slab," *J. Adv. Concr. Technol.*, vol. 18, no. 7, pp. 420–436, 2020, doi: 10.3151/jact.18.420.
[2]   K. Huang, M. Deng, L. Mo, and Y. Wang, "Early age stability of concrete pavement by using hybrid fiber together with MgO expansion agent in high altitude locality," *Constr. Build. Mater.*, vol. 48, pp. 685–690, 2013, doi: 10.1016/j.conbuildmat.2013.07.089.
[3]   C. Chen, C. Tang, and Z. Zhao, "Application of MgO concrete in China Dongfeng arch dam foundation," *Adv. Mater. Res.*, vol. 168–170, pp. 1953–1956, 2011, doi: 10.4028/www.scientific.net/AMR.168-170.1953.
[4]   J. Zhou, X. Chen, and J. Zhang, "Early-age temperature and strain in basement concrete walls: field monitoring and numerical modeling," *J. Perform. Constr. Facil.*, vol. 26, no. 6, pp. 754–765, 2012, doi: 10.1061/(asce)cf.1943-5509.0000294.
[5]   M. Collepardi, R. Troli, M. Bressan, F. Liberatore, and G. Sforza, "Crack-free concrete for outside industrial floors in the absence of wet curing and contraction joints," *Cem. Concr. Compos.*, vol. 30, no. 10, pp. 887–891, 2008, doi: 10.1016/j.cemconcomp.2008.07.002.
[6]   R. Troli, G. Iannis, and S. Maringoni, "Use of a shrinkage compensating concrete for the construction of a crack free slab foundation," in *XVI ERMCO Congress*, 2012, pp. 1–9.
[7]   J. Richardson, S. Eskildsen, B. Schiller, and M. Jones, "Measured strains in post-tensioned concrete parking deck Made with shrinkage-compensating concrete," *ACI Struct. J.*, vol. 107, no. 6, pp. 718–725, 2010, doi: 10.14359/51664020.
[8]   C. Ramseyer, K. Renevier, and S. Roswurm, "Behavior of shrinkage compensating concrete in an unrestrained and restrained environment," in *American Concrete Institute*, 2012, vol. 2012, no. SP 307, pp. 107–126.
[9]   S. H. Myint, G. Tanapornraweekit, and S. Tangtermsirikul, "Investigation of expansive concrete structures through strain monitoring in field structures," *Asian J. Civ. Eng.*, vol. 22, no. 3, pp. 565–578, 2021, doi: 10.1007/s42107-020-00332-1.
[10]   Q. Cao, S.-D. Hwang, K. H. Khayat, and G. Morcous, "Design and implementation of self-consolidating concrete for connecting precast concrete deck panels to ribdge girders," *J. Mater. Civ. Eng.*, vol. 28, no. 8, pp. 1–12, 2016, doi: 10.1061/(asce)mt.1943-5533.0001563.
[11]   American Concrete Institute Committee, *ACI 223R-10 Guide for the use of shrinkage*

compensating concrete. Farmington Hills: American Concrete Institute, 2010.

[12]   Japan Society of Civil Engineers Committee, *JSCE No. 23: Recommended practice for expansive concrete*, no. 23. Tokyo: Concrete Library of JSCE, 1994.

[13]   T. Kim, K. Y. Seo, C. Kang, and T. K. Lee, "Development of eco-friendly cement using a calcium sulfoaluminate expansive agent blended with slag and silica fume," *Appl. Sci.*, vol. 11, no. 1, pp. 1–24, 2021, doi: 10.3390/app11010394.

[14]   S. H. Myint, G. Tanapornraweekit, and S. Tangtermsirikul, "Prediction of restrained expansion and shrinkage strains of reinforced concrete specimens by using finite element analysis," in *Lecture Notes in Civil Engineering*, 2021, vol. 101, pp. 1849–1859. doi: 10.1007/978-981-15-8079-6_170.

[15]   R. Dumaru, W. Saengsoy, and S. Tangtermsirikul, "Effect of restraining and curing conditions on expansion and shrinkage of expansive concrete," *Proc. 2020 Int. Multi-Conference Adv. Eng. Technol. Manag.*, pp. 165–170, 2020.

[16]   L. Xu, J. Pan, and X. Yang, "Mechanical performance of self-stressing CFST columns under uniaxial compression," *J. Build. Eng.*, vol. 44, no. 103366, pp. 1–14, 2021, doi: 10.1016/j.jobe.2021.103366.

[17]   W. Huang, Z. Fan, P. Shen, L. Lu, and Z. Zhou, "Experimental and numerical study on the compressive behavior of micro-expansive ultra-high-performance concrete-filled steel tube columns," *Constr. Build. Mater.*, vol. 254, no. 119150, pp. 1–10, 2020, doi: 10.1016/j.conbuildmat.2020.119150.

[18]   F. W. Lu, S. P. Li, and G. Sun, "Nonlinear equivalent simulation of mechanical properties of expansive concrete-filled steel tube columns," *Adv. Struct. Eng.*, vol. 10, no. 3, pp. 273–281, 2007, doi: 10.1260/136943307781422271.

[19]   X. S. Qu, Y. Deng, G. J. Sun, Q. Liu, and Q. Liu, "Eccentric compression behaviour of rectangular concrete-filled steel tube columns with self-compacting lower expansion concrete," *Adv. Struct. Eng.*, vol. 25, no. 3, pp. 491–510, 2022, doi: 10.1177/13694332211054228.

[20]   H. Prayuda, R. Dumaru, G. Tanapornraweekit, S. Tangtermsirikul, W. Saengsoy, and K. Matsumoto, "Estimation of restrained expansion strain of reinforced expansive concrete considering mixture and curing conditions," *Constr. Build. Mater.*, vol. 322, no. 126386, pp. 1–15, 2022, doi: 10.1016/j.conbuildmat.2022.126386.

[21]   J.-X. Zhang, H.-M. Lyu, S.-L. Shen, and D.-W. Hou, "Investigation of crack control of underground concrete structure with expansive additives," *J. Mater. Civ. Eng.*, vol. 33, no. 1, pp. 1–8, 2021, doi: 10.1061/(asce)mt.1943-5533.0003528.

[22]   X. Y. Jing, X. H. Liu, and X. Zhang, "Thermal stress compensation of MgO concrete in construction of high arch dams in cold areas," *Adv. Mater. Res.*, vol. 852, no. February 1994, pp. 427–431, 2014, doi: 10.4028/www.scientific.net/AMR.852.427.

[23]   L. Wang *et al.*, "Pore structural and fractal analysis of the effects of MgO reactivity and dosage on permeability and F-T resistance of concrete," *Fractal Fract.*, vol. 6, no. 113, pp. 1–17, 2022, doi: 10.3390/fractalfract6020113.

[24]   L. Mo *et al.*, "Synergetic effects of curing temperature and hydration reactivity of MgO expansive agents on their hydration and expansion behaviours in cement pastes," *Constr. Build. Mater.*, vol. 207, pp. 206–217, 2019, doi: 10.1016/j.conbuildmat.2019.02.150.

[25]   N. D. Van, E. Kuroiwa, J. Kim, H. Choi, and Y. Hama, "Influence of restrained condition on mechanical properties, frost resistance, and carbonation resistance of expansive concrete," *Materials (Basel).*, vol. 13, no. 2136, pp. 1–16, 2020.

[26]   Y. Peng, S. Tang, J. Huang, C. Tang, L. Wang, and Y. Liu, "Fractal analysis on pore structure and modeling of hydration of magnesium phosphate cement paste," *Fractal Fract.*, vol. 6, no. 337, pp. 1–18, 2022, doi: 10.3390/fractalfract6060337.

[27]   L. Wang *et al.*, "Influence of MgO on the hydration and shrinkage behavior of low heat

portland cement-based materials via pore structural and fractal analysis," *Fractal Fract.*, vol. 6, no. 40, pp. 1–20, 2022, doi: 10.3390/fractalfract6010040.

[28] L. Mo, J. Fang, B. Huang, A. Wang, and M. Deng, "Combined effects of biochar and MgO expansive additive on the autogenous shrinkage, internal relative humidity and compressive strength of cement pastes," *Constr. Build. Mater.*, vol. 229, no. 116877, pp. 1–9, 2019, doi: 10.1016/j.conbuildmat.2019.116877.

[29] N. D. Van, H. Choi, and Y. Hama, "Modeling early age hydration reaction and predicting compressive strength of cement paste mixed with expansive additives," *Constr. Build. Mater.*, vol. 223, pp. 994–1007, 2019, doi: 10.1016/j.conbuildmat.2019.07.290.

[30] ASTM International, *ASTM C157/C157M-08: Standard test method for length change of hardened hydraulic cement mortar and concrete*. West Conshohocken, 2008. doi: 10.1002/9781118702956.ch15.

[31] ASTM International, *ASTM C39/C39M-20: Standard test method for compressive strength of cylindrical concrete specimens*. 2020.

[32] ASTM International, *C150/C150M-16: Standard specification for portland cement*, ASTM Inter. West Conshohocken: ASTM International, 2015. doi: 10.1520/C0150.

[33] Thailand Standards Association, *TIS 2135-2545: Coal fly ash for use as an admixture in concrete*. Bangkok: Thailand Industrial Standard, 2003.

[34] Z. Q. Siddique, "Finite element simulation of curling on concrete pavements," Kansas, 2004. doi: 10.1017/S0165115300023299.

[35] Y. D. Murray, *Users manual for LS-DYNA concrete material model 159*, no. May. Virginia, 2007.

[36] R. M. Brannon and S. Leelavanichkul, "Survey of four damage models for concrete," 2009.

[37] M. C. Jaime, "Numerical modeling of rock cutting and its associated fragmentation process using the finite element method," 2011.

[38] CEIB, *CEB Bulletin No. 213/214: CEB-FIP model code 90*. Lausanne: Thomas Telford Services, 1990.

[39] L. E. Schwer and Y. D. Murray, "Continuous surface cap model for geomaterial modeling: A new LS-DYNA material type," *7th Int. LSDYNA Users Conf.*, no. 2, pp. 35–50, 2002.

[40] B. Abdelwahed, B. Belkassem, and J. Vantomme, "Reinforced concrete beam-column inverted knee joint behaviour after ground corner column loss-numerical analysis," *Lat. Am. J. Solids Struct.*, vol. 15, no. 10, pp. 1–15, 2018, doi: 10.1590/1679-78254515.

[41] M. Bermejo, J. M. Goicolea, F. Gabaldón, and A. Santos, "Impact and explosive loads on concrete buildings using shell and beam type elements," *3rd Int. Conf. Comput. Methods Struct. Dyn. Earthq. Eng.*, no. May, pp. 1–14, 2011.

[42] O. Mkrtychev, M. Dudareva, and M. Andreev, "Verification of the reinforced concrete column bar model based on the test results," *MATEC Web Conf.*, vol. 251, pp. 1–6, 2018, doi: 10.1051/matecconf/201825104014.

[43] Y. Parfilko, *Study of damage progression In CSCM Concretes Under repeated impacts*. Rechester Institute of Technology, 2017.

[44] S. Paudel, G. Tanapornraweekit, and S. Tangtermsirikul, "Numerical study on seismic performance improvement of composite wide beam-column interior joints," *J. Build. Eng.*, vol. 46, no. September 2021, pp. 1–26, 2022, doi: 10.1016/j.jobe.2021.103637.

[45] Y. Wu, J. E. Crawford, and J. M. Magallanes, "Performance of LS-DYNA concrete constitutive models," in *12th International LS-DYNA Users conference*, 2012, no. 1, pp. 1–14.

[46] LSTC, *LS-DYNA keyword user's manual volume II: material models*, vol. II. LIVERMORE SOFTWARE TECHNOLOGY CORPORATION (LSTC), 2018.

[47]   R. Dumaru, *Performance of expansive concrete under the influence of mix proportions, restraining conditions and curing conditions*. Bangkok: Sirindhorn International Institute of Technology, Thammasat University, 2021.

[48]   S. Tongaroonsri, *Prediction of autogenous shrinkage, drying shrinkage and shrinkage cracking in concrete*. Pathum Thani: Sirindhorn Inernational Institute of Technology, Thammasat University, 2008.

CHAPTER 5
CONCLUSION AND RECOMMENDATION

5.1 Conclusions

This study focuses on the investigation and estimation of restrained concrete expansion and shrinkage strain. This study is divided into two major sections, including estimating restrained expansion strain for laboratory level (prism specimens) and estimating restrained expansion and shrinkage strain for actual expansive concrete structures. This study proposes a method for estimating the restrained expansion strain based on the effective free strain. Effective free strain is obtained from the free expansion strain through direct measurement, which is reduced using the reduction factor equation. The reduction factor generated in this study is one of the novelties of the research results. The important conclusion obtained from this study can be summarized as follows.

Several conclusions can be drawn based on the free and restrained expansion of expansive concrete specimens in this study.

1) The expansion behavior in expansive concrete is influences by various factors, including the amount of binder, amount of fly ash, amount of expansive additive, curing conditions, water to binder ratio, and reinforcement ratio.

2) Free and restrained expansion strain increases when one or more of the following factors which are the amount of expansive additive, binder content, fly ash content, water to binder ratio, and curing temperature are increased.

3) In expansive concrete, the curing type plays an important role in the expansion mechanism. The expansion strain of concrete with moist curing is larger than that of concrete with sealed curing.

4) A larger reinforcement ratio causes a lower the restrained expansion strain. This is because the reinforcing bar causes compression stress during the expansion.

5) Results of FE analysis of restrained expansion overestimate the test results if the loss of ability to produce expansion due to void filling of expansive products and compression creep are not considered. This loss of ability to produce expansion in restrained expansive concrete is considered by introducing a reduction factor to determine effective free expansion strain from the free expansion strain.

6) The reduction factor equation considers several factors, including binder content, expansive additive dosage, fly ash content, water to binder ratio, reinforcement ratio, curing temperature, and type of curing.

7) The use of effective free strain obtained from the proposed equations, as input in FE analysis, can accurately predict the restrained expansion strain of the tested expansive concrete prism specimens.

Based on the field investigation and FE analysis of the expansive concrete structures in this study, the following conclusions can be drawn.

1) The reduction factor used to determine the free strain can effectively estimate the restrained expansion strain in expansive concrete structures.

2) The level of expansion and shrinkage strains can be estimated by considering various factors affecting the expansion level on expansive concrete structures, such as mix proportion, degree of internal and external restraint, and strain direction.

3) Structures with expansive concrete show higher expansion than normal concrete structures. The level of expansion of the C-S-A-based expansive concrete is higher than the CaO + C-S-A-based expansive concrete.

4) The observed crack pattern indicates that expansive concrete effectively prevents shrinkage cracking, as evidenced by the field investigation and FE analysis.

5) In expansive concrete structures, structural configuration and degree of restraint significantly affect the level of expansion and shrinkage. The area with higher restraint conditions always produced lower restrained expansion strain.

5.2 Recommendation for future study

To improve the quality of research regarding the application of expansive concrete structures. Some recommendations can be made for future studies as follows.

1) The reduction factor equation to calculate the effective free strain used as input in the FE analysis was generated using experimental results with limited data. To improve the accuracy and applicability, it is recommended to expand the range of experiments, such as the effect of a larger range reinforcement ratio, water to binder ratio, amount of binder, and fly ash.

2) Experiments on expansion behavior in expansive concrete use only two types of expansive additives. Additional research with other types of expansive additives can increase the range of applicability of the reduction factor equation.

3) The development of reduction factor equations only considers the longitudinal expansion strain from prism specimens, multi-direction strain can be considered for further research.

4) Future research can include experiments on the effects of curing, such as duration and other types of curing, to improve the quality of the reduction factor equations.

5) This analysis only takes fly ash as a cementitious material into account. Other pozzolanic materials, such as blast furnace slag, bottom ash, and silica fume, require additional study.

6) The FE analysis simulation on the actual structure produces results that are very compatible with the field investigation results. Thus, the research can be continued by conducting a parametric study considering the influence of the configuration of the structure.

7) The construction stage is one factor that affects the expansion level during the expansion process. Simulation and investigation of the effect of the construction stage can be carried out as a further study.

8) Completing the equation of reduction factor by considering more comprehensively the effect of external restraint can be done for future studies.

9) Finally, the guideline for the design of structures using EA concrete should be proposed to be able to design the shrinkage crack resisting expansive concrete structures by calculating the required amount of EA for various degrees of restraint.

BIOGRAPHY

Name	Hakas Prayuda
Education	2013: Bachelor of Engineering (Civil Engineering)
	Universitas Muhammadiyah Yogyakarta.
	2015: Master of Engineering (Civil Engineering)
	Universitas Gadjah Mada.

International Journal

H. Prayuda, R. Dumaru, G. Tanapornraweekit, S. Tangtermsirikul, W. Saengsoy, & K. Matsumoto, (2022), Estimation of Restrained Expansion Strain of Reinforced Expansive Concrete Considering Mixture and Curing Conditions, *Construction and Building Materials*, Vol. 322(126386), pp. 1-15.
https://doi.org/10.1016/j.conbuildmat.2022.126386

H. Prayuda, G. Tanapornraweekit, S. Tangtermsirikul, K. Matsumoto, P. Jongvisuttisun, & C. Snguanyat, (2022), Field Investigation and Finite Element Analysis on Expansion and Shrinkage Strains of Expansive Concrete Structures, *Construction and Building Materials*, Vol. 360(129598), pp. 1-22.
https://doi.org/10.1016/j.conbuildmat.2022.129598

International Conference

H. Prayuda, R. Dumaru, G. Tanapornraweekit, S. Tangtermsirikul, W. Saengsoy, K. Matsumoto, (2022), Reduction Factor Used to Account for Effective Free Expansion Strain for Expansive Concrete, *Regional Conference in Civil Engineering (RCCE) and Sustainable Development Goals (SGDs) in Higher Education Institutions 2020*, Malaysia, 23-25 January 2021. (**Accepted**)